Analysis of the Impact of Closed-Loop Power Flow Control Strategies on Power System Stability Characteristics

by

As'ad Ally

Submitted in fulfillment of the academic requirements for the degree of Master of Science in Engineering in the School of Electrical, Electronic and Computer Engineering at the University of KwaZulu-Natal, Durban, South Africa.

April 2005

I hereby declare that all the subject matter contained in this thesis is my own original and unaided work except in the case where a specific numbered reference is made. Furthermore the work contained in this thesis has not been submitted for a degree at any another university.

Name: A.Ally Signature: _____

This Thesis is dedicated to my

parents,

who have taught me the importance of education.

ABSTRACT

The demand for electrical energy in industrialised countries continues to increase steadily. As a result of this growing demand for electrical energy, there is a need for optimisation of the power system in terms of transmission and control. One option could possibly be an increase in transmission facilities to handle the increase in growth; however factors such as environmental issues as well as the possible cost incurred could hamper this particular approach. An alternative resides in loading the existing transmission network beyond its present operating region but below its thermal limit, which would ensure no degradation of the system. For this approach to be realised, improved control of the flow of power in an interconnected network would be advantageous so as to prevent unwanted loop flows and inadvertent overloading of certain lines.

This approach can be made possible by the use of Flexible AC Transmission Systems (FACTS) technology. The concept of FACTS incorporates power-electronic compensation devices that can be typically used in an ac power system to enhance the system's power transfer and controllability. There exists a number of FACTS devices, where each device can be utilised differently to achieve the broad objective. One such device is the Thyristor Controlled Series Capacitor (TCSC). The TCSC is a class of FACTS device that makes it possible to alter the net impedance of a particular transmission line in an effort to force the flow of power along a "contract path".

This thesis identifies, in the published literature, a set of strategies for the scheduling of power flow by use of variable compensation; such strategies are then considered in more detail in the analysis of the thesis. Firstly, a detailed dynamic model of a TCSC is developed together with its various controls and associated circuitry within the power systems simulation package PSCAD. In addition to this, a power flow controller scheme is then implemented, which exhibits the functionality of the power flow controller strategies reviewed in the literature. In order to test the validity and

operation of the TCSC model as well as the analysis of the power flow controller scheme, a single-machine infinite bus (SMIB) study system model is developed and used as part of the investigation.

This thesis, firstly, presents a theoretical analysis of two particular modes of power flow control in an interconnected ac transmission system. Secondly it confirms the results of an analytical study in previously published work with the implementation of the two control modes, and further extends the scope of the previous study by examining the impact of the power flow controller's design on the small-signal and transient stability characteristics of the study system.

The key findings of this extended investigation are that the power flow controller's mode of operation has an important influence on both small-signal and transient stability characteristics of a power system: in particular, it is shown that one mode can be detrimental while the other beneficial to both system damping and first swing stability. Finally, the thesis applies the understanding of the power flow controller's operation obtained from the SMIB study system to the problem of inter-area mode oscillations on a well-known, two-area, multi-generator study system. Real-time simulator results are presented to exhibit the effect of the power flow controller modes and controller design on the oscillatory characteristics of the two-area study system.

Acknowledgements

I would like to thank my academic supervisor, Dr Bruce Rigby for his guidance, direction and patience throughout the course of my thesis. Furthermore, I would like to express my gratitude towards Eskom for affording me the opportunity to study towards a masters degree, I intend on making every effort to share and apply the knowledge that I have learned to make a contribution to the organisation. Finally, many thanks, to my family and friends that have supported me during the course of my studies.

CONTENT

CHAPTER THREE DESIGN AND IMPLEMENTATION OF POWER FLOW CONTROLLERS

CHAPTER FOUR MATHEMATICAL MODELLING

LIST OF SYMBOLS AND ABBREVIATIONS

The symbols and abbreviations utilised throughout this thesis are listed and explained below.

Symbols

C	- Capacitance
L	- Inductance
ω_S	- System Frequency
ω_R	- Resonant Frequency
$\propto$	- Thyristor Firing Angle
β	- Thyristor Conduction Angle
λ	- Ratio of Resonant Frequency to System Frequency
X_O	- Overall Transmission Reactance
X_{SC}	- Controllable Series Capacitive Reactance
X_L	- Inductive Reactance
X_C	- Fixed Capacitive Reactance
X_{TCSC}	- Net Compensating Reactance of the TCSC
X_{TCR}	- Variable Inductive Reactance
X_{order}	- Reactance Order of the TCSC
$X_{order\ 0}$	- Initial Steady State Reactance Order of TCSC
$X_{order\ min}$	- Minimum value of Reactance Order of TCSC
$X_{order\ max}$	- Maximum value of Reactance Order of TCSC
k	- Degree of Capacitive Compensation
R_L	- Transmission Line Resistance
I_{LINE}	- Transmission Line Current
V_C	- Capacitor Voltage
θ_{IINE}	- Instantaneous Angle of the Transmission Line Current

θ_{Vc}	- Instantaneous Angle of the Capacitor Voltage
V_S	- Voltage at the Sending End of the Transmission Line
V_R	- Voltage at the Receiving End of the Transmission Line
δ/θ	- Transmission Angle
P_{L1}	- Active Power Transfer in Transmission Line L1
P_{L2}	- Active Power Transfer in Transmission Line L2
P_{L3}	- Active Power Transfer in Transmission Line L3
P_{TCSCL1}	- Active Power Transfer in Additional Transmission Line Compensated by a TCSC
P_{reqL1}	- Required Power Transfer in Transmission Line L1
$P_{desiredL1}$	- Set Point Value of Transmission Line L1's Power Transfer
ε_{PL1}	- Error in Power Transfer in Transmission Line L1
ΔP_t	- Change in Active Power Dispatch
ΔP_m	- Change in Mechanical Input Power to the Generator
ΔP_{G1}	- Change in Output Power of Generator Unit 1
SW	- Toggle Switch
PI	- Proportional Integral
K_P	- Proportional Gain
K_I	- Integral Gain
K_{PLANT}	- Plant Gain
T_S	- Settling Time Constant
τ_P	- Closed-Loop Pole Time Constant
τ_Z	- Closed-Loop Zero Time Constant
ζ	- Damping Ratio
f	- Frequency
G1	- Generator Unit 1
G2	- Generator Unit 2
G3	- Generator Unit 3
G4	- Generator Unit 4

Abbreviations

AVR	- Automatic Voltage Regulator
PLL	- Phase Lock Loop
FFT	- Fast Fourier Transform
DFT	- Digital Fourier Transform
PSS	- Power System Stabiliser
PSCAD	- Power Systems Computer Aided Design
RTDS	- Real-Time Digital Simulator
RTPSS	- Real-Time Power System Studies
HVDC	- High Voltage Direct Current
SVC	- Static Var Compensator
SMIB	- Single-Machine Infinite Bus System
TCR	- Thyristor Controlled Reactor
UPFC	- Unified Power Flow Controller
SSSC	- Static Synchronous Series Capacitor
TCSC	- Thyristor Controlled Series Capacitor
FACTS	- Flexible AC Transmission System

CHAPTER ONE

INTRODUCTION

1.1. General Background

In an ac power system electrical generation and load must be balanced at all times in order to maintain stable operation of the system. For this reason there has always been a need for the effective control of power flow along an ac transmission system. Suggestions in the past have shown that a power system could be operated closer to its thermal limit, while still remaining dynamically stable and safe. In order to institute such a concept, the issues that needed to be examined involved: optimising line impedance; minimising voltage variation and the control of power flow under steady state conditions. Traditionally these requirements were met by transmission systems being installed with mechanically-switched series and shunt reactive compensation, in addition to voltage regulating and phase shifting transformer tap changers. However, since these control and compensation techniques were largely slow-operating in nature, the transmission systems were typically designed with generous stability margins such that they could recover from general outages and usual operating contingencies. This trend has led to transmission systems often being under utilised. With growth in the size and complexity of modern power systems it has become increasingly clear that high-speed operation is a pre-requisite for power system control applications [1].

In recent years however, key advances in the area of high-power semiconductor devices and control technologies have yielded the emergence of the broad concept of Flexible AC Transmission Systems or FACTS technology. The FACTS concept refers to the incorporation of power electronic compensation devices into an ac power system with the objectives of enhancing firstly these systems' power transfer capability and secondly, their controllability [2].

This broad objective can be achieved in various ways by applying FACTS devices both individually or in co-ordination with each other to enhance the power system's flexibility and controllability. A typical application incorporates the use of FACTS devices to directly control the amount of power flow in a particular transmission line or group of lines in an interconnected ac system [3,4]. There exists a range of possible benefits for this form of closed-loop power flow control, such as: allowing power to be directed along a contract path; preventing inadvertent overloading of lines already near their thermal limits and preventing unwanted loop flows in an interconnected system [3,5].

Closed-loop power flow control can be achieved using a number of FACTS devices: a thyristor controlled series capacitor (TCSC), a static synchronous series compensator (SSSC) or a unified power flow controller (UPFC). Such FACTS devices have the ability to control dynamically one or more of the factors that influence power transfer in the line they compensate, thus giving them the capability to direct the flow of power. Previous literature highlights various schemes that have been proposed employing each of these devices [4,6,7].

The TCSC in particular is a series-compensating device, which consists of a series capacitor shunted by a thyristor controlled reactor (TCR). The main applications of the TCSC are twofold: line power scheduling, and the control of electromechanical oscillations. The first application considers the use of the controllable series compensation provided by the TCSC to ensure a desired amount of power flow on parallel transmission paths. In the second application, careful dynamic control of the TCSC's capacitive compensating reactance can be used to influence the electromechanical oscillations between a generator and the rest of the power system. This thesis is concerned with the first of these two applications, that is using the TCSC for line power scheduling by implementing closed-loop control of ac power flow in a transmission system.

1.2. Thesis Objectives

Stability of a power system can be defined by the system's characteristic response when exposed to two different types of operating condition. Firstly, during normal operating conditions the system must have the capability to remain in a state of operating equilibrium. Secondly, the system must be able to recover from a disturbance and subsequently return to a state of acceptable equilibrium [8]. Stability of a power system is categorised according to two criteria following a major disturbance. The first criterion is transient (first-swing) stability, implying the system's ability to survive the first few swings and maintain synchronism after being subjected to a severe disturbance. Dynamic (small-signal) stability is the second criterion, and refers to the characteristics of the electromechanical oscillations that occur in the system following a small disturbance or after surviving a transient event. Generally in systems where power transfer is limited as a result of stability concerns, the inclusion of FACTS devices can prove to be a cost effective approach to utilise the power transmission system more effectively. It is for this reason that the use of variable impedance control has become an attractive option to enforce desired steady state power flow along parallel transmission paths.

This thesis considers the use of a TCSC to carry out closed-loop control of ac power flow in a transmission system. This TCSC-based, closed-loop power flow controller is used to implement two different strategies for transmission line power flow control that have been proposed in the literature: constant power control and constant angle control [3,6]. In particular, the thesis aims to investigate the effect that each power flow control strategy has on system stability as a whole. Furthermore, for each strategy, an investigation is carried out into the influence of the design of the power flow controller's response time on transient and small-signal stability of a single-generator study system. Finally, the TCSC-based power flow controller is applied to a well-known four-generator study system [8]. This thesis examines whether the TCSC-based power flow controller has an influence on the damping of the inter-area mode oscillations of this system.

1.3. Thesis Layout

This thesis consists of five subsequent chapters, which present the development of various simulation models used in the analyses, and the results and findings of the various studies conducted. The subject matter has been arranged as follows.

At the outset, a literature review of the technical aspects regarding the use of series compensation devices for the application of power flow control had to be addressed. Chapter Two discusses a brief history as well as the theory related to power flow control using firstly fixed, and then controllable series compensation. This chapter also reviews the various FACTS devices that can be used for this particular application of power flow control.

Chapter Three considers the design and implementation of the TCSC-based power flow controller. Within this chapter the concept of altering the net impedance of a transmission line by use of the two control strategies is examined in detail. This chapter also highlights the basic operation and attributes of the power flow controller as well as the design method used to obtain its controller gains. During the course of the thesis a number of simulation models were developed in both PSCAD [9] and RSCAD [10]. Chapter Four presents the simulation model of a single machine infinite bus (SMIB) study system that was developed in PSCAD. This chapter also includes the simulation models of the TCSC that were developed in both PSCAD and RSCAD respectively.

Chapter Five examines the performance of the SMIB study system, which was supplemented by a TCSC, operating in conjunction with a power flow controller. The first part of this study involved reconfirming the findings of previously published work to establish confidence in the simulation models used. The published work consisted of investigations into the application of a TCSC for line power scheduling using two control strategies.

Using these findings as a base, the investigations were extended by considering the effect and possible benefit that each control strategy would have on the SMIB study system during transient and dynamic conditions. In particular this chapter investigates the effect of the power flow controller on the small-signal and large signal stability characteristics of the study system. The investigations consider different operating conditions and various designs of the power flow controller's response time.

The results of Chapter Five indicate that a power flow controller can influence the stability characteristics of the SMIB study system, particularly the damping of the electromechanical oscillations. Chapter Six, therefore considers a two-area four-generator study system in order to ascertain what effect the power flow controller's operation would have on the electromechanical oscillations of a larger, multi-machine study system.

Chapter Seven summarises the results and findings of the thesis as well possible future work that could be of relevant interest in this particular area of research.

1.4. Findings of the Thesis

The previous section outlined the structural arrangement of the thesis. This section now highlights the main results and findings of the thesis.

The achievements and findings of the thesis maybe summarised as follows:

(i) A detailed simulation model of a TCSC has been developed for the simulation package PSCAD; this model includes the TCSC's power electronic switches and their low-level firing controls. The model has been verified against the theoretical characteristics of a TCSC and has been integrated into a model of a SMIB study system in PSCAD. A closed-loop power flow controller has also been implemented on this

SMIB and TCSC study system in order to allow a study of the two different power flow control strategies proposed in the literature.

(ii) A series of studies is presented to demonstrate the impact of closed-loop power flow control on the stability characteristics of the SMIB study system. These studies consider the influence of controller response time and power flow control mode on the small-signal and transient stability characteristics. The findings show that the closed-loop power flow controller does have an impact on the system's stability characteristics and that this impact depends on both the controller's response time and its operating mode. In particular, it is shown that in one mode the power flow control has an adverse impact on system stability whereas in another mode the impact is beneficial to these characteristics.

(iii) The influence of the closed-loop power flow controller on the small-signal stability characteristics of a multi-generator system is also examined using a real-time simulator. An existing real-time simulation model of a well-known four-generator study system has been extended in this thesis to include a TCSC and power flow controller. As with the single machine study system, a series of studies is then presented to confirm the influence of the power flow controller, its operating mode and response time, on the inter-area mode oscillations of this four-generator study system.

1.5. Research Publications

Findings from this thesis have been presented at national and international conferences [11,12].

CHAPTER TWO

CONTROLLABLE SERIES COMPENSATION FOR CLOSED-LOOP POWER FLOW CONTROL

2.1. Introduction

The previous chapter has highlighted the importance of the control of power flow along an ac transmission system in order to ensure system stability. The previous chapter stated that system stability can be achieved by balancing the electrical output power of the generators and the system loads. The discussions of the previous chapter showed that a FACTS device has the ability to alter and control dynamically the factors that influence power transfer in the particular line it compensates. This characteristic of a FACTS device gives it the capability to control the flow of power in an interconnected ac network.

This chapter reviews the applications of FACTS devices, and in particular the TCSC, that have been proposed in the literature for closed-loop power flow control. In particular the chapter examines the control strategies proposed by various researchers for power flow control. In addition, practical considerations as well as potential problems when implementing these strategies in a power system are highlighted from the previously published literature. However, the following section begins by introducing the basic concept of series compensation and explaining how it can be used to influence the power transfer capability of an ac power system.

2.2.Theory of Increased Power Transfer via Series Compensation

It is well known that the transmitted power in a simple ac two generator system is determined by the series line impedance and the angle between the end voltages of the line. In the past power system operators and researchers have considered various techniques to alter the flow of power in a transmission line to allow the system to operate closer to its thermal stability limit. Kimbark in the mid-1960s considered a method of switching in series capacitors mechanically using circuit breakers to alter the flow of power in a transmission line [13]. The fundamental concept of series compensation is to reduce the overall series line impedance, thus enabling the line to appear electrically shorter. This interest in series compensation is most likely a result of it being recognised that power transmission, particularly over long transmission lines is limited pre-dominantly by the line's series inductive reactance [14]. In addition, the justification of controllable series compensation can be explained in terms of the simple two-machine power system diagram shown in Fig. 2.1 below.

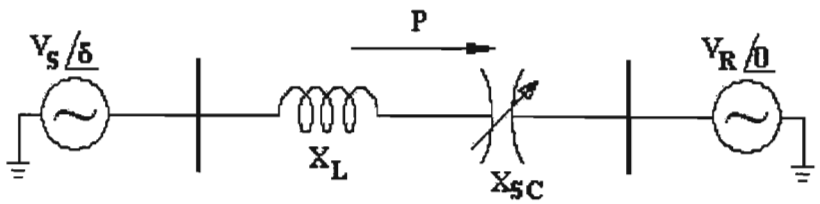

Fig.2.1. Effect of series compensation on power flow in an ac network

Fig. 2.1 comprises a two-machine system interlinked by the inductive reactance of the transmission line and a controllable series capacitance of reactance X_{SC}. The derivation of the relationship between the power flow and the controllable series compensating reactance is largely based on [1]. The overall transmission line reactance (X_O) can be written as:

$$X_O = X_L - X_{SC} \tag{1}$$

The degree of the compensation (k) can be defined as the ratio of the series capacitive reactance and the inductive line reactance (X_{SC}/X_L), such that:

$$X_O = (1-k)X_L \tag{2}$$

where the degree of series compensation is bound between the limits zero and one. Using the relationship for the overall line impedance, the power flow in Fig.2.1 can be approximated as:

$$P \cong \frac{|V_S||V_R|}{X_O} \sin\delta \tag{3}$$

Fig. 2.2 below shows the relationship between the electrical output power and the angle across the transmission line. From the graph, it is evident that the electrical output power increases steadily as the degree of compensation is increased.

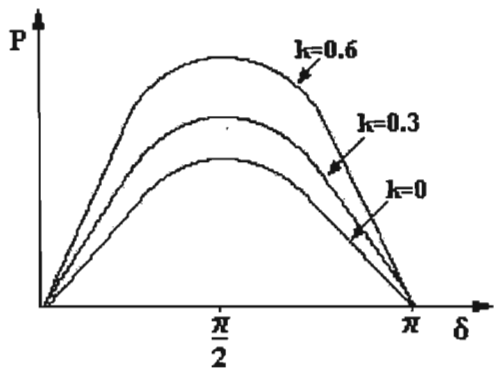

Fig.2.2. Active power vs. angle characteristic for two-machine power system

The use of series compensation to alter the flow of power can prove to be of benefit in a transmission system with multiple parallel paths during contingencies and line outages. In the case of a line outage in such a network, the power carrying capability of a particular line can be changed by altering its degree of series compensation in order to allow a continuous uninterrupted flow of power. This concept of power flow scheduling has been proposed in [3,4] and will be discussed in further detail in the subsequent sections.

2.3. Controllable FACTS Series Compensation

2.3.1. Overview

The initiative of FACTS technology emerged in the late 1980s as an alternative to the traditional methods used to solve the problem of increasing power demand: the two main objectives of FACTS technology were firstly, to direct the flow of power over designated routes and secondly to increase the power transfer capability of the existing transmission system through improved control [2]. The realisation of these objectives however would require the development of high-powered controllers. As a result of major advances in the area of high-powered semi-conductor technology, the concept of FACTS technology was conceived. Hingorani proposed the FACTS concept and the use of this technology in an effort to increase the usable power capacity in a power system [1].

The cornerstone of FACTS technology was initially the thyristor, which is an example of a high-powered semi-conductor device with control capabilities. These characteristics of the thyristor earlier saw application in the high-voltage direct current (HVDC) systems and static var compensator (SVC) technologies [14]. This was followed by the rapid development of various controllable series compensators, in particular the TCSC. The following subsection considers the three different types of controllable compensation devices for the application of power flow control. This thesis is concerned primarily with a particular type of series compensator, namely the TCSC. However the UPFC and SSSC can also be used for closed-loop power flow control as a result of them being able to influence the variables in eqn (1). Hence their basic concepts and power flow control capabilities are summarised in the following subsection.

2.3.2. Unified Power Flow Controller (UPFC)

The unified power flow controller was proposed by Gyugyi in the early 1990s. A schematic diagram of the UPFC is shown in Fig. 2.3 together with a brief description of its basic operation which is largely based on [4].

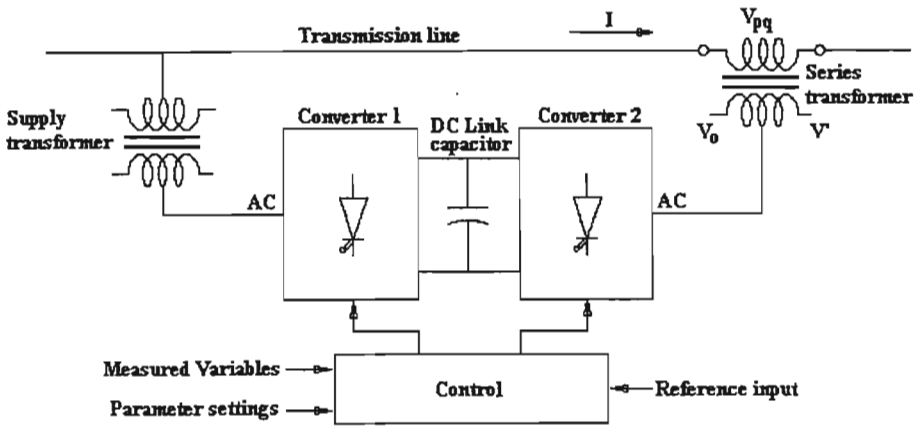

Fig.2.3. Schematic diagram of the UPFC

The UPFC consists of two back-to back voltage sourced converters that are operated from a common dc link, represented by a dc storage capacitor. The arrangement of the UPFC functions as a basic ac-to-ac converter, where each converter can independently generate reactive power at its own ac terminals. Converter 2 injects a voltage with a controllable magnitude and phase angle via an insertion transformer, where the injected voltage serves as a synchronous voltage source.

Active and reactive power exchange can thus occur between the ac system and this voltage source as a result of the flow of transmission line currents through the voltage source. Converter 1 supplies or can absorb the active power requested by converter 2 at the dc link in an effort to restore the active power exchange. The power demand of converter 2 at the dc link is then converted to ac by converter 1 and coupled to the transmission line. The UPFC is capable of controlling, simultaneously, one or more of the parameters (voltage, impedance, phase angle) that affect the flow of power in a transmission system [4,15].

2.3.3. Static Synchronous Series Compensator (SSSC)

A schematic diagram of an SSSC is shown in Fig. 2.4 followed by an explanation of the device's principles of operation which is based on [7].

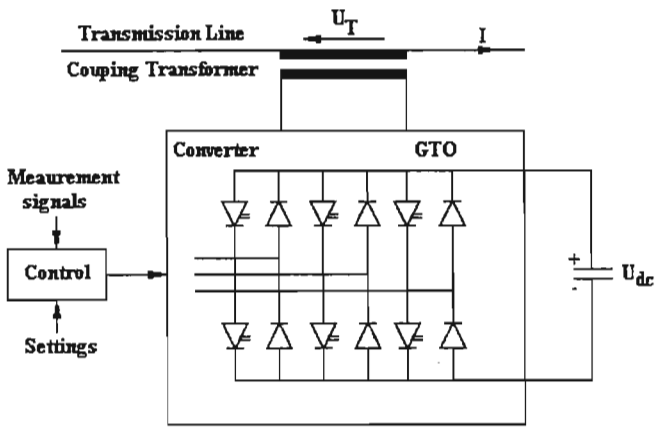

Fig.2.4. Schematic diagram of the SSSC

The SSSC is a voltage sourced converter that injects a voltage in series with the transmission line to which it is connected. The injected voltage is variable and is almost in quadrature with the line current. This injected voltage can emulate a capacitive or inductive reactance in series with the transmission line. The SSSC is then capable of influencing the flow of power in a transmission line by controlling the magnitude of this emulated reactance. Mihalič proposed the use of the SSSC in [7] as part of a fast-responding, closed-loop power flow controller in a simplified network.

2.3.4. Thyristor Controlled Series Capacitor (TCSC)

The thyristor controlled series capacitor was the first hardware controller to be developed under the FACTS initiative [3]. The TCSC makes it possible to vary the impedance of a particular transmission line in an interconnected network so as to force the flow of power along a contract path. A schematic representation of the TCSC is shown in Fig. 2.5 followed by a description of its principles and operating characteristics.

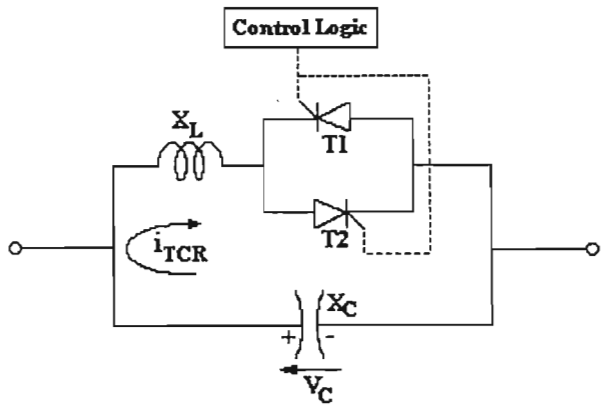

Fig.2.5. Schematic representation of the TCSC

A TCSC consists of a series capacitor connected in parallel with a thyristor-controlled reactor (TCR). The TCSC is inserted in series with the transmission line, in the same manner as a series compensating capacitor. Reference [3] proposed that several TCSC modules can be connected in series in order to obtain the required voltage rating and operating characteristic. The net compensating reactance X_{TCSC} that the TCSC provides to the system is the combination of the fixed capacitive reactance X_C and the variable inductive reactance X_{TCR} of the TCR. The magnitude of the variable inductive reactance is a function of the thyristor delay angle. The thyristor delay angle is determined by low-level firing controls. In a conventional TCSC arrangement, where the inductive reactance X_L is smaller in magnitude than the capacitive reactance X_C, the TCSC has two operating modes: capacitive mode and inductive

mode. Using this concept of variable series compensation of a TCSC, reference [3] proposed the idea of enforcing desired steady state power flows on parallel transmission paths of an interconnected network.

This section has reviewed three different FACTS devices that can be used to achieve closed-loop control of power flow. In general, inverter based devices, in particular the UPFC, provide more functional flexibility and better operational performance than thyristor controlled systems. However these devices are inherently more expensive than their equivalent thyristor-based counterparts, which is likely to be the reason for the TCSC being the most common series FACTS device being utilised for actual utility applications. Indeed, the TCSC is already in wide use in power utilities around the world at transmission voltage levels up to 500kV [16,17,18] whereas to date, the UPFC has only been installed at a test site at 138kV [19].

2.4. Closed-Loop Power Flow Control

2.4.1. Background

The concept of power flow control in an ac transmission system can be understood as the means by which those parameters of the system that are responsible for the flow of power can be altered [4,5,6,20]. Influencing the flow of power using controllable series components can result in improvements in the power system's performance by allowing operation closer to its thermal limits [6]. As pointed out in the previous section, the power flow along a transmission line is a function of the line impedance and the phase angle between the end voltages of the line. In the past the capacitive and inductive reactances were the parameters of the system that were either fixed or varied using a slow steady-state scheduling approach. With this traditional approach, during dynamic conditions, the power flow was a function of the angles across the system; however there existed no form of direct control of these angles.

FACTS devices however can be used to directly control the capacitive reactances and other parameters to achieve fast direct control of power flow in an interconnected ac network [1,20]. In situations where the angles across the system change, the capacitive reactance can be altered such that the desired power flows can be maintained. This form of impedance control can be programmed to react in a planned way to contingencies so as to greatly enhance power system stability [3].

This application of FACTS devices to provide direct control over the amount of power flow has been described in the literature as power flow control [5,7], closed-loop control of ac power flow [21] and power scheduling [3,6]. The ability to schedule the flow of power over particular transmission lines can yield several benefits [3,5]: preventing overloading of lines that are already operating close to their thermal limits; preventing undesired loop flows in an interconnected ac network; restricting the flow of power to selected transmission corridors.

Previous literature has highlighted the application of various FACTS devices for closed-loop power flow control [4,6,7]. This thesis, however, specifically considers the effect of such power flow control on the stability of the study system as a whole. This thesis considers the use of a FACTS device to direct the flow of power while examining the additional influences that this form of control might have on small and large signal behaviour of the generators feeding the interconnected system. Although the impact of power scheduling control on system stability has been presented in [6], this particular area of study has not yet received a thorough treatment.

2.4.2. Literature Review

In order to attain the objective of this thesis, which is to analyse the impact of closed-loop power flow control strategies on power system stability characteristics, the following issues need to be addressed with regards to closed-loop power flow control:

i). control approaches implemented using the TCSC;

ii). typical range of controller response rates considered;

iii). requirements for practical implementation in a real system; and

iv). potential problems for application in a real system.

This section reviews the published literature and examines the various issues regarding closed-loop power flow control.

Researchers have previously described methods in the literature for controlling the series compensation of a particular line in an interconnected network to improve the power flow capability in that system. References [3,6] have proposed two distinct strategies for the purpose of power flow control, namely the constant power strategy and the constant angle strategy. These control strategies are applied to a system consisting of at least two parallel transmission lines, where one of these lines is compensated by a TCSC. Reference [3] states that the objective of the constant power strategy is to force all the uncompensated lines to absorb any increase in dispatched power; control logic is then used to adjust the amount of series compensation provided by the TCSC, to ensure that the power in the line compensated by the TCSC is regulated accordingly. Conversely, reference [3] also proposed the concept of the constant angle strategy which forces the line compensated by the TCSC to absorb any increase in dispatched power; in this approach, by adjusting the TCSC's capacitive reactance, the increased power is transferred whilst maintaining a constant transmission angle across all the parallel lines. The operating principles of these two control strategies are explained in more detail in Chapter Three.

Reference [6] considered the impact of a TCSC on the stability characteristics of a study system. The TCSC formed part of a closed-loop power flow controller and power oscillation damping controller operating simultaneously. The findings from [6] showed no impact on the generator's synchronising and damping torque by the combined control action. However, the individual effects of power flow control and power oscillation damping were not separately considered in [6]. As such it is not

possible to obtain any conclusions from [6] on the stability impact of the power flow control algorithms themselves. Reference [6] also considered the influence of the power flow controller on the transient performance of their power oscillation damping controls. In this particular case the system's oscillations became poorly damped as a result of the saturation in the TCSC's output, but this was rectified by adjusting the power oscillation damping controller design. Reference [3] has considered the use of a power flow controller to damp power swings. The authors of [3] state that in order to improve the damping of power swings, the amount of compensation must be varied. This variation in the TCSC's compensation is required such that the resultant changes in power transfer caused by the variation of the capacitive reactance tend to counteract the power swings.

A number of researchers have considered the issue of the appropriate speed of response of a power flow controller, with a range of controller response times proposed in the literature [3,4,6,7]. Reference [6] suggested that the proportional integral (PI) controller in such a scheme should be slow acting, with the controller action carried out over a period of approximately 30 seconds. Reference [3] also supports this suggestion, where a response time on the order of 10 seconds is utilised. However, other researchers have also considered fast scheduling of power [4,7] using both the UPFC and SSSC respectively. Both references [4] and [7] suggest response times of tens of milliseconds for their respective controller designs.

Considering that previously published literature has considered closed-loop power flow control utilising both fast and slow response times, this thesis will focus on response times in the range of 5 to 25 seconds. This chosen range of response times is examined in order to obtain a more complete understanding and to take note of any effects that are present for both shorter and longer response times. Reference [21] documents techniques for simplifying power system models for the purposes of designing the response time of a power flow controller. The controller design process adopted in this thesis follows the approach used in [21], where simplified system representations of detailed simulation models were developed for controller design

purposes. However, whenever the influence of power flow control on stability is to be assessed in the thesis, the detailed simulation models are used.

Reference [6] investigates the implications of implementing the constant angle control strategy in a practical system. Reference [6] states that in the case where the location of generation is remote, telecommunication of some control signals would be required for the constant angle strategy. Reference [6] in addition states that using remote signals for this application would tend to have an impact on cost, but not on the reliability of the system. This is as a result of the requirement of the line power scheduling process being performed over a long period.

Similarly reference [3] also proposes the concept of scheduling of power flow in a remote location using the adjustment of the TCSC compensation. For their method, the power flow and approximate angle across the system would be determined by using the control system to measure the local voltage and current. Reference [3] states that the adjustment of the capacitive compensation would be programmed into an energy management system, which would send a desired set point value to a regulator. The compensation would then be varied continuously by the regulator in order to obtain the required power and estimated system angle relationship.

On the issue of the practicalities of implementing power flow control, in a real system, reference [6] has reported on potential problems that may arise during specific operating conditions in a parallel transmission system. Reference [6] considers the problems associated with the TCSC controls during conditions involving line outages. In particular, the authors of [6] consider the situation where the alternate line is outaged, leaving only the line compensated by the TCSC in operation. When the power flow controller is operated in constant power mode, the generator is shown to lack synchronising torque. The authors attribute [6] this problem to the PI controller trying to maintain the flow of power in the compensated line, irrespective of there being no alternate path for any additional power to flow: their suggestion is that the

constant power and angle strategies should be applied to systems with two or more parallel paths.

Thus in a situation involving a line outage, having more than one alternate line would assist the power flow controller's function to regulate the flow of power without resulting in the system becoming unstable. The second problem that [6] reports is the characteristic of the TCSC's output drifting arbitrarily to its minimum and maximum value following a system disturbance. The authors of [6] suggest that a protection scheme be utilised to disconnect the TCSC's controls during severe contingencies; however damping controls need to be maintained [6], or otherwise introduced during such a condition, in order to keep the system stable.

2.5. Summary

This thesis aims to investigate the effect of closed-loop power flow control on system stability as a whole. To this end, this chapter has reviewed the relevant research literature on this subject. By adopting the two control strategies proposed in the literature, the effect of both the transient and dynamic behaviour of a SMIB study system will be investigated. Furthermore by selecting a range of controller response times based on the published literature, the effect of both a fast and slow acting power flow controller on the stability characteristics of the system will be examined. This investigation will be conducted to identify the possible effects on the dynamic and transient behaviour of the study system for each of the two power flow control strategies.

CHAPTER THREE

DESIGN AND IMPLEMENTATION OF POWER FLOW CONTROLLERS

3.1. Introduction

The previous chapter highlighted the various control approaches undertaken in the published literature for closed-loop power flow control. In that chapter, aspects regarding the effective scheduling of power flow were reviewed and three devices that can be used for power flow control were identified and examined. Chapter Two also discussed the two particular control strategies suggested by researchers, namely the constant power and constant angle strategies. The previous chapter has also highlighted the range of response rates proposed by various researchers for power flow control. Based on these findings obtained from the published literature, the effect of closed-loop power flow control on small and large signal stability will be investigated.

This chapter however, focuses on the design and implementation of a specific power flow control scheme in a single-machine infinite bus (SMIB) study system. In the chapter the various components of the SMIB study system and their respective functionality will be discussed. The general theory of power flow control with regards to the SMIB study system will be examined using the power flow equation. In addition the constant power and angle control strategies will be discussed in detail. Furthermore this chapter outlines the method used for designing the gains of the power flow controller, so as to obtain a desired response time, and includes an example case to illustrate the various steps followed.

3.2. Power Flow Control Theory

3.2.1. The SMIB Study System

In this chapter a single machine infinite bus (SMIB) study system is outlined. This relatively simple SMIB system is used in this chapter so as to allow a clear explanation of the concepts and design of closed-loop power flow controllers. In addition, this study system is used in the initial studies of Chapter Five to enable the impact of a power flow controller on system stability to be readily understood. Subsequently, in Chapter Six, a more detailed, multi-generator system is considered for further analysis.

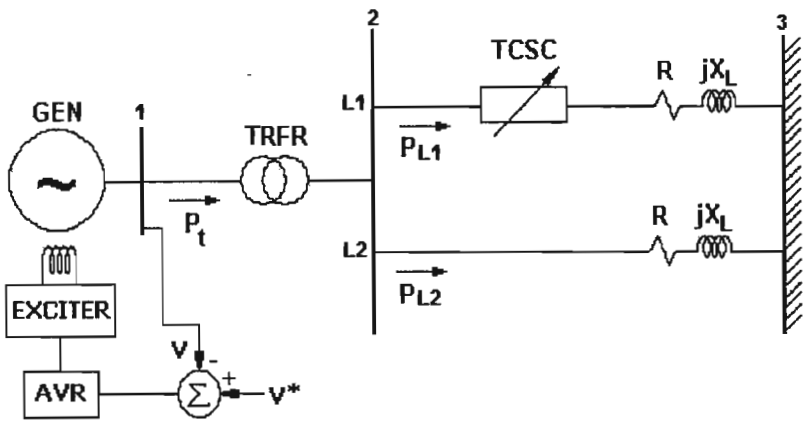

Fig.3.1. Single-line diagram of the SMIB study system

Fig. 3.1 above shows a diagram of the single-generator study system considered in the initial studies of the thesis. The system consists of a synchronous generator that is connected to an infinite busbar via a transformer and two parallel transmission lines. Transmission line L1 is compensated with a TCSC, while L2 is uncompensated. The *structure* of the study system shown in Fig. 3.1 is based on that which was used to study line power scheduling in [6]. In this thesis however, the *parameters* of the study system are different from those in [6], and are based on those of the Machines Research Laboratory at the University of KwaZulu-Natal.

The generator at the sending end of the transmission line is equipped with an automatic voltage regulator (AVR). The inclusion of the generator's AVR is important when considering the stability characteristics of a study system, since the AVR is known to have a significant impact on both small-signal and transient stability characteristics [8]. The TCSC provides a variable compensating reactance (X_{TCSC}) that is used to alter the overall impedance of line L1. The parameters of the TCSC used in the SMIB study system are based on those of a laboratory-scale TCSC that has been designed for use in the Machines Research Laboratory [22] and whose parameters are currently being revised for improved performance [23]. The full details of the parameters of the study system are given in Appendix A.

3.2.2. Basic Concepts of Power Flow Control

The previous subsection outlined the SMIB study system to be considered in the thesis. This subsection will now address the concept of power flow control with reference to the SMIB system in Fig 3.1. In Fig. 3.1 the active power transfer in transmission line L1 is given by

$$P_{L1} \approx \frac{|V_2||V_3|}{X_L - X_{TCSC}} \sin\theta_{23} \qquad (4)$$

where $|V_2|$ and $|V_3|$ are the magnitudes of the voltages at buses 2 and 3 of the system and θ_{23} is the transmission angle between these bus voltages.

Equation (4) highlights the principle by which series compensation can be used to manipulate the net impedance of a particular transmission line and hence influence its power transfer. When the TCSC's reactance is increased for a given transmission angle θ_{23}, the net reactance $X_L - X_{TCSC}$ of the compensated line is reduced, thereby increasing the active power transfer. Hence, the magnitude of the active power transfer in the compensated line can be increased for a given transmission angle by

increasing the amount of TCSC compensation. Alternatively, an increase in the amount of TCSC compensation can be used to reduce the transmission angle required for a given active power transfer in the compensated line.

These two observations underlie the two distinct strategies that have been proposed for closed-loop control of line power flow [3]: the "constant power strategy" which keeps the power flow in the compensated line constant, and the "constant angle strategy" which ensures that the compensated line absorbs any increase in generated power. Each of these strategies will now be explained in more detail.

3.2.2.1. Constant Power Strategy

Consider the system shown in Fig. 3.1 initially operating at steady state, and then subjected to an increase in the output power of the generator. This increase in the generator output power (P_t) causes the common transmission angle θ_{23} across the two parallel lines L1 and L2 to increase, and hence the active power transfer across both lines initially increases. However in the constant power strategy the TCSC is to be used to keep the power flow in line L1 constant at some desired set point value. The relationship in equation (4) shows that to achieve this, the TCSC's capacitive reactance has to be altered to counter any change in angle across line L1. In other words, under this control strategy, when the generator output power is increased, (and θ_{23} increases), the TCSC's reactance is then decreased accordingly so that the power transfer in line L1 remains unchanged from the desired set point value. Consequently, in this mode of control, all the increase in dispatched power from the generator is then forced to flow through line L2.

3.2.2.2. Constant Angle Strategy

Consider, once again, the situation when the generator output power in the system of Fig. 3.1 is increased, but now with the TCSC used to maintain a constant transmission angle θ_{23} across both lines. From equation (4), in order for additional power to be

transmitted, either the capacitive reactance of the TCSC has to be increased or the transmission angle θ_{23} has to be increased. Under this control strategy, where the angle across lines L1 and L2 is to be kept constant, when the generator output power increases the TCSC's capacitive reactance has to be increased accordingly. Increasing the TCSC's reactance in this manner results in the compensated line L1 transferring all the additional power dispatched. This ensures that the angle across line L1 and L2 is kept constant and that the power transfer in the uncompensated line L2 remains unchanged.

In this thesis, each of these two power flow control strategies is implemented on the SMIB study system of Fig 3.1. In each case, the impact of the particular strategy on system stability is studied for different response times of the power flow controller. The following section therefore outlines the method used to design the gains of a power flow controller so as to achieve a specified controller response time.

3.3. Design of Power Flow Control Parameters

3.3.1. Overview

Chapter Two has shown that a wide range of response times have been proposed by various researchers for power flow controllers. In order to be able to study the impact of these response times on system stability, a method has to be derived for designing a power flow controller's response time to match a user-specified value. The following subsection will now highlight the method utilised for simplifying the study system in Fig. 3.1 for the purpose of designing the appropriate response time of the power flow controller. The design method that will be discussed in the following subsection is taken from [21].

3.3.2. Design Method

Figure 3.2 below shows a simplified representation of the SMIB study system of Fig. 3.1. As in Fig 3.1, this simplified representation still consists of two nominally identical transmission lines with line L1 being compensated by a TCSC. However the rest of the original system of Fig 3.1 is now represented by two ideal sources on either end of the transmission network. The sending end voltage (V_S) is at some angle δ, while receiving end voltage V_R is taken to be the reference phasor at an angle of zero degrees.

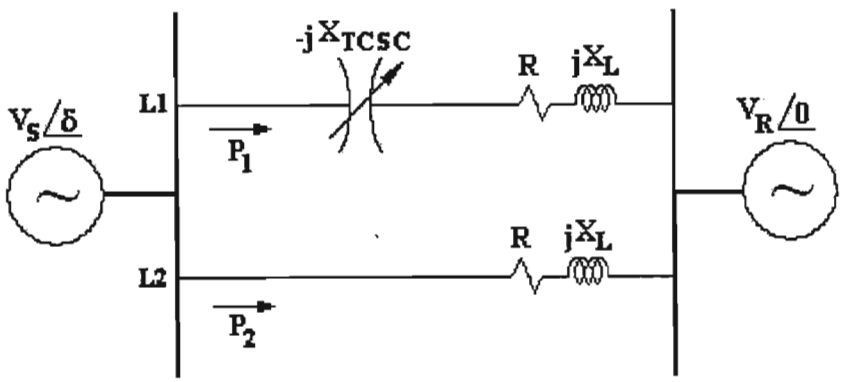

Fig. 3.2 Simplified single-line diagram of study system

As already explained using equation (4), the power flow in the compensated line is a function of the magnitudes and angles of the voltages at each end of the line and the size of the capacitive compensating reactance. However, a variable series capacitive compensator, together with suitable feedback control can be used to make the power transfer down a line track a desired value irrespective of the transmission angle or system voltages.

Fig.3.3 shows a diagrammatic representation of a simple feedback controller that can be used for this purpose. At the heart of the power flow controller diagram shown in Fig 3.3 is a block representing the plant itself (i.e. the transmission system). In the plant, the variable to be controlled is the power flow in the compensated line (P_1) and

the controller influences this variable by adjusting the size of the TCSC's compensating reactance X_{TCSC}. The relationship between the TCSC's reactance X_{TCSC} and the controlled variable P_1 has already been described in equation (4), but it is now re-written in terms of the variables defined in the simplified model used for controller design (Fig 3.2) as follows:

$$P_1 \approx \frac{|V_S||V_R|}{X_L - X_{TCSC}} \sin\delta \tag{5}$$

In a particular TCSC installation, the compensating reactance X_{TCSC} is an output of the device. The control input to a TCSC (manipulated by a high-level device such as a power flow controller) is actually the reactance order (X_{order}) of the TCSC. The reactance order of a TCSC is defined [1] as the ratio of its net reactance X_{TCSC} to the reactance of its internal capacitor X_C as follows

$$X_{order} = \frac{X_{TCSC}}{X_C} \tag{6}$$

Thus, in the feedback control scheme of Fig 3.3, the desired value of the power flow P_1^* is compared to the actual value P_1, and the error is used to drive a PI controller whose output ΔX_{order} adjusts the reactance order of the TCSC, around some set point value $X_{order\,0}$ to force P_1 to track P_1^*.

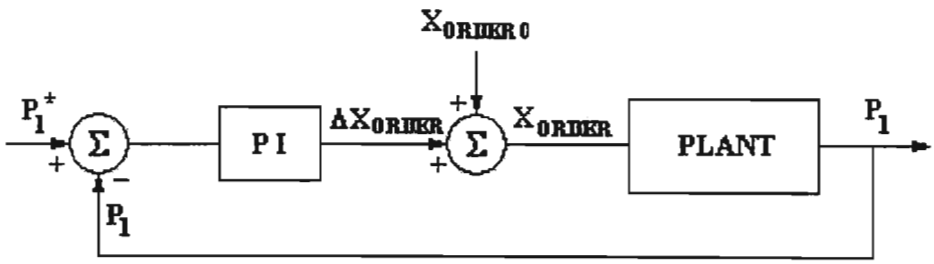

Fig. 3.3 Block diagram representation of a TCSC-based power flow controller

Reference [21] has presented a theoretical basis for selecting the proportional (K_P) and integral gains (K_I) of a power flow controller such as that shown in Fig 3.3 in order to achieve a specified response time of the controller. The following discussions now explain the design method of reference [21] which is used in this thesis for design of the power flow controller.

In order to design the closed-loop power flow controller of Fig 3.3 to achieve a specified response time, it is necessary to derive an expression for the plant, that is an equation relating the control input to the plant (X_{order}) to the controlled variable (P_1). The relationship between X_{order} and P_1 can be obtained simply by combining equations (5) and (6). However, an inspection of equation (5) shows that the resulting plant equation would be a non-linear, multi-variable relationship. Hence the approach taken to design the controller in this thesis is to linearise this plant equation at a specific operating point: this linear approximation to the true plant equation will be valid for small changes in X_{order} (and hence X_{TCSC}) around the selected operating point and will therefore be suitable for designing a small-signal power flow controller at a given operating point.

A linearised approximation to the relationship between P_1 and X_{TCSC} in equation (5) can be obtained [21] by evaluating the partial derivative of P_1 with respect to X_{TCSC} as follows:

$$\frac{\Delta P_1}{\Delta X_{TCSC}} \approx \left.\frac{\partial P_1}{\partial X_{TCSC}}\right|_{\substack{\delta=\delta_0 \\ V_i=V_{i0}}} \tag{7}$$

where $\Delta P_1 = P_1 - P_{10}$ and $\Delta X_{TCSC} = X_{TCSC} - X_{TCSC\,0}$ are small changes (deviations) in the quantities P_1 and X_{TCSC} from their steady state values (i.e. from the values P_{10} and $X_{TCSC\,0}$ at which the linearisation is carried out).

From equation (5), the partial derivative of P_1 with respect to X_{TCSC} can be derived as

$$\frac{\partial P_1}{\partial X_{XTSC}} = \frac{|V_S||V_R|}{\{|X_L| - |X_{TCSC}|\}^2} \sin\delta \tag{8}$$

Substituting equation (8) into equation (7) and rearranging yields

$$\Delta P_1 \approx \left(\frac{\partial P_1}{\partial X_{TCSC}}\bigg|_{\substack{\delta=\delta_0 \\ X_{TCSC}=X_{TCSC0}}} \right) \Delta X_{TCSC} \tag{9}$$

From equation (8) and equation (9), one can then write

$$\Delta P_1 = K_{PLANT}' \cdot \Delta X_{TCSC} \tag{10}$$

where

$$K_{PLANT}' \approx \frac{|V_S||V_R|}{\{|X_L| - |X_{TCSC0}|\}^2} \sin\delta_0 \tag{11}$$

Equations (10) and (11) are a form of the plant equations that relate changes in the TCSC's reactance to changes in P_1. However since the actual control input to the TCSC is the reactance order X_{order}, equation (10) must be re-written in terms of this control input to the TCSC, by applying the following relationship

$$\Delta X_{TCSC} = \Delta X_{order} \cdot |X_C| \tag{12}$$

where $|X_C|$ is the magnitude of the TCSC's internal capacitive reactance and $\Delta X_{order} = X_{order} - X_{order\,0}$. By defining

$$\begin{aligned} K_{PLANT} &= |X_C| \cdot K_{PLANT}' \\ &= |X_C| \frac{|V_S||V_R|}{\{|X_L| - |X_{TCSC0}|\}^2} \sin\delta_0 \end{aligned} \tag{13}$$

this yields

$$\Delta P_l = K_{PLANT} \cdot \Delta X_{order} \tag{14}$$

For given steady-state values of X_{TCSC}, V_S, V_R and δ, equations (13) and (14) describe the relationship between changes ΔX_{order} at the control input to the TCSC in line L1, and the resulting changes ΔP_l in active power transfer, and are valid for small values of ΔX_{order} and ΔP_l. These equations can then be integrated into the controller block diagram in Fig 3.3 to yield a linearised model of the closed-loop power flow control scheme as shown in Fig 3.4.

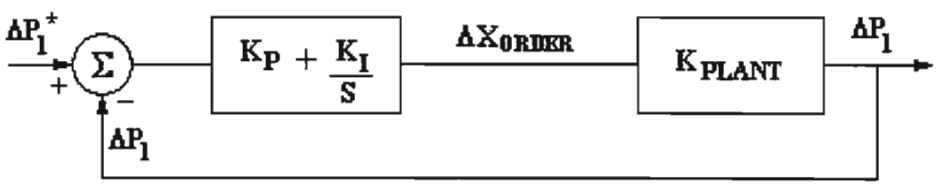

Fig. 3.4 Linearised model of the power flow controller

Using the linearised model in Fig 3.4, controller design rules can be derived in order to meet specified small signal dynamic response requirements. From Fig. 3.4, the closed loop transfer function $\Delta P_l/\Delta P_l^*(s)$ can be written in terms of the controller proportional gain (K_P), integral gain (K_I) and the plant gain (K_{PLANT}) as follows:

$$\frac{\Delta P_l}{\Delta P_l^*} = \frac{K_P K_{PLANT}}{1 + K_P K_{PLANT}} \cdot \frac{\left(s + K_I / K_P\right)}{\left(s + \dfrac{K_I K_{PLANT}}{1 + K_P K_{PLANT}}\right)} = K \frac{(s+b)}{(s+a)} \tag{15}$$

Equation (15) shows that the closed-loop system has a single pole and a single zero, the time constants of which can be set independently according to the power flow controller's performance specifications.

As explained in [21] a desired settling time of the controller can be achieved by appropriate choice of values for the time constant $\tau_P = 1/a$ of the closed loop pole and the time constant $\tau_Z = 1/b$ of the closed loop zero in the transfer function of equation (15). Since it is possible to set these time constants independently, the closed loop zero can be positioned anywhere relative to the closed loop pole in the complex plane. For example:

1. by choosing $K_P = 0$, the zero is effectively removed from the closed loop dynamics, at which point the controller reduces to a simple integral control scheme;
2. alternatively, astute positioning of the closed loop zero can be used to compensate for the physical response time of the TCSC itself, or for other delays in the system.

For the generalized case where the designer specifies the desired dynamic response in terms of particular values of τ_P and τ_Z, the required gains K_P and K_I can be determined directly from equation (15) as follows:

$$K_I = \frac{1}{K_{PLANT}(\tau_P - \tau_Z)} \tag{16}$$

$$K_P = \frac{\tau_Z}{K_{PLANT}(\tau_P - \tau_Z)} \tag{17}$$

3.3.3. Example Case: Calculation of Design Parameters

This section will now explain the process by which the two controller gains (i.e. K_P and K_I) are calculated by means of a numerical example. In order for the computations for K_P and K_I to be carried out, the correct steady state values of the variables in the simplified system model of Fig 3.2 must first be determined. These steady state values are obtained by running a detailed simulation model of the full

SMIB study system in Fig 3.1 at the desired system operating point, but without the power flow controller enabled (i.e. with the value of X_{order} at the input to the TCSC kept fixed at $X_{order} = X_{order\ 0}$). Furthermore, the steady state value of the reactance order of the TCSC ($X_{order\ 0}$) is set to a value of 2 (The typical control range of a TCSC is $1 \leq X_{order} \leq 3$; the value $X_{order\ 0} = 2$ is thus chosen so that the TCSC is in the middle of its control range at the design operating point). The steady state response of the detailed simulation model at the desired operating point is then used to calculate the steady state values of the variables in the simplified model of the system at the same operating point.

In the case of the numerical design example about to be presented, upon running the detailed simulation model at the desired steady state operating point it was found that the power flow in each line was measured to be P_{L1}= 0.462pu and P_{L2} = 0.307pu. The voltage at bus 2 in Fig 3.1 (i.e. the voltage at the coupling point of the two transmission lines in the detailed model) was measured to be 1.065pu. Note that for the purposes of design calculations, the bus voltage V_2 in the detailed simulation model is measured and not the voltage at the generator terminals: this is done to accommodate the simplified network topology (Fig 3.2) that is used for the controller design calculations (i.e. in Fig 3.2 an ideal source is assumed to be connected directly to the sending end of the parallel lines). Thus, for controller design purposes, the value of $|V_s|$ in the simplified model of Fig 3.2 was set to 1.065pu (equal to the bus 2 voltage in the detailed system model) and the value of $|V_R|$ in Fig 3.2 was set to 1.0pu (equal to the actual magnitude of the infinite bus voltage in the detailed system model).

In order to apply equation (13) to evaluate the plant gain, the correct value of the angle δ_0 between the sending end and receiving end buses in the simplified model had to be evaluated for the chosen steady state operating point. By using equation (5) and solving for δ_0, we obtain the following

$$\delta_0 = \sin^{-1}\frac{P_1(X_L - X_{TCSC0})}{|\overline{V_S}||\overline{V_R}|} = \sin^{-1}\left\{\frac{0.462(0.75-0.248)}{1.065\times 1.0}\right\}$$

$$= \sin^{-1}(0.2178)$$

$$\delta_0 = 12.57^\circ$$

where $X_L = 0.75$pu is the line's inductive reactance and $X_{TCSC\,0} = 0.248$pu is the value of the TCSC's reactance corresponding to $X_{order\,0} = 2$.

With this value of δ_0, the plant gain can be evaluated using equation (13) as follows:

$$K_{PLANT} = 0.124\frac{(1.065)(1.0)}{(0.75-0.248)^2}\sin(12.57^\circ)$$

$$= 0.1104$$

To illustrate the design procedure further, the proportional and integral gain values required to yield a specific settling time (T_S) of the power flow controller will be calculated using the formulae derived above. For a first order system, the relationship between the settling time T_S and the time constant of the system's pole τ_P is given by

$$T_S = 5\tau_P \qquad (18)$$

In this numerical design example, the desired value of the power flow controller's settling time was specified as $T_S = 5$ seconds, so that $\tau_P = 1$ second according to equation (18). A desired time constant $\tau_Z = 0.1$s was then specified for the controller zero such that it lies significantly to the left of the controller pole in the complex plane. With these values of τ_P, τ_Z and K_{PLANT}, the controller gains K_P and K_I were then determined using equations (16) and (17) as follows:

$$K_I = \frac{1}{0.1104(1-0.1)} = 10.06$$

$$K_P = \frac{0.1}{0.1104(1-0.1)} = 1.006$$

The numerical example shown above illustrates how the feedback controller of Fig 3.3 can be designed to achieve a specific settling time for power flow control in the SMIB study system of Fig 3.1 at a particular operating point. In the subsequent studies of the thesis, this same design procedure is used to obtain a range of different power flow controller response times for comparative analysis. It should be noted that the simplified transmission network model in Fig 3.2 is used only for the purpose of designing the power flow controller's gains for each comparative study. When analysing the influence of the power flow controller on the stability of a power system in subsequent chapters, the full power system model associated with the particular system under study is always used. In addition, because a simplified (and somewhat idealised) network model is used to derive power flow controller gains, before each comparative study is carried out, the intended (designed) response time of the power flow controller is first verified using the full network model, before embarking on stability comparisons.

3.4. Conclusion

This chapter has explained the concepts of power flow control using a SMIB study system as an example. The operation of the two different power flow control strategies proposed in the literature, namely the constant power and constant angle strategies, was discussed in detail. This chapter also included a theoretical derivation of the method used in the rest of the thesis for designing the power flow controller to meet a specified settling time in its dynamic response. Furthermore a numerical example case was documented, in which the power flow controller gain values were determined for a specific settling time and operating condition in the SMIB study system.

By applying the design method discussed in this chapter, the required controller gains will be calculated to yield power flow controller settling times of 5, 10 and 25 seconds. Each of these three settling times will then be considered for both modes of power flow control (constant power and constant angle control). In each case, the stability characteristics of the SMIB study system will then be examined following small-signal and transient disturbances. However, prior to considering these stability studies, the following chapter describes the detailed models of the SMIB study system, and the TCSC itself, that have been developed to conduct these studies.

CHAPTER FOUR

MATHEMATICAL MODELLING

4.1. Introduction

The previous chapter explained the concepts of power flow control for the SMIB study system being considered in this thesis. The previous chapter also considered the various parameters responsible for altering the flow of power in a specific line in the SMIB study system. The two control strategies proposed in the literature, namely the constant power and constant angle strategies, were also discussed with reference to the SMIB study system. Furthermore, Chapter Three also included a theoretical method, in conjunction with a numerical example, for designing the power flow controller to meet a specified settling time in its dynamic response.

This chapter now focuses on the mathematical models of the various system components required in order to study the influence of power flow control on power system stability. The chapter describes the development of a simulation model of the SMIB study system that is to be used to analyse the effect of closed-loop control on small and large signal stability in Chapter Five. In addition, this chapter discusses the various components of the SMIB study system and describes how they are represented in the simulation model. Furthermore a detailed description and analysis of the TCSC and power flow controller models developed for this study will be outlined in this chapter. Finally a simulation model of a two-area, four-generator study system together with its associated components will be presented; this latter system is used to study the impact of power flow control on multi-generator systems in Chapter Six.

4.2. The SMIB Study System

In order to study the effect of closed-loop control on small signal and large signal stability, a single machine infinite bus study system is initially considered. In this chapter the detailed PSCAD model of the single machine infinite bus (SMIB) study system is described. Fig 4.1 shows a single-line diagram of the SMIB study system modelled in PSCAD. The full graphical schematic of the PSCAD model itself is shown in Fig A.1 of Appendix A. Fig 4.1 shows that the SMIB study system consists of two parallel transmission lines, each of lumped impedance $R_L + jX_L$, connecting a 3-phase synchronous generator to an infinite busbar.

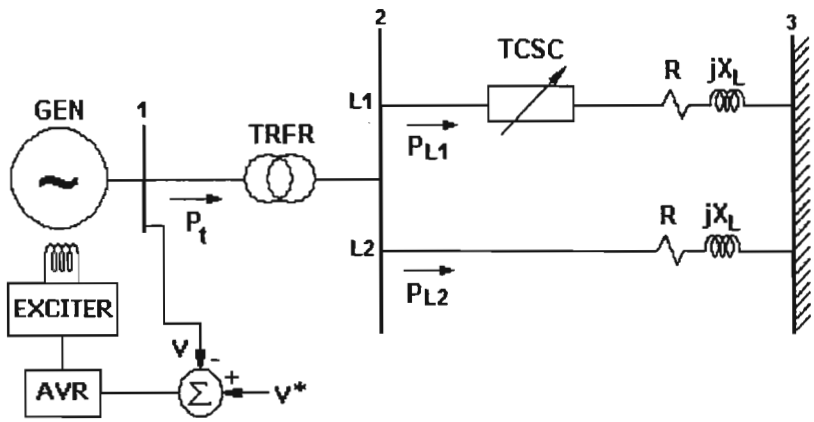

Fig.4.1. Single-line diagram of the SMIB study system

Transmission line L1 is supplemented with a thyristor controlled series capacitor, which is a device that makes it possible to alter the impedance of a transmission line by providing a variable series compensating reactance. The generator's step-up transformer is represented in the simulation model by its leakage reactance. The synchronous generator is represented by a detailed two-axis model provided in PSCAD [9] that includes stator and field circuit dynamics and the effect of damper windings.

Finally, the synchronous generator in Fig 4.1 is equipped with an automatic voltage regulator (AVR) and a static exciter. The inclusion of the generator's AVR and exciter is important when considering the stability characteristics of a study system, since the combination of the AVR and exciter is known to influence these stability characteristics [8].

4.3. Detailed TCSC Model

4.3.1. Overview

The thyristor controlled series capacitor is an actively controlled device that is capable of altering the reactance (capacitive or inductive) that it provides in series with a transmission line. In this thesis, the variable capacitive reactance facility of a TCSC is used as a means of controlling the power flow in an interconnected transmission system. The following subsections will now discuss the operating characteristics of the TCSC and will describe the detailed simulation model of a TCSC that was developed in PSCAD.

4.3.2. TCSC Characteristics

Fig 4.2 shows a single-line diagram of a TCSC, which comprises a capacitor in parallel with a thyristor-controlled reactor. This device is inserted in series with the transmission line, much like a series compensating capacitor. The net compensating reactance $-jX_{TCSC}$ that the TCSC provides to the system is the parallel combination of its fixed capacitive reactance $-jX_C$ and the variable inductive reactance, jX_{TCR} of its TCR where the latter's magnitude is a function of the thyristor firing angle α. Fig 4.2 illustrates the main circuit of the TCSC, where the main circuit parameters are defined as:

$$X_C = -\frac{1}{\omega_S C} \tag{19}$$

and,

$$X_L = \omega_S L \tag{20}$$

where ω_S is referred to as the system frequency.

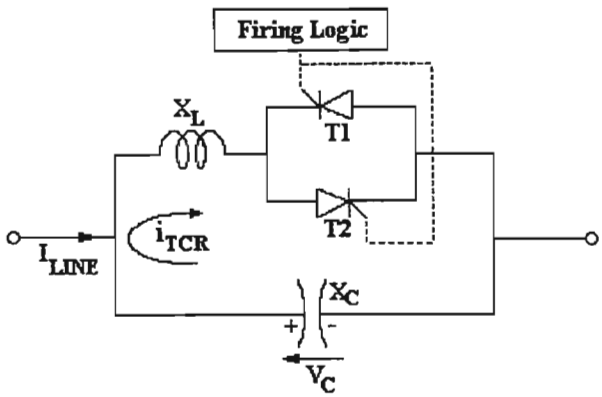

Fig 4.2: Single-line diagram of a TCSC

The resonant frequency (ω_R) of the TCSC in Fig 4.2 is the frequency at which the capacitive reactance (X_C) equals the inductive reactance (X_L) of the TCR branch. The resonant frequency is thus defined by the following equation,

$$\omega_R = \frac{1}{\sqrt{L\,C}} \tag{21}$$

Solving for the capacitance (C) and inductance (L) in equation (19) and (20) respectively, and substituting these terms in equation (21), yields a representation of the resonant frequency (ω_R) of the TCSC as a function of the system frequency (ω_S):

$$\omega_R = \omega_S \sqrt{\frac{|-X_C|}{|X_L|}} \tag{22}$$

The quotient between the resonant frequency of the TCSC (ω_R) and the system frequency (ω_S) is defined as the parameter λ, where:

$$\lambda = \frac{\omega_R}{\omega_s} = \sqrt{\frac{|-X_C|}{|X_L|}} \tag{23}$$

Generally, numerical values of λ for a TCSC lie between 2 and 4 [14], which means that at the system frequency, the reactance of a TCSC's capacitor is typically 4 to 16 times larger than that of its inductor. For the purpose of interfacing a TCSC to a high-level controller, the device's control input is not the thyristor firing angle α but rather the TCSC's reactance order X_{order}. The reactance order X_{order} of a TCSC is a dimensionless ratio (gain) that defines the extent to which the device's net compensating reactance (X_{TCSC}) is increased over the value of its fixed internal capacitive reactance (X_C). A mathematical formula can be used to calculate the reactance order of the TCSC as a function of the conduction angle (β) of its thyristors [14]:

$$X_{order} = 1 + \frac{2}{\pi}\frac{\lambda^2}{\lambda^2 - 1}\left[\frac{2\cos^2\beta}{\lambda^2 - 1}(\lambda\tan\lambda\beta - \tan\beta) - \beta - \frac{\sin 2\beta}{\beta}\right] \tag{24}$$

where λ is defined in equation (23), and β = 180 - α.

The TCSC is capable of operating in various modes, where each mode exhibits unique values of net compensating reactance. The following operating modes will now be outlined:

- Blocking Mode
- Bypass Mode
- Vernier Mode

4.3.2.1. Blocking Mode

In this mode of operation, the thyristor gates are not triggered (α=180°), so that the thyristors do not conduct current. Hence at α=180° the TCSC is regarded as operating in *blocking* mode. As a result of the line current (I_{LINE} in Fig 4.2) passing only through the capacitor, the TCSC's net reactance is effectively the reactance of the capacitor ($-jX_C$) in blocking mode. Furthermore, according to equation (24), the value of X_{order} is 1 in blocking mode.

4.3.2.2. Bypass Mode

In this mode of operation, the thyristors are gated continuously (α=90°) and conduct constantly, with the resulting net TCSC reactance being the parallel combination of $-jX_C$ and jX_L. In this mode of operation, with the thyristors gated continuously, most of the current flows through the TCR branch as a result of its reactance being 4 to 16 times smaller than that of the series capacitor. Thus only a small amount of current flows through the capacitor of the TCSC, which results in this mode being referred to as the *bypass* mode.

4.3.2.3. Vernier Mode

The vernier operation mode consists of two categories: the inductive mode and the capacitive mode. Although a TCSC can also operate as a variable inductive reactance, in this thesis, only the capacitive vernier mode of operation will be considered. In the capacitive vernier mode of operation, the TCSC's reactance can be varied from a minimum value, equal to the capacitive reactance of its internal capacitor ($-jX_C$), to approximately four times the value of $-jX_C$, as α is decreased below 180°. Thus the range of the reactance order X_{order} lies between 1 and 4, where the maximum reactance order $X_{order\ max}$ at a particular line current is determined by the design of the TCSC's main circuit parameters.

4.3.3. Impedance Characteristic

In order to illustrate further the relationship between the reactance order of the TCSC and the firing angle α, equation (24) can be modelled using software to obtain the X_{order} versus α characteristic.

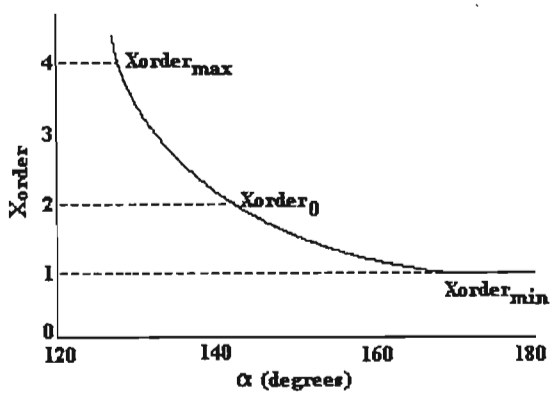

Fig 4.3 X_{order} versus α characteristic curve

Fig 4.3 shows the two important aspects related to variation of the TCSC's reactance order as a function of firing angle. Firstly, the relationship between the reactance order X_{order} and the firing angle α is highly non-linear; this non-linearity has to be catered for when designing high-level control systems around the TCSC. Secondly, in a control application the TCSC's initial (steady-state) value of reactance order (X_{order0}) is typically set to a value that lies approximately in the middle of its control range.

4.3.4. TCSC Modelling

The previous subsections have considered the principles of operation of a TCSC together with its impedance characteristics in its various operating modes. This subsection now describes the detailed simulation model of the TCSC developed in this thesis in the simulation package PSCAD. Fig 4.4 below shows a single-line diagram of a TCSC together with its internal controls as they have been modelled in

PSCAD. Fig A.2 in Appendix A shows the full schematic diagram of this TCSC and controller model developed in PSCAD.

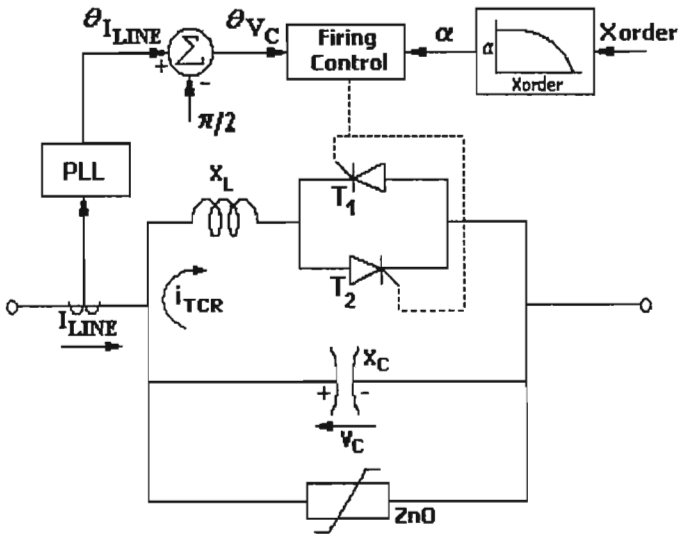

Fig 4.4: Single-line diagram of a TCSC with its internal controls

As explained previously, the control input to the TCSC that is manipulated by a high-level device is the desired value of reactance order (X_{order}). In the PSCAD model of the TCSC used in this study, a linearisation function, (in the form of a look-up table for X_{order} to thyristor firing angle (α) mappings), is used to calculate the correct value of TCSC firing angle α for the demanded X_{order} value at the input to the TCSC [21]. The PSCAD model of the TCSC developed in this thesis represents the individual power electronic switches of the device in all three phases, as well as their low-level firing controls. The firing angle α of a TCSC is defined as the angle from the zero crossings of its capacitor voltage V_C, to the start of conduction of the forward-biased thyristor. However, in practice the synchronisation of the thyristor firing controls is usually carried out indirectly by means of a phase locked loop (PLL) synchronized to the transmission line currents [14] in order to ensure stable operation of the TCSC. In other words, the PLL determines the instantaneous angle $\theta_{I_{LINE}}$ of the transmission line currents; subtracting 90° from this angle then yields the instantaneous angle θ_{V_C}

of the TCSC's capacitor voltages required for calculation of the thyristor firing instants. The PSCAD model of the TCSC includes a detailed representation of a phase locked loop which calculates the instantaneous angle θ_{V_C} of the TCSC voltages from the measured line currents; the model also includes the low-level controls used to generate thyristor firing signals in each phase by comparing θ_{V_C} to α. Finally, the PSCAD model includes a surge arrester connected across each phase of the TCSC as shown in Fig 4.4. Such surge arresters are always a feature of TCSC installations in the field [1,14]; it has been found necessary to include them in the TCSC model in transient stability studies [24] to ensure satisfactory performance of the TCSC's capacitor voltages, and hence of its PLL-based firing controls, following short-circuit faults in the transmission line.

A characteristic curve of the TCSC's reactance order versus firing angle for the PSCAD model was generated and compared to the theoretical curve in order to verify the correctness of the PSCAD model, and to develop a linearisation function for the simulated TCSC based on its actual characteristics. The reactance order versus firing angle for the theoretical curve was generated using equation (24) for a range of firing angles between 140° and 180°(capacitive vernier mode). The component values for the capacitive reactance (X_C) and the inductive reactance (X_L) are based on those of a laboratory-scale TCSC that has been designed for use in the Machines Research Laboratory [22]. The full details of the parameters are given in Appendix A. In order to measure the reactance order versus firing angle for the TCSC modelled in PSCAD, the net compensating reactance (X_{TCSC}) of the TCSC had to be determined. In practice, in a TCSC, there are harmonics, particularly within the capacitor voltage (V_C). Therefore, in order to measure the reactance of the TCSC, the fundamental frequency components of the line current (I_{LINE}) and capacitor voltage (V_C) have to be distinguished from their harmonic components. The fundamental frequency component of the line current and capacitor voltage were obtained in the simulation model by means of a Fast-Fourier Transform (FFT). Using these fundamental frequency components of the line current (I_{LINE}) and the capacitor voltage (V_C), the

net compensating reactance (X_{TCSC}) of the TCSC was determined for each value of α within the specified range. Fig 4.5 below shows the comparison of the simulated and the theoretical curve.

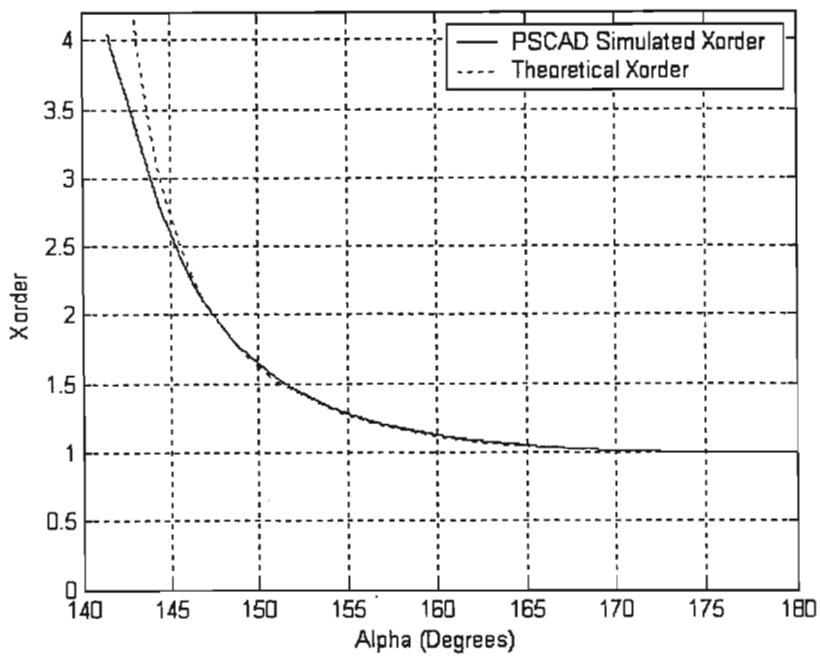

Fig 4.5 Theoretical and simulated X_{order} as a function of α

From the result shown in Fig 4.5, the general shape of the simulated TCSC's X_{order} characteristic is similar to the theoretical curve, with close agreement between the two curves occurring over most of the range of trigger angles. However, at low trigger angles (i.e. below 145°), the steepness of the simulated curve is less than that of the theoretical curve. The reasons for this deviation are twofold. Firstly, in a digital simulation model, a desired firing angle cannot ever be recreated exactly. Secondly, because of the nature of the non-linearity in the X_{order} vs. α characteristic, X_{order} values at low firing angles are more sensitive to small errors in firing angle. Hence the small percentage error in firing angle due to the discrete nature of the simulation model yields a larger percentage error in the reactance order at low values of firing angle α.

4.4. Power Flow Controller Model

Chapter Three described the concept of power flow control, with reference to two particular control strategies, namely the constant power strategy and the constant angle strategy. Chapter Three also outlined the method used to design the proportional and integral gains of a power flow controller to obtain a desired settling time for a particular operating condition. This subsection now discusses the actual structure of the control loops used in the thesis to implement power flow control in both the constant power and constant angle modes of operation. In each case a block diagram representation (detailed model in Fig A.2 of Appendix A) will be included to ensure clarity and to show how certain controller components differ functionally in each mode.

4.4.1. Structure of the Power Flow Controller

As mentioned previously in Chapter Three, the power flow controller developed in this thesis can apply either of the aforementioned two modes of control to the SMIB study system shown in Fig 4.1. The SMIB study system in Fig 4.1 consists of a line L1 compensated by a TCSC while the parallel line L2 is uncompensated. A simplified block diagram of the power flow controller is considered for the purposes of explaining each mode of control.

4.4.1.1. Constant Power Mode

In the constant power mode of control, the task of the TCSC-based power flow controller is to ensure that the active power transferred by the compensated line L1 remains constant at some set-point value (determined by an operator) despite any changes in generator output power. Fig 4.6 illustrates how the power flow controller performs its functions so as to maintain a constant power transfer in line L1.

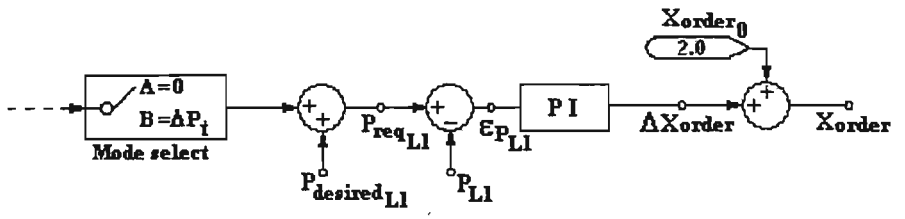

Fig 4.6: Block diagram of the power flow controller for constant power mode

At the beginning of its operation, the power flow controller is always set to constant power mode by default: that is, the "Mode select" switch in Fig 4.6 is set to position A, such that the output of this switch is zero. The required power transfer in line L1 (shown as signal $P_{req\ L1}$ in Fig 4.6) is then obtained by adding the output of this mode select switch to the set-point value of line L1's power transfer, as determined by the operator (input signal $P_{desired\ L1}$ in Fig 4.6). In other words, in constant power mode, the required power transfer in line L1 is the same as the set-point input value, i.e. $P_{reqL1} \equiv P_{desired\ L1}$. The actual (measured) value of power transfer in line L1 (P_{L1}) is then subtracted from the required value $P_{req\ L1}$ to form the error ε_{PL1} at the input to the PI controller. The PI controller then adjusts the reactance order of the TCSC via its output ΔX_{order} in order to drive the error ε_{PL1} in the power transfer in line L1 to zero. The change in reactance order (ΔX_{order}) at the output of the PI controller is added to the set-point value of the reactance order (X_{order0}) to form the overall commanded value of the reactance order X_{order} at the input to the TCSC. This overall commanded reactance order is then mapped to a corresponding firing angle by the TCSC's internal controls as explained before.

Thus, depending on the overall commanded X_{order} at the output of the power flow controller, the net reactance of the TCSC in line L1 will be altered, which will in turn result in the flow of power in the compensated line L1 (P_{L1}) being altered until the actual power in line L1 is equal in magnitude to the requested power ($P_{req\ L1}$).

4.4.1.2. Constant Angle Mode

In the constant angle mode of control, the function of the power flow controller is to ensure that the compensated line L1 absorbs any change in power dispatched from the generator in Fig 4.1. Hence in this mode, the power transfer in the uncompensated line L2 should remain constant, at its initial (set-point) value, thus keeping the angle across both transmission lines constant. The block diagram in Fig 4.7 below illustrates how the TCSC-based power flow controller performs this task.

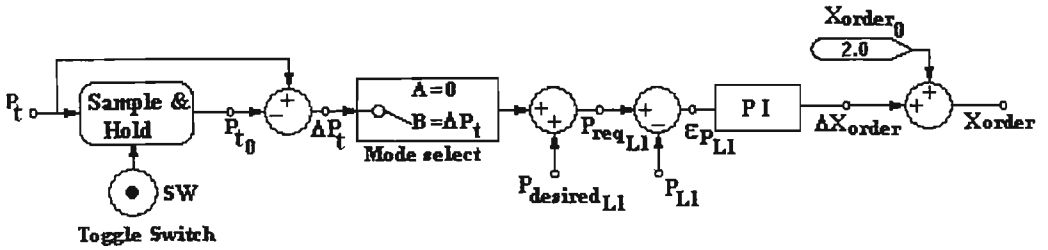

Fig 4.7: Block diagram of the power flow controller for constant angle mode

As explained previously, at the beginning of its operation the power flow controller is always set by default to the constant power mode of operation. Once started in constant power mode, the controller can be switched to constant angle mode by activating the toggle switch "SW" in Fig 4.7. When switch "SW" is activated in this way, it performs two functions:

(i) it changes the Mode select switch to position B (for constant angle mode);

(ii) it activates a sample and hold circuit which samples the active power P_t measured at the terminals of the generator and saves the particular value of P_t recorded at the onset of constant angle control to a value P_{t_0}.

Fig 4.7 shows that a signal ΔP_t is then created by subtracting the continuously-measured value of P_t from its value P_{t_0} that was sampled and held at the onset of constant angle control. In other words, the signal ΔP_t represents the change in active power dispatch from the generator (either positive or negative) from the time at which

constant angle control commenced. In constant angle mode (Mode select switch in position B) this signal ΔP_t is then added to the initial set-point value of power transfer in line L1 ($P_{desired\ L1}$) to form the new power transfer required in line L1 ($P_{req\ L1}$) at the input to the power flow controller. In this way, when the power flow controller is switched to constant angle mode, the reference input to the power flow controller (i.e. the desired value of power transfer in line L1) is now $P_{req\ L1} = P_{desired\ L1} + \Delta P_t$ such that line L1 is forced to transfer its initial power, plus any change in generator dispatch ΔP_t.

Note that the power flow control loop itself functions in the same way in constant angle mode as it does in constant power mode – that is, the actual value of power transfer in line L1 is subtracted from the reference value $P_{req\ L1}$ and used to drive a PI controller that adjusts the reactance order of the TCSC in line L1. However, in constant angle mode, as a result of the different calculation method for the reference *input* $P_{req\ L1}$ to the power flow controller, the end result of forcing P_{L1} to follow $P_{req\ L1}$ is that all additional dispatch flows in line L1 so that the power transfer in line L2 remains constant.

4.5. The Multi-Generator Study System

4.5.1. Overview of the Real-Time Digital Simulator (RTDS)

In addition to single-generator system studies, Chapter Six of this thesis considers the performance of the power flow controller in a multi-generator study system. The multi-generator system chosen for study is a two-area four-generator system that has been used extensively in other research for the analysis of inter-area mode oscillations. This section thus discusses the simulation models used to study the impact of closed-loop power flow control on this two-area system. The modelling and analysis of the multi-generator study system was conducted at the Real Time Power System Studies (RTPSS) centre at the Durban Institute of Technology. The RTPSS centre is equipped with real-time digital simulator (RTDS) hardware [10] for simulating complex power systems in real time.

In the RTDS environment, a real-time simulation model of a power system is developed using specialised software referred to as RSCAD, on a computer host. The RSCAD software comprises two important sub-programs, namely Draft and Runtime. The Draft sub-program includes pre-coded simulation models of all major power system components such as generators, transformers, transmission lines and symmetric or asymmetric faults. Once the user has constructed a desired power system model using these building blocks, this model is then compiled to produce real-time executable code that is downloaded to the RTDS simulation hardware (rack). The second sub-program (Runtime) is then used to run the simulation model and apply different disturbances and faults to the study system to evaluate its performance.

4.5.2. Four-Generator Model

For many years, researchers have studied a particular small-signal stability problem that occurs in many power systems, that being poor damping of the electromechanical oscillations between interconnected synchronous generators. Oscillations between groups of generators in different parts of a power system are referred to as inter-area mode oscillations. Generally inter-area mode oscillations and their characteristics are complex to study and require a detailed representation of the interconnected system. In order to study and analyse the factors that affect inter-area mode oscillations, researchers [25,26] have considered the use of a two-area, four-generator study system; although this system is relatively small, its system parameters and general structure are realistic.

Fig B.2 of Appendix B shows a single-line diagram of the four-generator study system as it has been used in [25,26]. The system consists of two distinct areas, (Area 1 and Area 2) which are interlinked by a weak tie line. Each area consists of two generators and step-up transformers. Each generator in this study system is represented by a detailed two-axis model, which is considered to have an automatic voltage regulator and a power system stabiliser (which can be turned on or off as required in the study). The dynamic data for the generators as well as the relevant parameters for the transformers and transmission system can be found in Appendix B. Shunt capacitors are installed at buses 7 and 9, in order to ensure a suitable voltage profile across the system. Furthermore, during normal operating conditions the system in Fig B.2 exports approximately 400MW of power from area 1 to area 2.

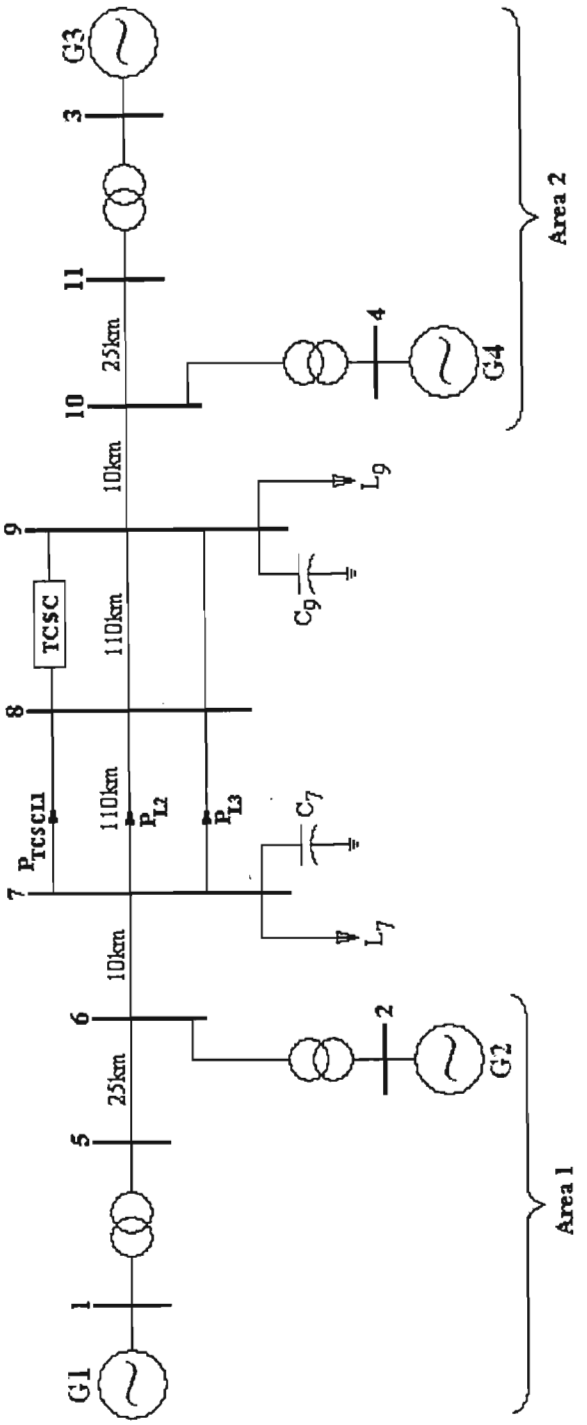

Fig 4.8: Single-line diagram of the two-area, four-generator study system with an additional transmission line and a TCSC.

The objective in Chapter Six of this thesis is to apply the TCSC-based power flow controller model to the aforementioned four-generator system, in order to ascertain if either mode of operation of the power flow controller is beneficial or detrimental to the damping of the system's inherent inter-area mode oscillations. As a result of other work done previously in the Real Time Power System Studies Centre [27], a working real-time model of the two-area study system (as it appears in [25,26]) was available for use in the work of this thesis. However for the purposes of this thesis, some additional components were added to this model of the two-area system obtained from [27] in order to study the impact of power flow control on this system. The modified version of this study system considered in Chapter Six is shown in Fig 4.8. Using the four-generator system model from [27] as a foundation, another transmission line (L1) with identical parameters to those of the two original transmission lines (L2 and L3) was added to the system as shown in Fig 4.8. Furthermore, a real-time model of a TCSC, together with its associated firing controls and a power flow controller was added to this new transmission line in the modified study system.

4.5.3. TCSC Model

4.5.3.1. Structure

The earlier parts of this chapter have outlined the development of a detailed PSCAD model of a TCSC and its firing controls. In RSCAD, a pre-coded, detailed real-time model of a TCSC is already available, so that for the studies in Chapter Six, only the TCSC's firing controls and power flow control loops had to be modelled. The structure of the TCSC firing controls and power flow control loops is similar to that developed in PSCAD as described earlier in this chapter. A schematic diagram of the RSCAD real-time models of these controls is shown in Fig B.4 of Appendix B. In the four generator study system, the line voltage of the transmission system in which the TCSC is to be connected is 230kV. Thus, parameters of a TCSC suitable for use in this system had to be found. A review of the literature uncovered a set of published

parameters for an actual TCSC that has been in service in a 230kV transmission system for some years [17] and these TCSC parameters were adopted for this study.

4.5.3.2. Impedance Characteristic

In order to verify that the real-time simulator model of the 230kV TCSC and its firing controls was functioning correctly, the reactance order versus firing angle characteristic obtained from this simulation model was compared with the theoretical characteristic governed by equation (24). In a similar manner to the verification of the PSCAD TCSC model, the real-time simulation was used to determine the reactance order of the 230kV TCSC for a range of trigger angles by carrying out a Digital Fourier Transform (DFT) to obtain the fundamental frequency components of the capacitor voltage and transmission line currents. By dividing the fundamental frequency component of the TCSC capacitor voltage by that of the transmission line current, the net compensating reactance (X_{TCSC}) of the TCSC at the fundamental frequency was obtained at each firing angle. The comparison of the theoretical and RSCAD simulated X_{order} versus α characteristic is shown in Fig 4.9 below.

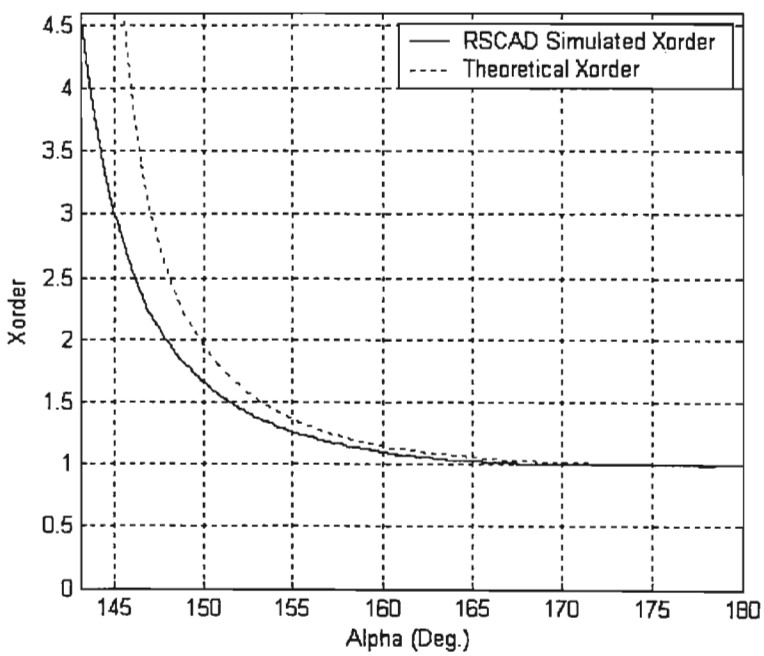

Fig 4.9: Theoretical and RSCAD simulated X_{order} as a function of α

From Fig 4.9, the general shape of the RSCAD simulated curve is similar to that of the theoretical curve, with once again, the simulated curve deviating from the theoretical curve at lower firing angles. As explained in section 4.3.4, the most plausible reason for this deviation is that, due to the non-linearity of the X_{order} versus α characteristic, X_{order} values at low firing angles are more sensitive to the small errors in firing angle caused by the discrete nature of the simulation.

4.5.4. Power Flow Controller Model

The structure of the power flow controller model that was applied to the four-generator study system in Fig 4.8 is identical to the model designed for the SMIB study system. The following two subsections discuss each mode of control, namely the constant power mode and constant angle mode, with the inclusion of a block diagram in each case illustrating the controller's actions.

4.5.4.1. Constant Power Mode

In the constant power mode of operation, the TCSC-based power flow controller ensures that the power in the compensated line L1 in Fig 4.8 remains constant irrespective of any increase or decrease in the dispatch of power from area 1 to area 2. When the constant power mode of control is activated, the power flow controller's actions are illustrated by the block diagram in Fig 4.10 below.

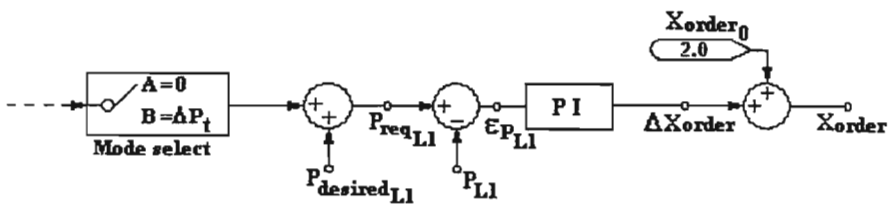

Fig 4.10: Block diagram of power flow controller in constant power mode

The functionality of the block diagram representation of the constant power mode of operation follows the explanation in section 4.4.1.1.

4.5.4.2. Constant Angle Mode

In the four-generator study system, the constant angle mode of operation of the power flow controller ensures that any increase in the dispatch of power from area 1 to area 2, is transferred by the line compensated with the TCSC. When the constant angle mode of control is activated, the power flow controller, depending on the change in power transfer from area 1 to area 2 (an increase or decrease in power dispatch), will alter the capacitive reactance of the TCSC in Line L1. This change in TCSC reactance ensures that the power transferred by the two uncompensated parallel lines (lines L2 and L3 in Fig 4.8) remains constant. This control action is depicted in Fig 4.11 below.

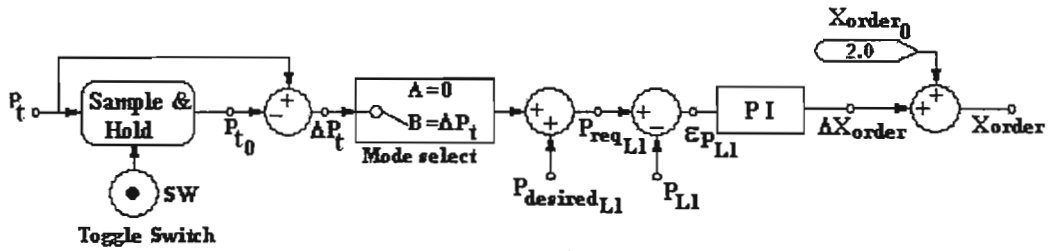

Fig 4.11: Block diagram of the power flow controller in constant angle mode

The detailed analysis of the controller block diagram for the constant angle mode of control follows the explanation in section 4.4.1.2.

4.6. Analytical Approach

The software programs PSCAD and RSCAD that are used in this thesis for stability analysis are time domain simulation tools. However, a main focus of study in this thesis is the impact of the power flow controller on the small-signal stability characteristics (damping) of the study system. In general, linearised models are recognised as the accepted tool for the analysis of small-signal stability issues, where an important linear systems analysis technique is the calculation of the eigenvalues of

the system model. Eigenvalues, when plotted in the complex plane, convey specific information about the small-signal stability characteristics of the system; in addition, they allow *quantitative* stability judgments about the system to be made at particular operating points. Nevertheless, it is still possible, using time domain simulation tools such as PSCAD and RSCAD, to make a *qualitative* analysis of the impact of the power flow controller on the small-signal stability characteristics of the study system.

4.7. Conclusion

This chapter has described the model of the single-machine infinite bus study system that was developed within PSCAD. The function of each of the pre-coded components that were used in the SMIB study system such as the synchronous generator, automatic voltage regulator and static exciter were outlined in this chapter. In addition this chapter has included a brief description of the two-area four-generator study system considered for the investigation of inter-area mode oscillations. The various modifications made to the original four-generator system were also outlined in this chapter. Furthermore, this chapter presented the model of the TCSC that was developed for the SMIB study system and for the four-generator study system. Both the low-voltage TCSC model and 230kV TCSC model, were benchmarked against the theoretical curve in order to test each model for correctness.

This chapter also included a detailed description of the power flow controller model that was implemented on both the single-machine infinite bus study system and the four-generator study system. For each mode of control and for each study system, a block diagram of the power flow controller was included to explain how the reactance of the TCSC in both the SMIB study system and the four-generator system can be manipulated, such that all additional power is either transferred by the compensated line or forced to flow through the parallel lines. Using the various simulation models developed in this chapter, the effect of closed-loop power flow control on small and large signal stability can be investigated. Secondly, by implementing the TCSC-based power flow controller on the four-generator system, the possible improvement of inter-area mode oscillations inherent to the four-generator system can be investigated.

CHAPTER FIVE

INFLUENCE OF POWER FLOW CONTROL STRATEGIES ON A SINGLE GENERATOR SYSTEM

5.1. Introduction

The previous chapter has described in detail the simulation model of the single machine infinite bus study system developed in PSCAD. In that chapter the representation of the various components in the SMIB study system, such as the synchronous generator, automatic voltage regulator and the transmission system were outlined. The previous chapter has also described and confirmed the correctness and performance of the TCSC model developed in PSCAD for the SMIB study system. In addition, Chapter Four has described the power flow controller model that was implemented on the SMIB study system for power flow scheduling.

This chapter now focuses on the effect of closed-loop power flow control on the stability characteristics of the single machine infinite bus study system. In particular this chapter presents a theoretical study into the influence of closed-loop control of ac power flow on the small-signal and transient stability characteristics of the SMIB study system. Both the constant power and constant angle strategies are examined for small and large signal disturbances to determine if either mode of control is beneficial or detrimental to the stability characteristics of the SMIB study system. Furthermore, the influence on the stability characteristics of the SMIB study system of the design of the power flow controller's settling time for each mode of control is investigated in this chapter.

5.2. Small-Signal Behaviour

5.2.1. Overview

Dynamic (small-signal) stability generally refers to the characteristics of the electromechanical oscillations that occur in a system following a small disturbance or after surviving a transient event. This section thus examines the impact of the two closed-loop power flow control strategies on the small-signal dynamic characteristics of the study system in Fig 5.1 below, which is the same study system as described in Chapter Three (Fig 3.1), the diagram being shown again here for convenience.

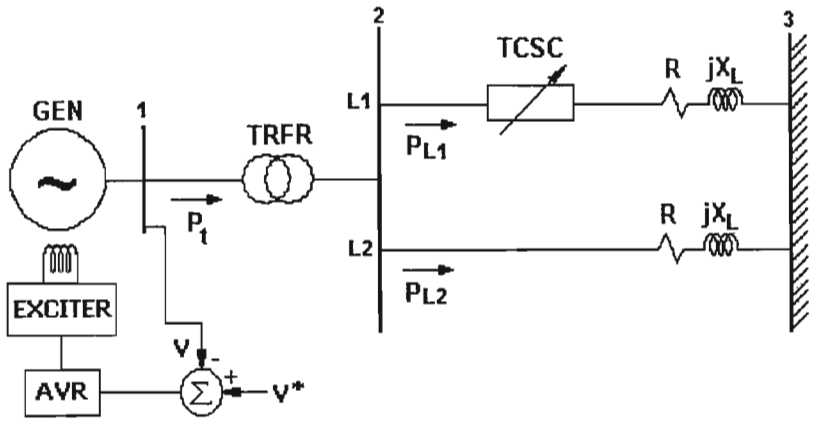

Fig 5.1: Single-line diagram of the SMIB study system

However, prior to considering the effect of closed-loop power flow control on small-signal stability, the characteristics of the two modes of power flow control need to be verified. The objectives of the following subsection are: firstly, to ensure that each mode of the power flow controller (constant power and constant angle mode) is operating correctly, and secondly, to confirm that the response rate of the power flow controller in each mode of control agrees with the response rate designed using the method described in Chapter Three. Once these two requirements were satisfied, the effect of closed-loop control on the small-signal stability characteristics of the SMIB study system was investigated.

5.2.2. Control Mode Verification

In order to test the performance of the power flow controller in each of its two modes of control, in each mode the simulation study was started from the same steady state condition in which the generator's active power output was P_t = 0.769 p.u, with this active power being initially transferred by the two lines L1 and L2 as follows: P_{L1} = 0.462 p.u and P_{L2} = 0.307 p.u. Subsequently, the mechanical input power to the generator was increased by a small amount ΔP_m = 0.04 p.u. such that the total active power P_t dispatched by the generator increased to 0.809 p.u. The response of the system to this increase in generator output power was then studied for the system with no power flow controller (i.e. with the TCSC's X_{order} held constant at a value of 2) as well as with the constant power and constant angle control modes activated with a settling time (T_S) of 10 seconds.

5.2.2.1. Control Disabled

Fig. 5.2 shows the simulated response of the study system to an increase in generator output power with the power flow controller disabled; the variables shown are the active power transfers in each line as well as the TCSC's X_{order} value.

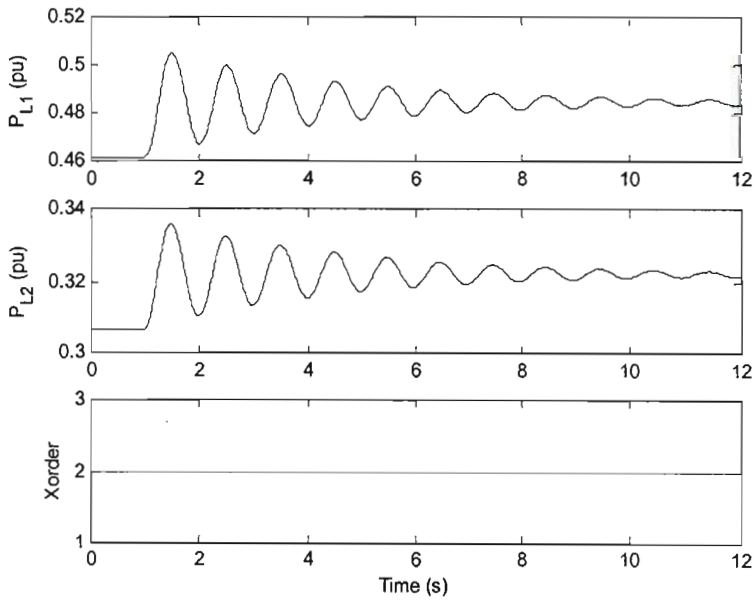

Fig 5.2: Response of the SMIB study system with the power flow controller disabled

The results in Fig 5.2 confirm that, with no power flow controller present, the additional power dispatched by the generator is shared between both of the two parallel transmission lines, with transmission line L1 transferring a larger proportion of the additional power: transmission line L1 transfers a larger share of the dispatched power since it is electrically shorter than line L2 as a result of the (in this case) fixed TCSC compensation. In this scenario (fixed TCSC compensation) any increase in generator output power (P_t) results in both transmission lines transferring a proportion of the increased power, and no form of power flow control along a contract path can be instituted.

5.2.2.2. Constant Power Mode

Fig. 5.3 now considers the study system with the power flow controller active and set to the constant power mode. The results show that, following the increase in the generator's output power, initially the power transfer in both lines L1 and L2 increases, which then results in the power flow controller reducing the degree of capacitive compensation provided by the TCSC.

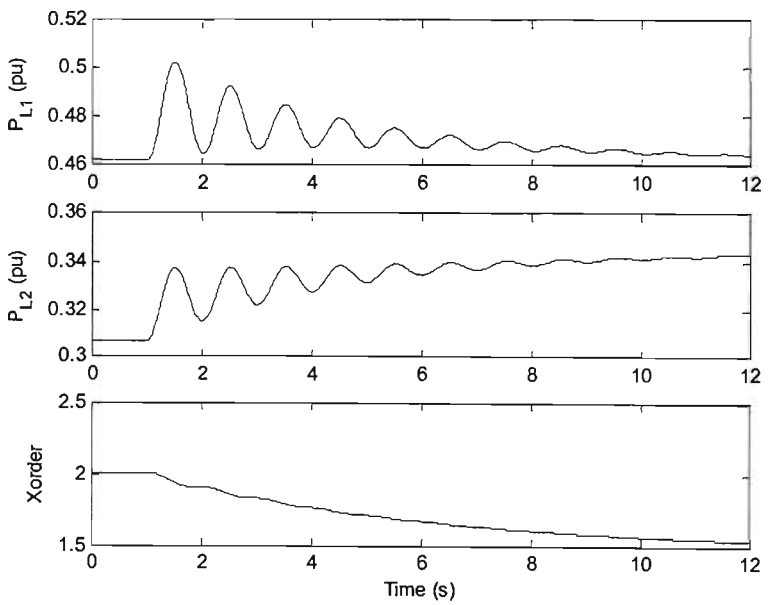

Fig 5.3: Response of the SMIB study system with the power flow controller operating in constant power mode

By reducing the capacitive reactance of the TCSC, the power transfer in transmission line L1 decreases accordingly and returns to its nominal operating point of 0.462 p.u. All of the additional power dispatched by the generator is thus forced to flow through transmission line L2, where the power transfer is increased to 0.347 p.u. This response thus satisfies the basic philosophy of the constant power strategy discussed in Chapter 3, and confirms that the constant power flow controller is correctly implemented in the PSCAD model of the SMIB study system shown in Fig.5.1.

5.2.2.3. Constant Angle Mode

Fig 5.4 shows the behaviour of the SMIB study system (Fig 5.1) following the increase in generator output power with the power flow controller now set to operate in constant angle mode. According to [3,6] the constant angle strategy should ensure that the compensated line (L1) transfers all the additional output power of the generator.

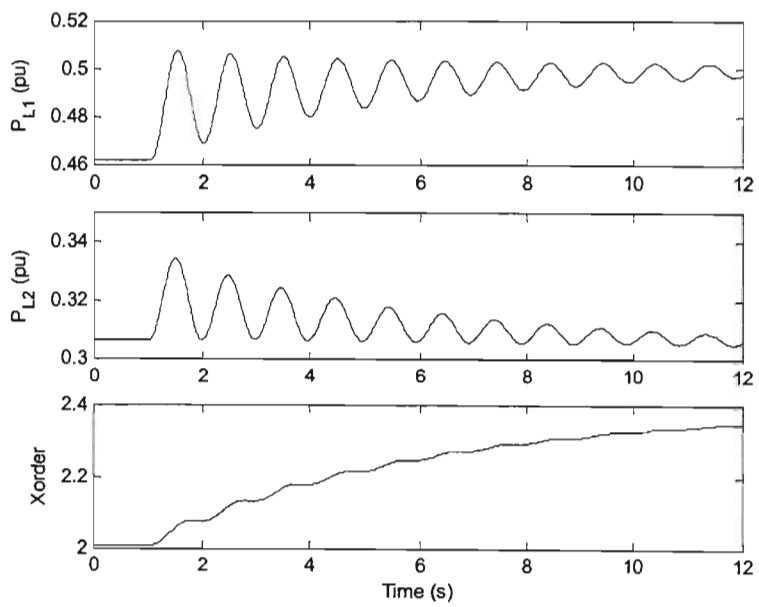

Fig 5.4: Response of the SMIB study system with the power flow controller operating in constant angle mode

Fig 5.4 shows that initially, following the increase in the output power of the generator, the active power transferred by both transmission lines (L1 and L2) increases; however, the power flow controller responds by increasing the degree of capacitive compensation provided by the TCSC such that the power transfer in transmission line L2 returns to its nominal operating point of 0.307 p.u and all the additional power dispatched by the generator is transferred by transmission line L1 (P_{L1} increases to 0.502 p.u). Fig 5.4 thus confirms that the constant angle controller is correctly implemented in the PSCAD model of the SMIB study system shown in Fig 5.1.

5.2.3. Influence of Power Flow Control on Small-Signal Stability Characteristics

The previous section has thus far confirmed the correct operation of the power flow controller in the constant power and constant angle modes of control for a settling time (T_S) of 10 seconds. This section now examines the impact that each of these power flow control modes has on the small-signal stability characteristics of the study system when the power flow controller is designed to respond at different rates. Chapter Three has described a technique for designing the dynamic response characteristics of the closed-loop power flow controller. In this subsection, the design method of Chapter Three has been used to arrive at three different settling times for the power flow controller implemented on the study system of Fig 5.1. The settling times considered are, T_S = 5s, T_S = 10s and T_S = 25s. For each of these settling times, and for both modes of power flow control, the response of the SMIB study system in Fig 5.1 was examined for a small step increase in the mechanical input power (ΔP_m = 0.04 p.u.) of the generator.

5.2.3.1. Constant Power Mode

Fig 5.5 compares the small-signal response of the study system to an increase in generator output power (P_t) for the three different settling time designs of the power flow controller in constant power mode.

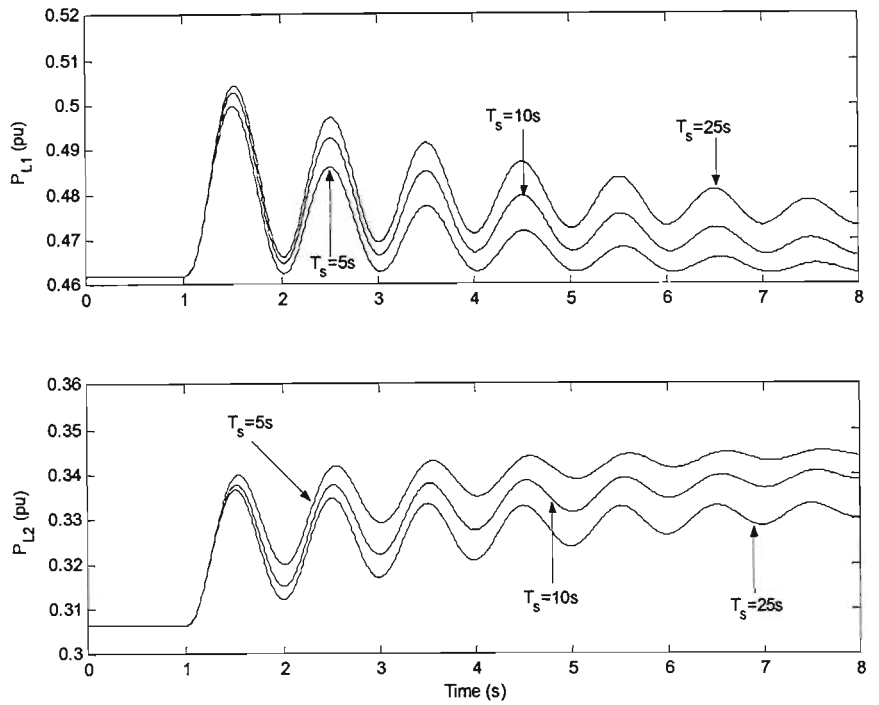

Fig 5.5: Small-signal response for different power flow controller settling times: constant power mode

In considering the responses in Fig 5.5, there are two aspects to the behaviour of the system that are affected by the design of the power flow controller. Firstly, the rate at which the power transferred by each line is returned to the correct post-disturbance steady state value is different in each case, which is the expected (and intended) consequence of adjusting the controller design. However the results show that the damping of the generator's electromechanical oscillations is also affected by the power flow controller's response time: close inspection of Fig 5.5 shows that the rate of decay of the oscillatory components of the line powers P_{L1} and P_{L2} becomes greater as the settling time of the power flow controller is made shorter. The electromechanical swing mode of the generator in this particular system has a frequency of approximately 1 Hz. As such, one would expect that the power flow controller would be more likely to influence the characteristics of this electromechanical swing mode (via the associated oscillations in the line power transfers) as the response of the power flow controller is made faster.

Conversely, one would expect the power flow controller to have less of an influence on the characteristics of the system's electromechanical oscillations when its response time is designed to be significantly longer than the period of these oscillations. However, the results in Fig 5.5 show not only that the power flow controller has a greater influence on the electromechanical oscillations of the study system as its response time is made shorter, but in addition that this influence is to *increase* the damping of these oscillations, at least in constant power mode.

5.2.3.2. Constant Angle Mode

Fig 5.6 once again compares the response of the SMIB study system to an increase in output power of the synchronous generator for the three different settling times of the power flow controller, but with the power flow controller now operating in constant angle mode.

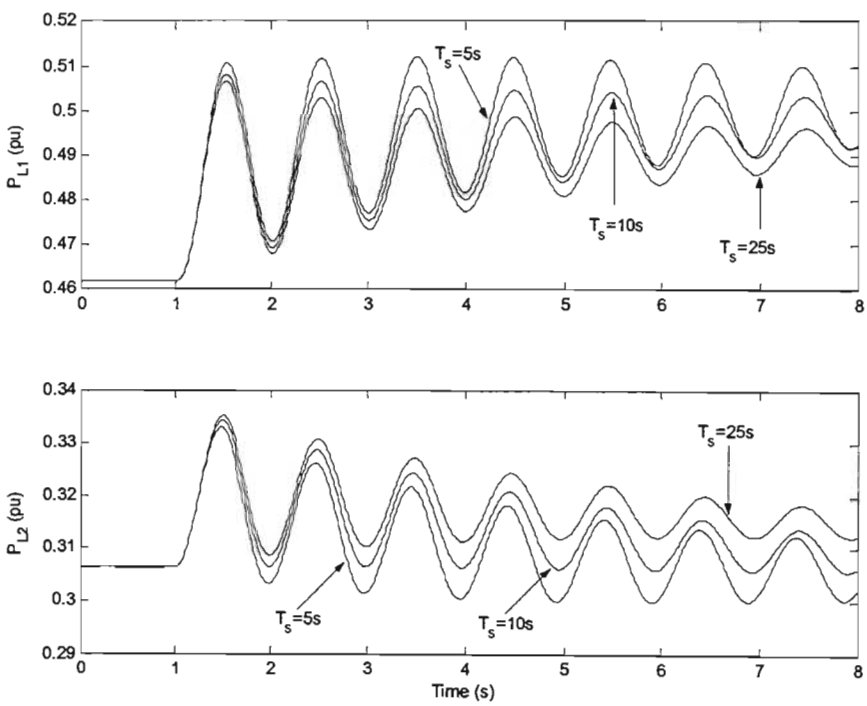

Fig 5.6: Small-signal response for different power flow controller settling times: constant angle mode

As in the case of constant power mode, the design of the controller's settling time influences not only the rate at which the power transfers in each line are returned to their correct steady state values, but also the damping of the post-disturbance oscillatory components present in these power transfers as a result of the generator's electromechanical swings. Close inspection of Fig 5.6 shows that in constant angle mode, the influence of the power flow controller is to *decrease* the damping of the system's electromechanical oscillations: the results show that as the settling time of the power flow controller is made shorter, the system's electromechanical oscillations take progressively longer to diminish following the disturbance.

5.2.4. Effect of Control Mode and Settling Time on Small-Signal Damping

The results of the small-signal investigations in this subsection have thus shown that in both modes of operation, the closed-loop power flow controller has an increasing influence on the damping of the system's electromechanical oscillations as its response time is made shorter. However the nature of this influence of the power flow controller has been shown to be dependent on its mode of operation. In the constant power mode of operation the influence is beneficial, i.e. a shorter settling time of the power flow controller tends to aid the inherent damping of the SMIB study system by increasing the rate of decay of the electromechanical oscillations. Conversely in the constant angle mode of control the influence is detrimental, i.e. a shorter settling time results in the power flow controller negating the system's inherent damping, which results in the electromechanical oscillations of the system taking longer to diminish. Although the reason for the opposite influences on system damping for the two power flow control modes cannot be categorically explained, the conclusion is clear: the operation of the power flow controller in constant angle mode is detrimental to the inherent damping of the system, particularly at short settling times of the power flow controller. As a result, careful design of a constant-angle controller would be required, in conjunction with any other damping controllers present in the system, prior to practical implementation of such a scheme.

5.3. Large Signal Behaviour

5.3.1. Overview

The previous section has considered the impact of power flow controller design and controller mode on the small signal characteristics of the SMIB study system shown in Fig 5.1. This section now examines the impact of closed-loop power flow control on the behaviour of the study system under the transient conditions that typically follow a large system disturbance such as a short circuit fault. Once again the characteristics of the SMIB study system in Fig 5.1 are investigated firstly with the power flow controller disabled (i.e. the X_{order} of the TCSC being set to a fixed value of 2), and thereafter with the controller enabled in each of the two modes of power flow control. For each mode of control, the controller parameters were designed (using the techniques outlined in Chapter Three) for a settling time (T_S) of 5 seconds. The SMIB study system shown in Fig 5.1 was then started from a steady state condition with the generator's total active power output (P_t) of 0.733 p.u. being shared between the two transmission lines (L1 and L2). Subsequently a three-phase short circuit fault was applied on transmission line L2, at a distance of 33% along the length of the transmission line. The short circuit fault was applied at this location for a duration of 700ms and thereafter removed.

5.3.2. Response of the System for Different Control Modes

5.3.2.1. Power Flow Control Disabled

Fig 5.7 shows the simulated response of the SMIB study system following the three-phase short circuit fault with the power flow controller disabled. The variables shown are the transmission angle and speed deviation of the generator as well as the TCSC's reactance order (X_{order}). The power flow controller is disabled, with the reactance order of the TCSC being set to a value of 2.

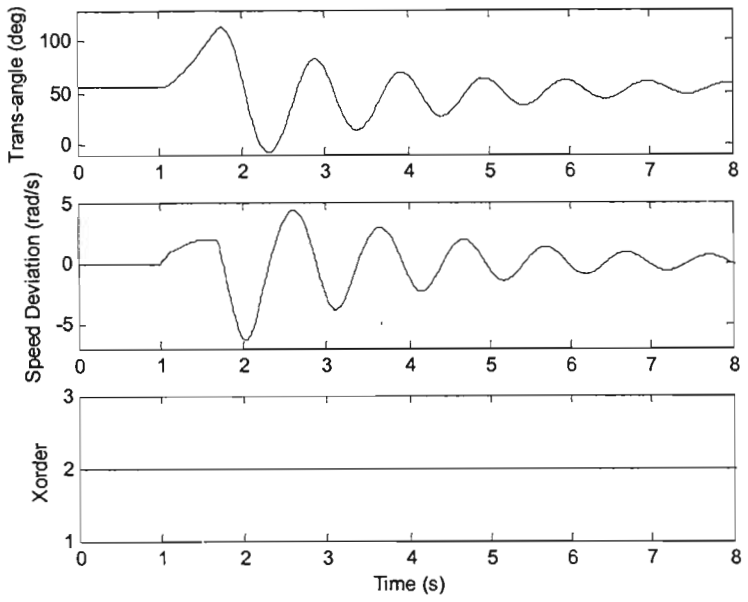

Figure 5.7: Response of SMIB study system to 3-phase short circuit fault: power flow controller disabled

From Fig 5.7, when the fault occurs, the electrical output power of the generator is reduced (since the fault is applied some distance from the generator, there is still some power transfer on the unfaulted line L1) while the mechanical input power remains constant. As a result of the imbalance between the mechanical input power and electrical output power (P_t) of the generator, during the fault, the transmission angle increases as the generator starts to accelerate. When the fault is removed the electrical output power increases abruptly, such that the electrical output power of the generator now exceeds the mechanical input power to the generator, hence causing the generator to decelerate. Fig 5.7 shows that, for this fault location and duration, the generator is transiently stable – that is, the generator rotor angle is bounded and the generator returns to synchronous speed following clearing of the fault.

5.3.2.2. Constant Power Mode

Fig 5.8 shows the response of the SMIB study system with the power flow controller now active in the constant power mode of operation. During the period that the fault is applied on transmission line L2, the total output power of the generator (P_t) decreases causing the power in the compensated line to fall below its nominal operating point (i.e. below the set-point to the constant-power mode power flow controller).

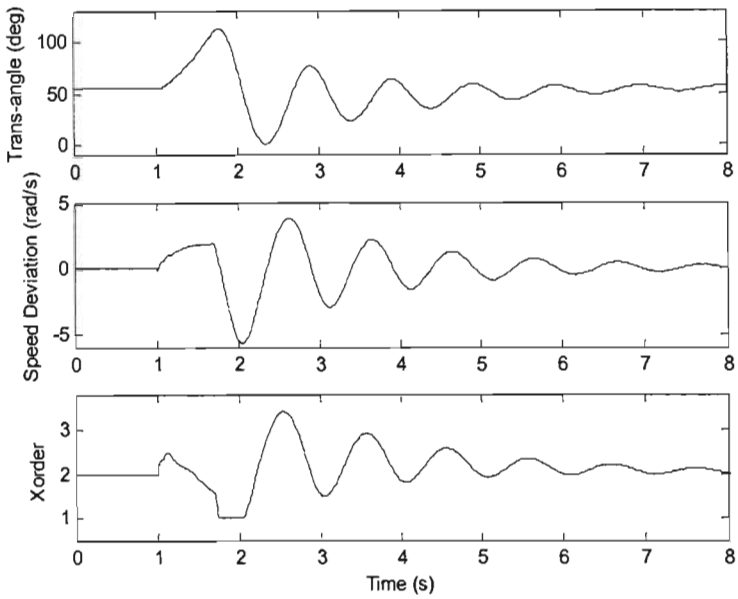

Fig 5.8: Response of the SMIB study system to a 3-phase short circuit fault: constant power mode

The results show that the response of the power flow controller in constant power mode is initially to increase the TCSC's reactance order X_{order} value in an effort to return the compensated line L1 to its nominal operating point. However once the short circuit fault is removed, the electrical output power of the generator increases, which results in the compensated line's power exceeding its nominal operating point value. This results in the power flow controller then decreasing the TCSC's reactance order accordingly in order to return the power in the compensated line (L1) to its pre-disturbance operating point value.

5.3.2.3. Constant Angle Mode

Fig 5.9 shows the response of the SMIB study system with the power flow controller now active in the constant angle mode of operation. The results show that in this mode of operation, the power flow controller responds to the short circuit fault by initially sharply decreasing the compensation in line L1 during the period that the fault is applied.

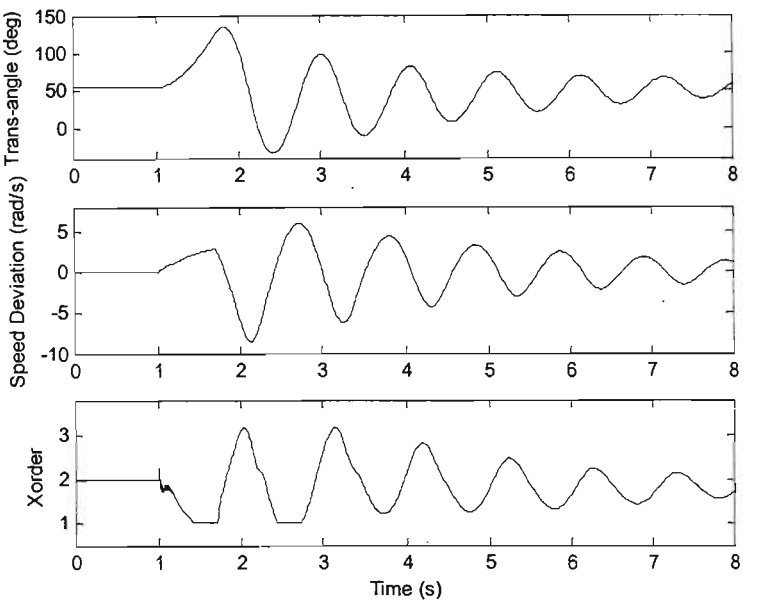

Fig 5.9: Response of the SMIB study system to a 3-phase short circuit fault: constant angle mode.

Recall that in constant angle mode of control all additional output power of the generator must be transferred by the compensated line (L1). With the short circuit fault applied to transmission line L2, the output power (P_t) of the generator temporarily decreases: this results in the power flow controller reducing the degree of compensation of transmission line L1 in an attempt to maintain a constant angle across both transmission lines. Once the fault is removed, the electrical output power of the generator increases, which results in the power flow controller increasing the amount of compensation accordingly to ensure that the compensated line (L1) absorbs all additional power dispatched by the generator.

5.3.3. Comparison of Control Modes

Comparison of Figs 5.8 and 5.9 shows that the power flow controller initially responds in the opposite manner to the same short-circuit fault in its two different modes of operation: in constant power mode the power flow controller initially responds by reducing the net impedance of the compensated line (L1), with the effect being that the total power transfer out of the generator during the fault is increased by the action of the controller; in constant angle mode, the controller initially responds by increasing the net impedance of the compensated line (L1), with the effect being that the total power transfer out of the generator during the fault is reduced by the action of the controller. It is well known that the transient (first swing) stability of a generator is enhanced by any action that results in improved transfer of active power out of the generator during, and immediately after a fault condition [21]. The results in Figs 5.8 and 5.9 therefore suggest that the mode of operation of the power flow controller will have an effect on the first swing characteristics of the generator in response to a short circuit fault.

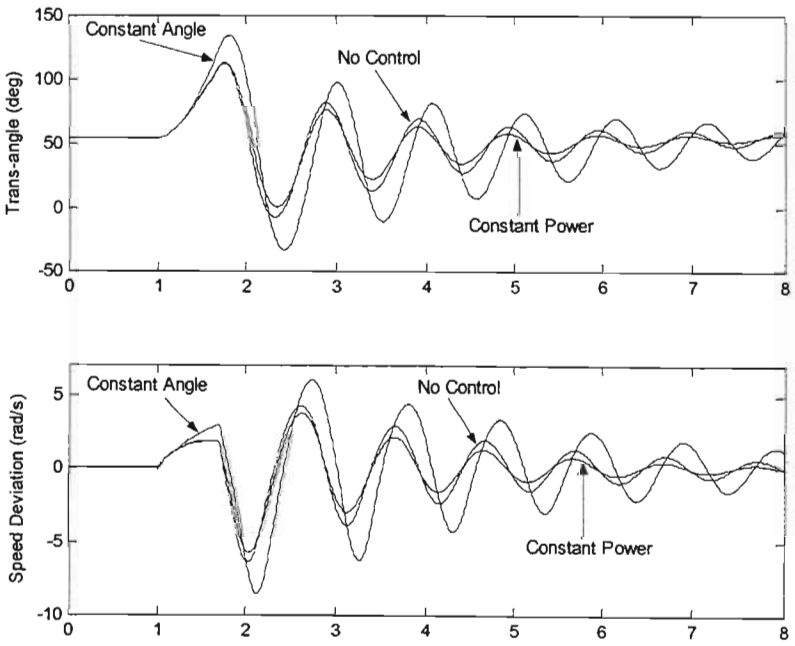

Fig 5.10: Comparison of responses to short-circuit fault: no control; constant power; constant angle

Fig 5.10 therefore compares the response of the generator's transmission angle and speed deviation to the short circuit fault for the cases where the power flow control is inactive; active in constant power mode; active in constant angle mode (i.e. the results of Figs 5.7, 5.8 and 5.9 are now plotted again on the same set of axes). The results in Fig 5.10 confirm that the power flow controller, and its mode of operation, both influence the first swing characteristics of the generator: the amplitude of the first swing of the generator angle is slightly smaller in constant power mode than for the case when there is no power flow control; by contrast, the amplitude of the first swing of the generator angle is noticeably larger when the power flow controller is in constant angle mode. The post-fault behaviour of the generator's speed deviation in Fig 5.10 is also consistent with the findings in section 5.2 – the small-signal damping is significantly improved by the power flow controller in constant power mode whereas the small-signal damping is clearly reduced by the power flow controller in constant angle mode.

5.4. Conclusion

This chapter has presented an investigation into a thyristor controlled series capacitor based closed-loop power flow controller for power flow control on a single machine infinite bus study system. The study included an investigation of the two power flow controller modes (constant power and constant angle) for both small-signal and large signal behaviour. Initially, for small-signal behaviour, the constant power and constant angle control modes were tested for correctness and to ensure that the rate at which the power flow controller responds correlated with the designed specifications. Furthermore, a series of results were presented to study the impact of closed-loop power flow control on the behaviour of the SMIB study system under transient conditions.

This chapter has demonstrated that the power flow controller's mode of operation has a noticeable influence on both the small-signal and transient stability characteristics of the SMIB study system. In particular, it has been shown that the constant angle mode of control can be detrimental to both small and large signal stability characteristics: the constant angle control acts so as to negate the system's inherent damping and increases the amplitude of the generator's first swing during a large disturbance. Conversely, the constant power mode of operation has been shown to have a beneficial impact on both small-signal and first-swing stability: the power flow controller's action adds to the inherent damping of the system and reduces the amplitude of the first-swing of the synchronous generator during transient conditions.

Furthermore, the small-signal investigations have also shown that the power flow controller has an increasing influence on the system's electromechanical oscillations for a faster responding power flow controller. This influence was shown to be dependent on the mode of operation: in constant power mode of control, as the settling time of the power flow controller was made shorter, the damping added to the

system by the power flow controller was found to be more pronounced. Conversely in constant angle mode of control, for a fast acting power flow controller (i.e. a short settling time), there was an increasing impact of the power flow controller negating the system's inherent damping.

The following chapter now makes use of these findings by considering a well-known four-generator study system and examines the influence of the two power flow controller modes on the inherent inter-area mode oscillation of that system.

CHAPTER SIX

INFLUENCE OF POWER FLOW CONTROL STRATEGIES ON A MULTI-GENERATOR SYSTEM

6.1. Introduction

The previous chapter has shown that the power flow controller's mode of operation has an important influence on both the small-signal and transient stability characteristics of the SMIB study system. In particular, it was shown in Chapter Five that for a fast acting power flow controller the constant angle mode of control can be detrimental to both small and large signal stability characteristics: the constant angle mode of control acts so as to diminish the system's inherent damping and increases the amplitude of the generator's first swing during a large disturbance. Conversely, the constant power mode of operation was shown to have a beneficial impact on both small-signal and first-swing stability characteristics: in this mode, the power flow controller's action adds to the inherent damping of the system and reduces the amplitude of the first-swing of the synchronous generator during transient conditions.

This chapter now focuses on the effect of the closed-loop power flow control strategies on the stability characteristics of the two-area, four-generator study system. This chapter initially reviews the well-known small-signal characteristics of the four-generator study system as described in [8], including the system's eigenvalues and mode shapes. The chapter then presents results to demonstrate the small-signal characteristics of the modified four-generator study system, which includes an additional transmission line and a TCSC-based power flow controller. In particular, investigations are presented to determine whether either mode of power flow control is beneficial or detrimental to the inter-area mode of oscillation of the modified study system. Finally, investigations are presented to determine whether the two modes of power flow control have any influence on the ability of power system stabilisers to damp this inter-area mode of oscillation.

6.2. Small-Signal Characteristics

Before considering the impact of the power flow controller on the modified two-area, four-generator study system, the small-signal characteristics of the original study system are reviewed in this section. The small-signal characteristics of the four-generator study system (in its original form as shown in Appendix B.3) are reproduced here from the information presented in [8]. In particular, reference [8] presents an analysis of the small-signal behaviour of the study system based on the linearised eigenvalues and mode shapes of the system. The following subsection thus presents an overview of the linearised eigenvalues and mode shapes of the original study system as found in [8], in order to obtain an understanding of the time-domain simulation results of the modified version of this study system that will be discussed in subsequent sections of the chapter.

6.2.1. Eigenvalues of the Four-Generator System

Table 6.1 below shows the eigenvalues, frequencies and damping ratios of the three main oscillatory modes of the four-generator study system as obtained from [8] for the specific case when the four-generators are fitted with high-gain thyristor exciters.

Table 6.1: Eigenvalues of the original four-generator study system shown in Appendix B.3 [8].

Parameters	Inter-area Mode	Area 1 Local Mode	Area 2 Local Mode
Eigenvalues	+0.031±j3.84	-0.490±j7.15	-0.496±j7.35
Frequency (Hz)	f = 0.61Hz	F = 1.14Hz	F = 1.17Hz
Damping Ratio	ζ = -0.008	ζ = 0.07	ζ = 0.07

Using the information in Table 6.1, the expected small-signal behaviour of the four-generator study system can be described. Table 6.1 shows that there are three main oscillatory modes in the four-generator system: there is an inter-area mode of oscillation and two local modes of oscillation (one in each area). The inter-area mode

of oscillation has a frequency of 0.61Hz and is negatively damped (ζ = -0.08). Conversely the local modes (Area 1 and Area 2) have an identical degree of positive damping (ζ = 0.07), whilst the frequencies of oscillation for the Area 1 and 2 local modes, are 1.14Hz and 1.17Hz respectively.

6.2.2. Mode Shapes of the Four-Generator System

The normalised eigenvector components (mode shapes) associated with the rotor speeds of each of the four generators in the study system are shown in Fig. 6.1 [8]. For the inter-area mode of oscillation (Fig. 6.1(i)), there are three important characteristics of the mode shape vectors that predict the behaviour of the generators in the inter-area mode of oscillation.

- From the phase of the eigenvectors shown in Fig 6.1(i), it is apparent that in the inter-area mode of oscillation, the generators in Area 1 (G1 and G2) swing in anti-phase with the generators of Area 2 (G3 and G4).
- The amplitudes of the eigenvectors of generators G3 and G4 are larger than those of generators G1 and G2 showing that in the inter-area mode, the amplitudes of the oscillations of the generators in Area 2 are larger than those of the generators in Area 1.
- From the phase of the eigenvectors it is also apparent that in the inter-area mode the generators of Area 1 (G1 and G2) swing approximately in phase with one another, as do the generators of Area 2 (G3 and G4).

Figs 6.1 (ii) and (iii) show the mode shapes of the local modes of oscillation in Areas 1 and 2 respectively. In particular, in the Area 1 local mode, generator G1 swings in anti-phase with generator G2; similarly in the Area 2 local mode generator G3 swings in anti-phase with generator G4.

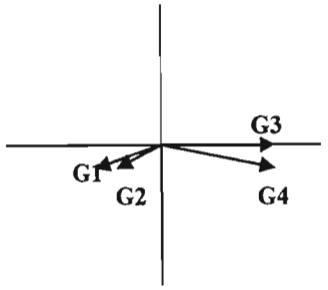

(i) Inter-area Mode

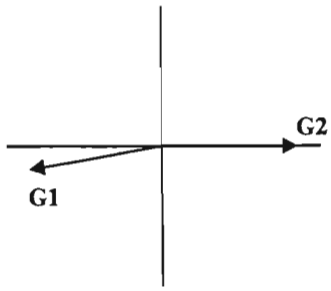

(ii) Area 1 local mode

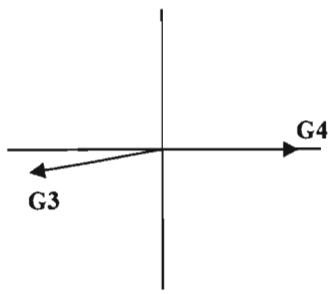

(iii) Area 2 local mode

Fig 6.1: Mode shapes of the three oscillatory modes of the four-generator study system in Fig. B.2 [8].

This section has thus far presented an overview of the small-signal characteristics of the original (unmodified) four-generator study system (Fig B.2) using eigenvalues and mode shape information obtained from [8].

The following sections present the results of simulation studies carried out using the real-time simulator model of the modified four-generator system that is shown in Fig. 4.8. In particular, the studies consider the impact on the inter-area mode oscillations of adding the TCSC-based power flow controller to the four-generator system, as well as examining the impact that the TCSC-based power flow controller has on the performance of the power system stabilisers (PSS) in the study system. However the following section is dedicated to first verifying the validity of the real-time model of the modified four-generator system.

6.3. Verifying the Validity of the Real-Time Model

The purpose of this particular section is to verify that the modified four-generator study system (shown in Fig 4.8) that has been developed in RSCAD, has similar inter-area mode characteristics to the original four-generator study system described in [8]. The detailed RSCAD model of the four-generator study system is shown in Appendix B.4 together with the parameters and initial operating conditions of the study system. The following subsection investigates the characteristics of the inter-area mode oscillations of the modified study system both with and without the power system stabilisers on the generators enabled but with the power flow controller *disabled* – that is, the reactance order of the TCSC (X_{order}) was set to a constant value of 2. Finally, additional results are presented with the power flow controller enabled in order to confirm the correctness of the power flow controller model developed in RSCAD, and to confirm that its dynamic response can be made to correspond to a design value of settling time.

6.3.1. Response with the Power System Stabilisers and Power Flow Controller Disabled

This subsection now considers the characteristics of the modified four-generator study system which includes an additional transmission line together with a TCSC-based power flow controller. The reactance order (X_{order}) of the TCSC is set to a value of 2,

which is approximately midway along the TCSC's control range. For this particular simulation study the power system stabilisers (PSS) on each of the generators were disabled. Fig 6.2 shows the response of the study system when a 5ms short circuit fault is applied at bus 7(Fig 4.8). Fig 6.2 shows the output power of all four generators together with the power transfer P_{TCSCL1} in the additional TCSC-compensated line (Fig 4.8) as well as the TCSC's constant reactance order (X_{order}). In order to obtain a clearer understanding of the characteristics of the individual generators (G1 to G4) in the various modes of oscillation, their responses are shown both immediately following the fault, as well as some time after the fault has been applied and removed.

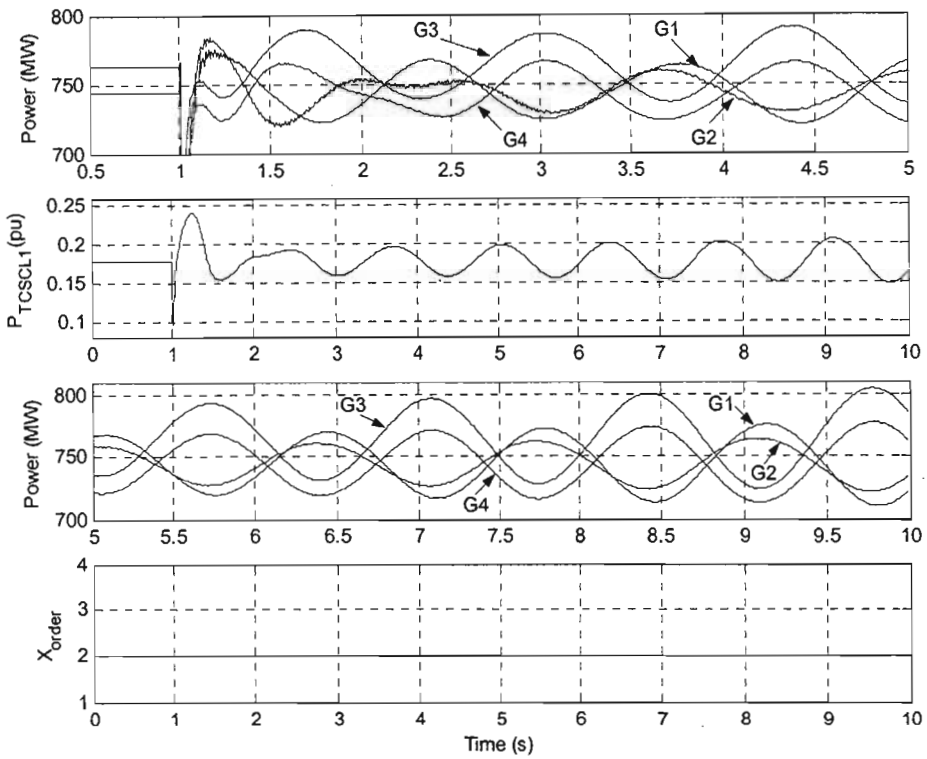

Fig 6.2: Response of the modified study system to a temporary fault with both the power system stabilisers and the power flow controller disabled.

Fig. 6.2 shows that immediately following the short circuit fault, the generators of Area 1 (G1 and G2) oscillate approximately 90° out of phase with one another: this corresponds to a combination of the Area 1 local mode of oscillation and the inter-area mode of oscillation. However Fig 6.2 shows that some time after the fault, the

generators of Area 1 oscillate almost in phase with each other, with generator 1 having a larger amplitude of oscillation than generator 2. Similarly, several seconds after the fault, the generators of Area 2 oscillate in phase with each other and in anti-phase with the generators of Area 1. Furthermore the generators of Area 2 (G3 and G4) oscillate with a larger amplitude than that of the generators in Area 1. Thus the nature of the system oscillations some time after the fault, when the well-damped local mode oscillations have died away, is consistent with the mode shape of the inter-area mode of the original study system as outlined in the previous section. Furthermore, the results in Fig. 6.2 show that these inter-area mode oscillations are slightly negatively damped. However, close inspection of Fig 6.2 shows that the frequency of the inter-area mode oscillations is 0.75Hz in the modified study system, which is greater than the value in Table 6.1 (0.61Hz) for the original study system.

This increased frequency of the inter-area mode oscillations in the modified study system is to be expected, because of the strengthening of the intertie between the two areas as a result of the inclusion of the third, TCSC-compensated line between busses 7 and 9. A strengthened transmission system (lower overall transmission system reactance) between the two areas results in higher synchronising torques in the generators in each area and hence in an increase in their natural frequency of oscillation in the inter-area mode. However, notwithstanding this change, the results in Fig 6.2 show that the modified study system still has the same essential characteristics in its inter-area mode of oscillation as does the original study system: the inter-area mode has the same mode shape and results in slightly negatively damped oscillations between the groups of generators in each area at a low frequency.

6.3.2.Response of the Study System with the Power System Stabilisers Enabled and the Power Flow Controller Disabled

This subsection now considers the behaviour of the modified four-generator study system (Fig 4.8), once again with the power flow controller disabled (i.e. the TCSC's reactance order set to a constant value of 2), but with the power system stabilisers at

each of the four generators enabled. Fig 6.3 shows the response of the modified four-generator study system under these conditions to a 5ms short circuit fault applied at bus 7. The plots in Fig 6.3 show the electrical output power of each of the generators (G1 to G4), the active power transfer (P_{TCSCL1}) by the line compensated by the TCSC and the TCSC's reactance order (X_{order}) for the duration of the simulation.

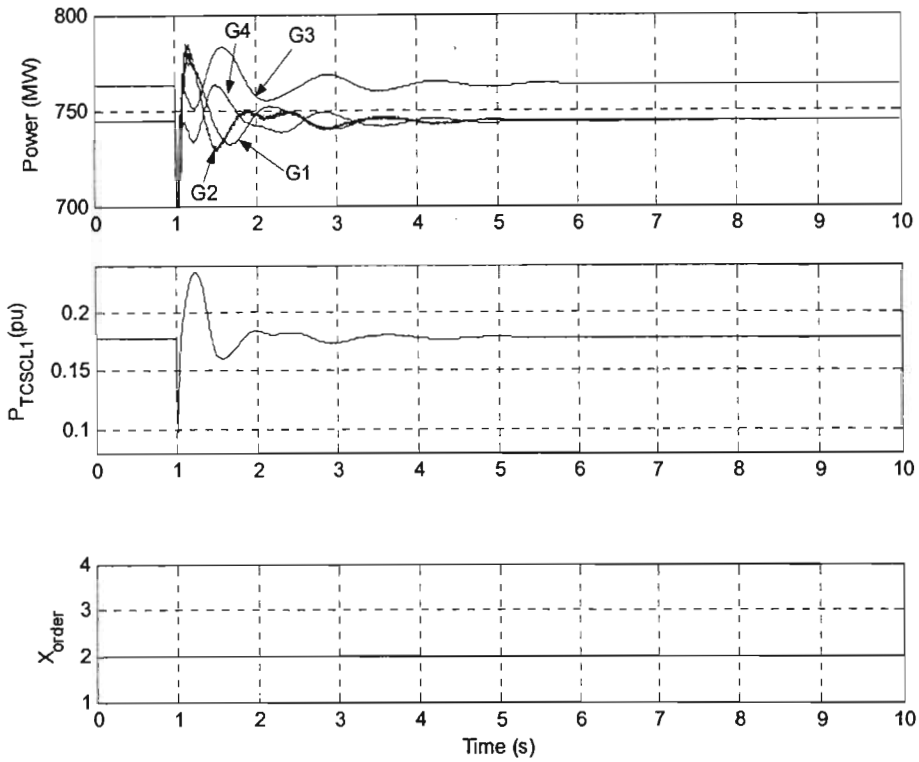

Fig 6.3: Response of the modified study system to a temporary fault with the power system stabilisers enabled and the power flow controller disabled.

Fig 6.3 shows that the responses of all the generators are now well damped; in particular, the 0.75Hz inter-area mode oscillations no longer increase in amplitude with time, but rather die out completely after a few seconds. This is the expected behaviour of the system with the power system stabilisers at each of the generators enabled, since their function is to damp out any inter-area mode oscillations [26]. The active power (P_{TCSCL1}) transferred by the line compensated by the TCSC is also

shown to be influenced by the action of the power system stabiliser, where the power oscillations are shown to be positively damped.

6.3.3. Verifying the Design of the Power Flow Controller

The objective of this subsection is to verify the correct operation of the power flow controller, for both its constant power and constant angle modes of operation, in the real-time model of the modified four-generator study system shown in Fig 4.8. In particular, the correct scheduling of the power (P_{TCSCL1}) transferred by the compensated line in each of the two modes of power flow control will be verified. In addition, the designed value of the response rate of the power flow controller will be verified by examining the rate at which the power flow controller adjusts the controlled variable (in this case the power P_{TCSCL1} transferred by the compensated line) to track the desired power flow for each of the two control modes. Such verification using the full four-generator system model is necessary because, as explained in Chapter Three, a simplified (and somewhat idealised) model of this system has initially been assumed *during the design calculations* for the power flow controller gains.

In order to perform these verifications, in each of the two modes of power flow control the real-time simulation model was started from a steady state condition in which the power transferred from Area 1 to Area 2 was shared between the three transmission lines as follows: P_{TCSCL1} = 0.178pu; P_{L2} = 0.141pu and P_{L3} = 0.141pu. The initial reactance order (X_{order}) of the TCSC was set to a value of 2. Subsequently the mechanical input power of generator G1 in Area 1 was increased by a small amount ΔP_{G1} = 0.039pu. The response of the study system was then investigated for the two modes of power flow control with a designed value of controller settling time (T_S) of 25s.

6.3.3.1. Constant Power Mode

Fig 6.4 shows the simulated response of the study system for the aforementioned small step increase in the mechanical input power to generator G1, with the power flow controller set to the constant power mode of operation; the variables shown are the active power transfers in each of the three transmission lines as well as the TCSC's reactance order (X_{order}). The results in Fig 6.4 show that following the increase in active power output from generator G1, the power transfer from Area 1 to Area 2 by all three transmission lines initially increases. The power flow controller subsequently reduces the TCSC's capacitive reactance in order to ensure that the power in the compensated line (P_{TCSCL1}) returns to its pre-disturbance operating point value, so that all the additional dispatched power from Area 1 is then forced to flow through transmission lines L2 and L3.

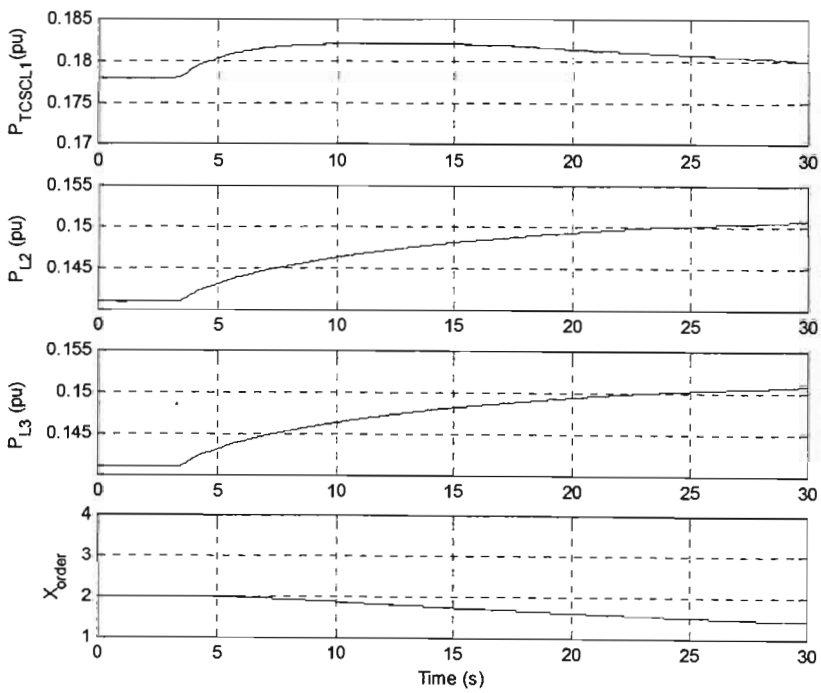

Fig 6.4: Response of the four-generator study system, with power system stabilisers enabled, to a small step increase in P_{mech} at generator G1; power flow controller operating in constant power mode.

Although the responses of the transmission line power transfers in Fig 6.4 thus confirm the correct operation of the power flow controller in constant power mode, the settling time of these responses is clearly somewhat longer than the nominal design value of 25 seconds in this case. The reason for this discrepancy can be attributed to the assumptions made in the design of the power flow controller gains in Chapter Three. Recall that in the design of the controller gains in Chapter Three, the assumption made was that the simple parallel transmission system was connected to fixed voltage sources at its sending and receiving ends. The controller gains were then calculated for a particular operating point and TCSC reactance order set point value. However in the four-generator study system, the transmission system is more complex, in that it is connected at its sending and receiving ends (buses 7 and 9) to a set of generators, resistive, capacitive and inductive loads as well as additional interconnecting transmission lines. In practice, dynamic changes in these abovementioned power system components result in some degree of variation in the voltage magnitudes at the sending and receiving end busses of the line in which the power flow controller is connected. However the result in Fig 6.4 shows that the power flow controller satisfies the basic philosophy of the constant power mode of control, even though the actual settling time of the power flow controller does not match the design value as closely as in the more simplified case of the SMIB study system of earlier chapters. Nonetheless, repeated such tests for a number of design values of controller settling time from T_S = 5s to T_S = 25s have shown that the power flow controller can still be designed to meet a specified response time with a reasonable degree of consistency over the range of desired settling times of interest.

6.3.3.2. Constant Angle Mode

Fig 6.5 shows the behaviour of the four-generator study system following the small step increase in the mechanical input power to generator G1 when the power flow controller is operating in the constant angle mode of control. Recall that in the constant angle mode of control, the transmission line compensated by the TCSC should transfer all additional output power dispatched from Area 1 to Area 2 of this study system. Fig 6.5 shows that following the increase in the active power output

from generator G1 the power transfer from Area 1 to Area 2 by all three transmission lines initially increases. The power flow controller then responds by increasing the TCSC's capacitive reactance such that the transmission lines L2 and L3 both return to their pre-disturbance values of power transfer, and all the additional output power dispatched from Area 1 is transferred by the compensated line. However, as was seen in the case of constant power mode (Fig 6.4), the settling time of the constant angle mode controller is not exactly 25 seconds as nominally intended, again as a result of the validity of the simplifying assumptions made in the controller design method used.

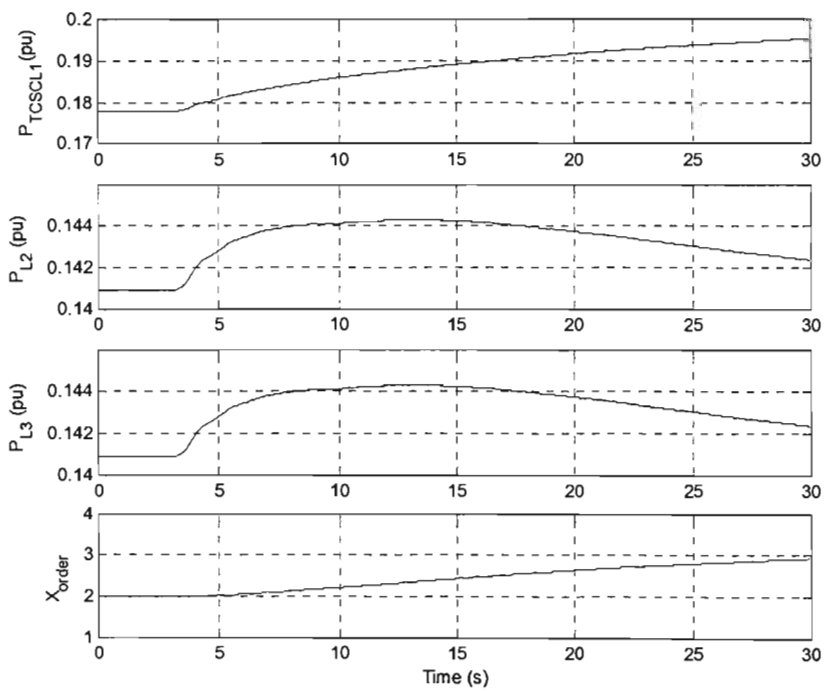

Fig 6.5: Response of the four-generator study system, with power system stabilisers enabled, to a small step increase in P_{mech} to generator G1; power flow controller operating in constant angle mode.

This section has thus far presented a review of the small-signal characteristics of the modified four-generator study system, and compared them with the known characteristics of the original four-generator system. Furthermore, this section has also verified the correct operation of the power flow controller for each of its control

modes in the modified four generator study system when its power system stabilisers are enabled. The following section now considers the impact that the power flow controller has on the four-generator study system for each of the two modes of power flow control when the power system stabilisers on the generators of the system are disabled.

6.4. Influence of the Power Flow Controller with the Power System Stabilisers Disabled

The previous section verified the correct operation of the power flow controller in the four-generator study system and has reviewed the various oscillatory modes of this study system. This section now considers the influence that the power flow controller has on the oscillatory modes of the modified four-generator study system for the case when the power system stabiliser on each of the four generators is disabled. In particular, the investigations are conducted for each of the two modes of power flow control and for three different nominal controller settling times: 5 seconds; 10 seconds and 25 seconds. To conduct these investigations, the system has been started from the same steady state operating condition in all cases, that is with the steady-state power transfers in each of the three lines connecting Area 1 to Area 2 set to the same initial values in each simulation study. Furthermore, in each case the same disturbance is used to provoke the system's oscillatory response: a 5ms short circuit fault at bus 7. The following subsections now present the time domain simulation results obtained for the constant power and constant angle modes of control.

6.4.1. Constant Power Mode

Fig 6.6 shows the behaviour of the active power outputs of each generator in the modified study system when the power system stabilisers are disabled and the power flow controller is in constant power mode for the three different nominal settling times of the controller. In considering the responses of Fig 6.6, there are two important observations that can be made regarding the inter-area mode oscillations of the system and how they are affected by the selected settling time of the power flow

controller. Firstly the behaviour of the active power outputs of each generator shows that for all three controller settling times, the inter-area mode oscillations of the system are negatively damped. Secondly, comparison of the system responses in Fig 6.6 demonstrates that the extent of this negative damping of the inter-area mode is influenced by the selection of the settling time of the power flow controller.

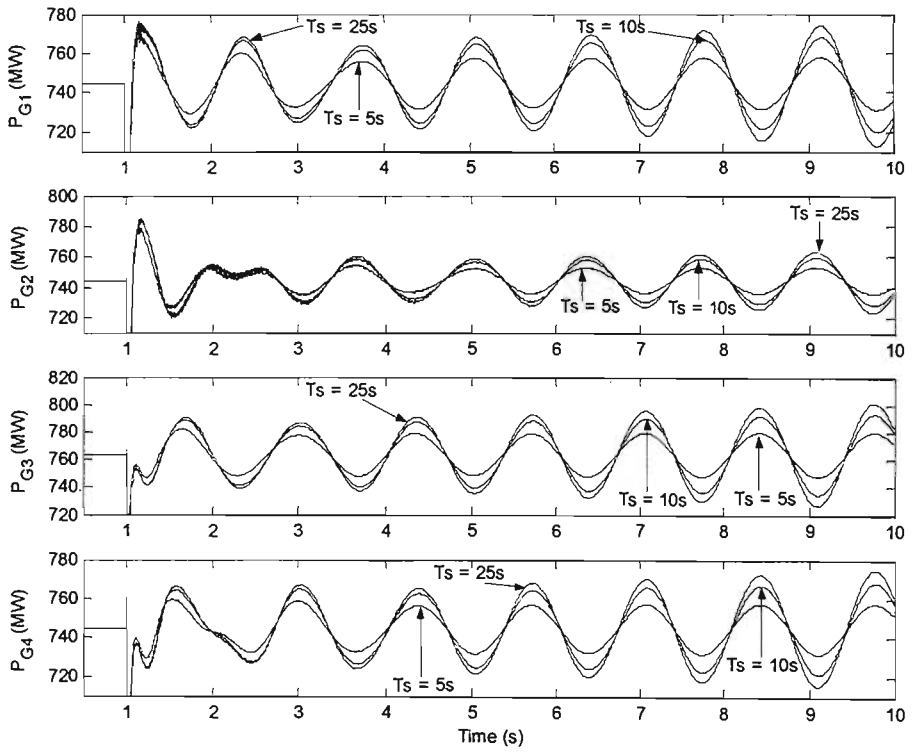

Fig 6.6: Response of the modified study system with no power system stabilisers and constant power mode power flow control for T_S = 5, 10 and 25 seconds.

In particular, as the settling time of the power flow controller is decreased, the system's inter-area mode oscillations become less negatively damped. The frequency of the inter-area mode oscillations is approximately 0.75Hz, corresponding to a period of oscillation of 1.33 seconds. Thus, superimposed on the output power of the generators is a 0.75Hz inter-area mode oscillation that gradually increases in amplitude with time, and this negatively damped oscillation is shown in Fig 6.6 to be

more pronounced for longer selected settling times. Thus a slow acting power flow controller (i.e. a power flow controller with a long settling time, in this case $T_S = 25s$) operating in constant power mode results in the inter-area mode oscillations of the system being more negatively damped, while the inter-area oscillations are less negatively damped with a fast acting power flow controller.

6.4.2. Constant Angle Mode

Fig 6.7 now compares the behaviour of the four-generator study system in response to a short circuit fault for the three selected settling times, with the power flow controller now operating in the constant angle mode of control. As in the case of the constant power mode of operation, Fig 6.7 shows that for all three settling times, the system's inter-area mode oscillations are negatively damped. In addition, the design of the power flow controller's settling time is also shown to influence the negatively damped inter-area oscillations of the study system. However, in contrast with the constant power mode of operation, for this mode of control as the settling time of the power flow controller is made shorter, the system's inter-area mode oscillations become *more* negatively damped. The results in Fig 6.7 therefore demonstrate that in the constant angle mode of control a fast acting power flow controller (i.e. a short settling time) results in the inter-area mode oscillations of the system being more negatively damped.

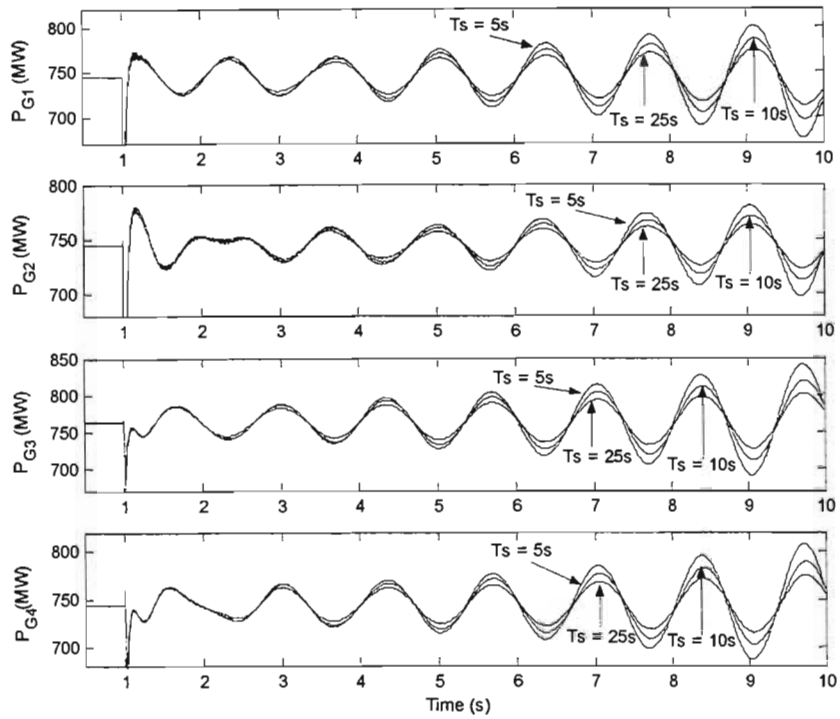

Fig 6.7: Response of the modified study system with no power system stabilisers and constant angle mode of control for T_S = 5; 10 and 25 seconds.

The results obtained in both the constant power and constant angle mode of control have demonstrated that the design of the power flow controller's settling time has a significant influence on the damping of the inter-area mode oscillation of the study system when the power system stabilisers are disabled. The nature of this influence has been shown to be mode dependent: in particular, in constant power mode of operation the influence is beneficial, i.e. as the settling time of the power flow controller is made shorter the system's inter-area mode oscillations become less negatively damped. Conversely in constant angle mode of control the influence is detrimental, in that, as the settling time of the power flow controller is made shorter the system's inter-area mode oscillations become more negatively damped. The findings of this chapter thus correlate with the results of the single generator studies presented in Chapter Five, and further emphasise that a power flow controller, depending on its mode of control, can be either beneficial or detrimental to the damping of system oscillations.

6.5. Influence of the Power Flow Controller on the Performance of the Power System Stabilisers

The results of the previous section have demonstrated that the power flow controller can have either a detrimental or beneficial impact on the damping of inter-area mode oscillations; furthermore, the influence was also shown to be dependent on the mode of operation of the power flow controller as well as the length of the settling time (T_S). This section now considers the impact that the power flow controller has on the performance of the power system stabilisers of the four-generator study system. Published literature has shown that the power system stabiliser is the accepted method for mitigation of inter-area mode oscillations [25]. Therefore it would be logical to consider what effect the power flow controller has on the performance of the power system stabilisers.

Hence, this section considers the influence that each of the two modes of power flow control (constant power and constant angle mode) have on the performance of the power system stabilisers for a single value of the controller settling time. Specifically, the investigation is carried out for a fast acting power flow controller (i.e. a power flow controller designed with a short settling time). In the previous section the shortest controller settling time (T_S = 5s) resulted in the inter-area mode oscillation of the system being least negatively damped (in comparison with the range of selected settling times) in the constant power mode of control while in the constant angle mode of control the inter-area mode oscillations of the system were most negatively damped for T_S = 5s. In other words, the shortest settling time of the controller was shown to have the most influence (either beneficial or detrimental) on the system oscillations when no power system stabilisers are employed. For this reason, only the shortest settling time (T_S = 5s) of the power flow controller has been selected for further study in this section. This section now considers the effect of a fast acting power flow controller on the power system stabilisers of the study system, as compared to the performance of the power system stabilisers when the power flow controller is disabled (i.e. X_{order} fixed to a value of 2).

In order to conduct such an investigation, the system was started from the same steady state operating condition in all cases, that is, with the steady-state power transfers in each of the transmission lines connecting Area 1 to Area 2 set to the same initial values in each simulation study. Subsequently in each case the same disturbance is used to provoke the system's oscillatory response: a 5ms short circuit fault at bus 7.

6.5.1. Constant Power Mode

Fig 6.8 shows a comparison of the response of the four-generator study system firstly with the power flow controller disabled, and then with the power flow controller operating in constant power mode of operation: in each case the power system stabilisers are enabled. The results in Fig 6.8 show the oscillations in speed of each generator for both simulation cases to be positively damped; this is an expected occurrence as a result of the action of the power system stabilisers. Comparison of the two simulation results shows that the amplitude of the initial oscillation in speed for the constant power mode of operation is slightly larger when compared with the response when the power flow controller is disabled. However, the long time scale plots in Fig 6.8 do not readily make clear what effect the constant power mode of control has on the subsequent damping of the oscillations in speed. In order to show the effect that the constant power mode of control has on the damping of the oscillations in speed of the generators, a zoomed-in version of the comparison of the speeds of generator G1 is shown in the second plot of Fig 6.8.

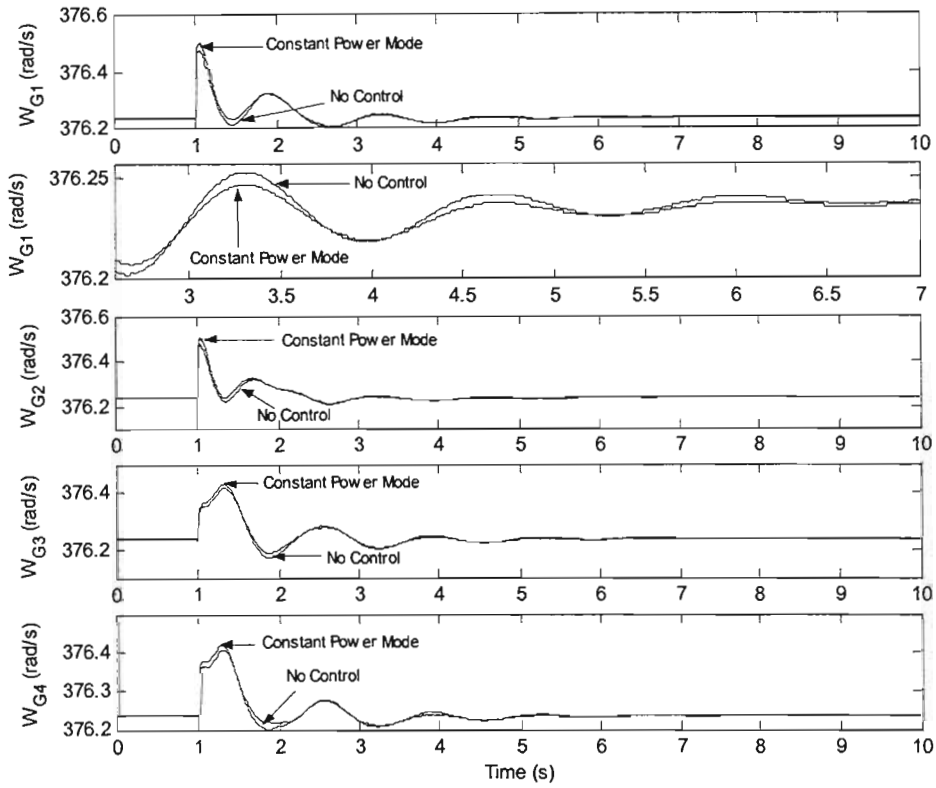

Fig 6.8: Influence of the power flow controller on the performance of the power system stabilisers: constant power mode of control.

The second plot of Fig 6.8 shows that when the power flow controller is operating in constant power mode, the oscillations in speed (w_{G1}) of generator G1 decay in amplitude at a faster rate in comparison with the response when the power flow controller is disabled. The response in Fig 6.8 thus demonstrates that the power flow controller operating in constant power mode of control, results in the inter-area mode oscillations of the study system being *more* positively damped in comparison with the oscillations when the power flow controller is disabled. Hence, the comparison in Fig 6.8 shows that the power flow controller operating in the constant power mode of control has a positive influence on the performance of the power system stabiliser: the ability of the power system stabiliser to mitigate the inter-area mode oscillations of the study system is improved.

6.5.2. Constant Angle Mode

Fig 6.9 shows a comparison of the response of the four-generator study system firstly with the power flow controller disabled (X_{order} set to a value of 2), and then with the power flow controller operating in constant angle mode of operation.

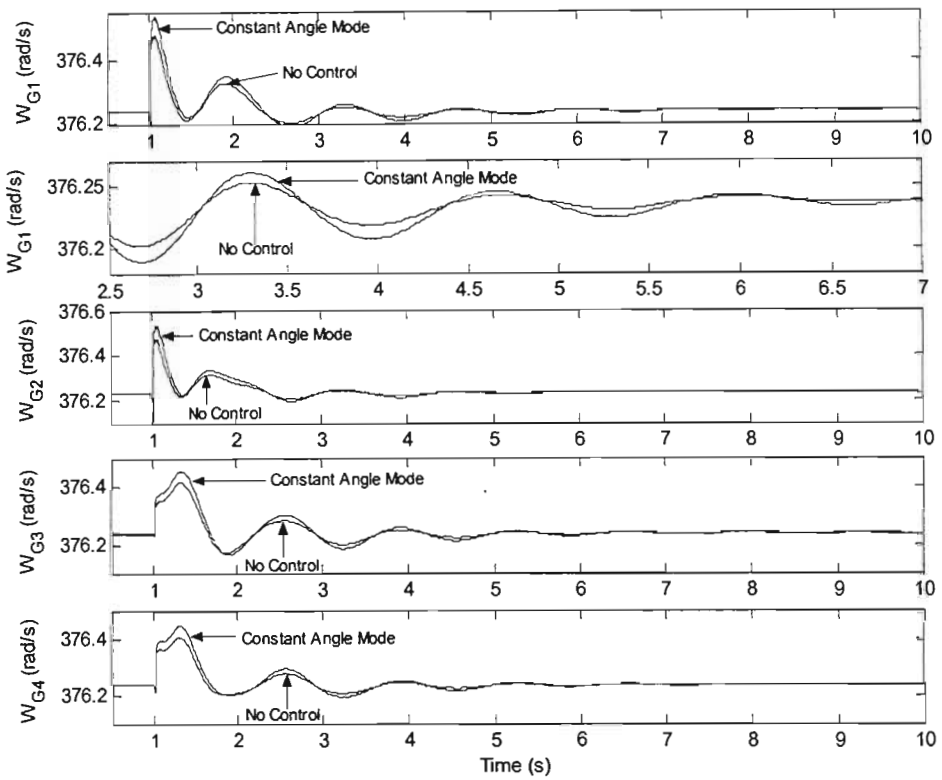

Fig 6.9: Influence of the power flow controller on the performance of the power system stabilisers: constant angle mode of control.

As was the case with the constant power mode of control (section 6.5.1), the oscillations in speed of each generator for both simulation studies in Fig 6.9 are shown to be positively damped. In addition, Fig 6.9 shows that when the power flow controller is operating in constant angle mode, the amplitude of the initial oscillation in speed of each generator is larger compared with that when the power flow controller is disabled.

However, in order to analyse the subsequent damping of the inter-area mode oscillations in more detail, a zoomed-in view of the comparison of the speeds of generator G1 is shown in the second plot of Fig 6.9. From the results shown in this second plot of Fig 6.9, the power flow controller operating in the constant angle mode of control clearly reduces the rate at which the oscillation in speed decays in amplitude, in comparison with the response when the power flow controller is disabled. In other words, the figure demonstrates that the subsequent inter-area mode of oscillation of the study system is *less* positively damped when the power flow controller operates in the constant angle mode of control compared with the response when the power flow controller is disabled. The results in Fig 6.9 therefore suggest that the action of the power flow controller operating in constant angle mode has a detrimental influence on the performance of the power system stabilisers (i.e. the inter-area mode oscillations of the study system take longer to diminish when the constant angle mode of control is enabled).

Based on the investigations conducted for the both the constant power and constant angle modes of control, the results have shown that the action of the power flow controller, depending on the mode of operation, has either a beneficial or detrimental influence on the performance of the power system stabilisers. In particular, the power flow controller operating in the constant power mode of control results in the inter-area mode oscillations of the study system being more positively damped, while in the constant angle mode of control, the inter-area mode oscillations of the system were shown to be less positively damped in comparison with response when the power flow controller is disabled. The behaviour of the generators' speed deviations in this section was found to be consistent with the results obtained throughout the earlier studies in this chapter as well as with those obtained in Chapter Five (i.e. the single generator studies), where the constant power mode of control proved to be beneficial and resulted in the small-signal damping of the study system being improved, while in the constant angle mode of control the influence was detrimental and resulted in a reduction in the small-signal damping of the study system.

6.6 Conclusion

This chapter has focussed on the implementation of a TCSC-based power flow controller in a two area four-generator study system, with the intention of investigating the impact of the power flow controller on the small-signal stability characteristics of the system. Initially, simulation results of the modified four-generator study system were presented in order to verify that the modified study system exhibits the same essential characteristics in its inter-area mode of oscillation as the original study system. In addition, this chapter also verified that the TCSC-based power flow controller operates correctly in each of its two modes of power flow control in the modified four-generator study system.

The chapter has considered the impact that the power flow controller has on the damping of the inter-area mode of oscillation of the system with the power system stabilisers disabled. The results have shown that the influence that the power flow controller has on the damping of the inter-area mode of oscillation of the system is once again control mode dependent. In particular, in the constant power mode of control, a fast acting power flow controller resulted in a beneficial influence on the damping of the inter-area mode oscillations. Conversely in the constant angle mode of control, a fast acting power flow controller resulted in a detrimental effect on the damping of the inter-area mode oscillations of the modified study system.

Finally, this chapter has demonstrated the impact that the power flow controller has on the performance of power system stabilisers (PSSs). Once again, the findings have correlated with earlier results, where the power flow controller, depending on its mode of control, has either a beneficial or detrimental impact on the performance of the power system stabilisers: the inter-area mode oscillations of the study system were shown to be *more* positively damped when the power flow controller operated in the constant power mode of control while the inter-area mode oscillations of the study system were shown to be *less* positively damped when the power flow controller operated in constant angle mode.

CHAPTER SEVEN

CONCLUSION

7.1. Introduction

This thesis has investigated the stability characteristics of a SMIB study system as well as the inter-area mode oscillations of a four-generator study system, when a thyristor controlled series capacitor was applied in each system as part of a power flow controller scheme. The results obtained from the above mentioned investigations have shown that a TCSC-based power flow controller can influence the stability characteristics of both single generator and multi-generator systems. This chapter highlights the various findings of the thesis, and thereafter suggests further work that could be carried out in this particular area of research.

7.2. Findings from the Literature Review

Chapter Two reviewed the broad subject area of controllable series compensation for closed-loop power flow control in an ac transmission system. In that chapter the concept of power flow control was outlined and explained in terms of its potential role in the performance of the power system as a whole. Three different FACTS devices that could be used for this application of closed-loop power flow control were reviewed, namely the UPFC, the SSSC and the TCSC. However, the particular focus of this thesis has been the use of the TCSC for closed-loop power flow control. A technical review of the published literature outlined the key issues regarding this particular form of closed-loop control. In particular, Chapter Two outlined two distinct control strategies that have been proposed for closed-loop power flow control, namely the constant power strategy and the constant angle strategy. In addition, Chapter Two considered the issue of the appropriate speed of response of a power flow controller and briefly described the range of response rates that have been

proposed by other researchers. The objective of this thesis was to consider the effect of both a fast and slow acting power flow controller on the stability characteristics of the study system. These investigations were to be conducted for each of the two possible modes of power flow control proposed in the literature in order to identify the effects on the dynamic and transient behaviour of the study system. Finally, a power flow controller design approach was identified from the literature review in Chapter Two, that enables a simplified system representation of a more-detailed study system to be used for controller gain design purposes.

7.3. Design of Power Flow Controllers

Chapter Three initially focussed on explaining the concepts of power flow control and then subsequently described the design and implementation of a power flow control scheme in a single-machine infinite bus (SMIB) study system. In particular, the various components that comprise the SMIB study system together with their functionality were discussed. Using the example of the SMIB study system presented in Chapter Three, the operating principles of both the constant power strategy and constant angle strategy of power flow control were described in detail.

Chapter Three also included a theoretical derivation of the method used in the thesis for designing the power flow controller to meet a specified settling time in its dynamic response. In addition a numerical example was presented in which the power flow controller gains were determined for a particular operating condition and various settling times in the SMIB study system. By utilising the design method discussed in Chapter Three, suitable controller gains were calculated for power flow controller settling times of 5, 10 and 25s for use in subsequent studies in later chapters.

7.4. Simulation Models Developed

Chapter Four described the development of detailed simulation models of the single machine infinite bus study system, and of a two-area, four-generator study system. The topology of the single machine infinite bus study system was based on a similar system considered by others, but in this study the system parameters were based on the equipment in the Machines Research Laboratory at the University of KwaZulu-Natal. The four-generator study system was based on a well-known system that has been used extensively by other researchers to study inter-area mode oscillation problems. Chapter Four presented a brief description of the original four-generator study system and subsequently outlined the various modifications made to the original study system for the evaluation of inter-area mode oscillations in the presence of a power flow controller. Chapter Four also described the detailed simulation models of the TCSC that were developed for each study system.

Finally Chapter Four provided a detailed description of the simulation model of the power flow controller itself that was developed for both the SMIB study system and the four-generator study system. A block diagram of the power flow controller was shown for each study system, and for each mode of control, in order to demonstrate how manipulation of the reactance of the TCSC is used to force the additional dispatched power in the system to be transferred by specific transmission lines in each case. The simulation models developed in Chapter Four were used in the subsequent investigations carried out on both the SMIB study system and four-generator study system in the remainder of the thesis.

7.5. Findings of the Thesis

7.5.1. Influence of Power Flow Controller on a Single-Machine Infinite Bus Study System

The literature review in Chapter Two identified two distinct strategies that have been proposed for controlling the flow of power in an interconnected transmission network using a particular FACTS device; each of these control strategies was implemented on the SMIB study system in order to then analyse the stability characteristics of the system. However, before analysing the effect that each mode of power flow control has on the small and large signal stability characteristics of the study system, the basic operating characteristics of the two modes of control were verified. The two objectives of this initial verification exercise were, firstly, to ensure that each mode of the power flow controller operated correctly (i.e. the power transfer in each transmission line was scheduled accordingly depending on the mode of control) and secondly, to confirm that the response rate of the power flow controller correlated with the designed response time. The findings from this exercise confirmed that both objectives were attained for a particular settling time.

Subsequently Chapter Five then examined the impact that each of the two modes of power flow control has on the small-signal stability characteristics of the SMIB study system when the power flow controller is designed to operate for different settling times. Using the design method described in Chapter Three the controller gains were computed for the three settling times of 5, 10 and 25 seconds – for each of these settling times, and for both modes of power flow control, the response of the study system was examined. The results from the small-signal investigation yielded the following findings:

(a) In both modes of power flow control (constant power and constant angle) the closed-loop power flow controller has a progressively larger influence on the damping of the system's electromechanical oscillations as the settling time of the controller is made shorter.

(b) However, the nature of the influence of the power flow controller on small-signal damping was shown to be control mode dependent, that is

(i) in constant power mode of control the influence was shown to be beneficial – as the settling time of the power flow controller is made shorter, the rate of decay of the system's electromechanical oscillations becomes more pronounced;

(ii) in constant angle mode, the influence was shown to be detrimental – as the settling time of the power flow controller is made shorter, the rate of decay of the system's electromechanical oscillations becomes less pronounced.

Although the reasons for this opposite influence of each mode of control on small-signal damping were not examined in detail, a clear conclusion was drawn: the constant angle mode of control with a short settling time is detrimental to the system's inherent damping, and as such a supplementary damping controller would be required in conjunction with the power flow controller, in a practical implementation of such a scheme.

The investigations in Chapter Five then considered the effect of the two closed-loop power flow control strategies on the large signal stability characteristics of the SMIB study system. As in the case of the small-signal investigation, the study system was initially analysed for the case when the power flow controller was disabled and then subsequently with the power flow controller enabled for each mode of control. These investigations were conducted to evaluate the transient stability characteristics of the SMIB study system for each mode of control. Comparison of the constant power and constant angle mode results showed that the power flow controller in each mode of control responds in the opposite manner to a short circuit fault: in constant power mode of control the power flow controller responds to a short circuit fault by initially increasing the degree of compensation provided by the TCSC, thereby increasing the

amount of power transferred out of the generator; in constant angle mode of control the power flow controller responds to a short circuit fault by initially decreasing the degree of compensation provided by the TCSC, thereby reducing the amount of power dispatched by the generator. Comparison of the rotor angle response of the generator following a short circuit fault for each mode of control led to the following findings: the power flow controller influences the first swing stability characteristics of the generator in both modes of control. In particular,

(a) the amplitude of the generator's first swing is reduced when the power flow controller is operated in constant power mode as compared to the response when the power flow controller is disabled;

(b) by contrast, the amplitude of the generator's first swing is increased when the power flow controller is operated in constant angle mode as compared to the response when the power flow controller is disabled.

These findings from the transient stability studies correlated with those of the small-signal investigations, where the power flow controller operating in constant power mode of control was shown to be beneficial to small-signal stability, whereas when operating in constant angle mode of control it was found to be detrimental to system stability.

7.5.2. Influence of Power Flow Controller on a Four-Generator Study System

Chapter Six of the thesis considered the implementation of a TCSC-based power flow controller in a well-known, two-area, four-generator study system in order to examine the influence of the power flow control strategies and their response times on the inter-area mode oscillations of the study system. Initially Chapter Six reviewed the small-signal characteristics of the original four-generator study system as presented in [8], which included the system's eigenvalues and mode shapes. Simulation results were then presented using a detailed real-time simulator model of the modified four-

generator study system to ensure that this modified study system still exhibited the same essential inter-area mode characteristics as the original study system.

In addition, Chapter Six verified the operation of the power flow controller for both the constant power and constant angle modes of control. Once again, the two aspects that were verified were firstly, the correct scheduling of the power transfers along the parallel transmission lines in both the constant power and constant angle modes, and secondly, the rate at which the power flow controller adjusted the controlled variable to track the desired power flow for each of the two control modes.

Chapter Six then considered the influence of the power flow controller on the inter-area mode oscillations of study system for the case when the power system stabilisers in the study system were disabled. In particular, the investigations were conducted for each of the two modes of power flow control and for three different controller settling times. Analysis of the results showed that with the power system stabilisers disabled, the power flow controller influences the damping of the inter-area mode oscillations of the study system. The nature of this influence was again shown to be mode dependent. In constant power mode the influence is beneficial: as the settling time of the power flow controller is made shorter, the inter-area mode oscillations of the study system become less negatively damped. Conversely in constant angle mode of control, the influence is detrimental: as the settling time of the power flow is made shorter the system's inter-area mode oscillations became more negatively damped.

Finally Chapter Six examined the effect of the power flow controller on the performance of the power system stabilisers in the study system for each of the two modes of power flow control. The results from the simulations demonstrated that the impact of the power system stabilisers is influenced by the action of the power flow controller. In particular the power flow controller operating in the constant power mode of control results in the inter-area mode oscillations of the study system being more positively damped than is the case when the stabilisers operate when no power flow control is employed. The power flow controller operating in the constant angle

mode of control results in the inter-area mode oscillations of the system being less positively damped in comparison with the response when stabilisers operate with the power flow controller disabled. The findings obtained from the study conducted in Chapter Six thus demonstrated that the power flow controller operating in the constant power mode of control, in conjunction with the power system stabilisers, could be used as an effective tool to successfully alleviate inter-area mode oscillations in a multi-generator system.

7.6. Further Work

This thesis set out to investigate the application of a TCSC for closed-loop power flow control in an ac transmission system. However, it was not possible to cover every aspect of the research problem. Nonetheless, the results obtained from the thesis have identified certain issues that require a more thorough treatment. Thus the particular areas that could not be addressed in this thesis and require further research work are highlighted below.

a) The small-signal analysis could be extended by developing linearised models of the study systems to allow for quantitative analysis of the trends established in the thesis.

b) In the stability studies for the single machine infinite bus study system, the torsional dynamics of the turbine shaft of the synchronous machine were not considered as part of the simulation model. Thus in order to simulate the characteristics of the synchronous machine more accurately, a more detailed multi-mass model of the synchronous machine's mechanical shaft should be considered; this will allow any impact of power flow control strategies on shaft torsional phenomena to be studied.

c) Part of the thesis focussed on the transient stability characteristics of the SMIB study system, in particular when a three-phase, short-circuit fault was applied

on the *uncompensated* line. This study could be extended by considering the impact of a three-phase, short-circuit fault applied on the *compensated* line itself for each mode of power flow control.

d) The results presented on the SMIB study system for both the small-signal and large signal stability characteristics showed that the constant angle mode of control is detrimental to both the transient and dynamic stability of the study system. As such, this study could be extended by considering the inclusion of a damping controller and transient stability controller in conjunction with the power flow controller, in order to improve the transient and small-signal stability characteristics of the SMIB study system in the constant angle mode of operation.

e) Finally, practical implementation of the power flow controllers developed in the thesis could be considered using the laboratory-scale TCSC that has been developed by other researchers in the Machines Research Laboratory.

APPENDIX A

PARAMETERS OF THE SINGLE MACHINE INFINITE BUS (SMIB) STUDY SYSTEM

This Appendix lists the parameters used in the SMIB study system in Chapter Five. This appendix also includes the PSCAD representation of the SMIB study system together with the TCSC internal controls and power flow controller models.

A.1. Parameters of the study system

A.1.1 Generators

R_a = 0.005 p.u
X_d = 0.920 p.u
X_d' = 0.3 p.u
X_d" = 0.22 p.u
X_q = 0.51 p.u
X_q' = 0.228 p.u
X_q" = 0.290 p.u
T_{d0}' = 5.2 s
T_{d0}" = 0.029 s
T_{q0}' = 0.85 s
T_{q0}" = 0.034 s
H = 5.68144 s

Base Voltage = 0.22 $kV_{(l\text{-}lrms)}$
Base Current = 0.007873 $kA_{(rms)}$
Base Power = 3 kVA

A.1.2 Transmission Line System

Line L1 & L2 : R_L = 0.033 p.u.

X_L = 0.75 p.u

Base Power = 3kVA

Base Voltage = 0.22kV

A.1.3 Transformer

R_{TRFR} = 0 p.u

X_{TRFR} = 0.13 p.u

Base Power = 3kVA

Base Voltage = 0.22kV

A.1.4 Thyristor-Controlled Series Capacitor

X_C = 0.124 p.u

X_L = 0.025 p.u

Base Power = 3kVA

Base Voltage = 0.22kV

A.2. PSCAD Representation of the SMIB study system

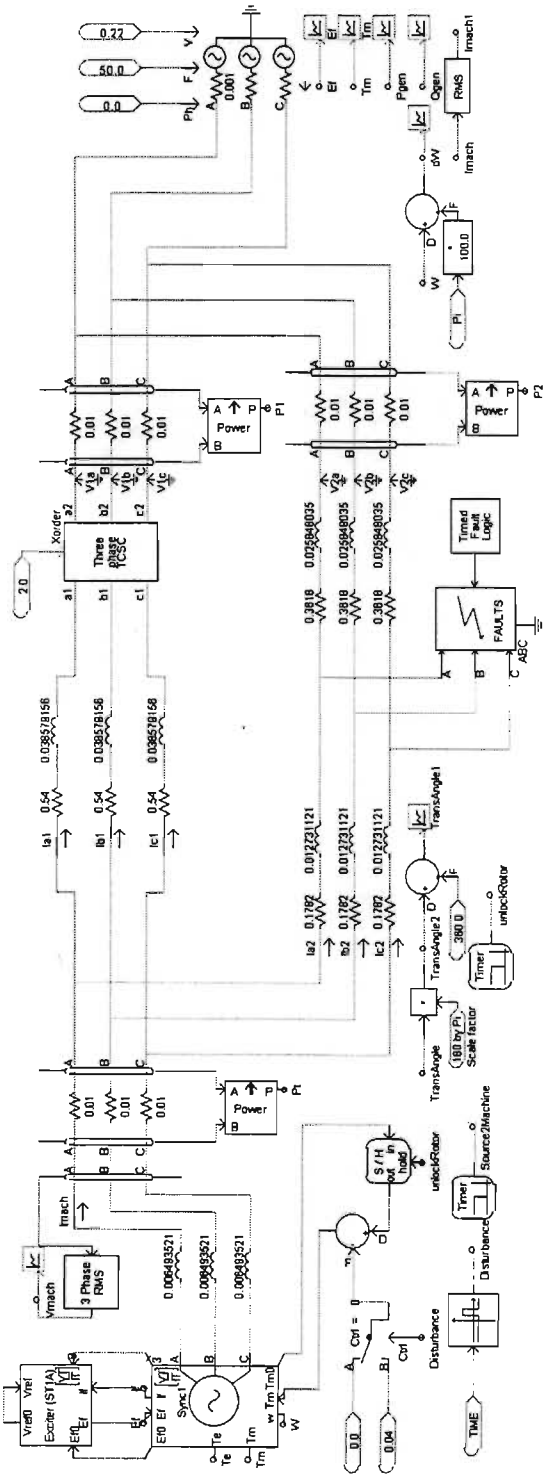

Fig A.1: A detailed PSCAD representation of the SMIB study system

A.3. Detailed Representation of the TCSC with its Internal Controls and the Power Controller Model.

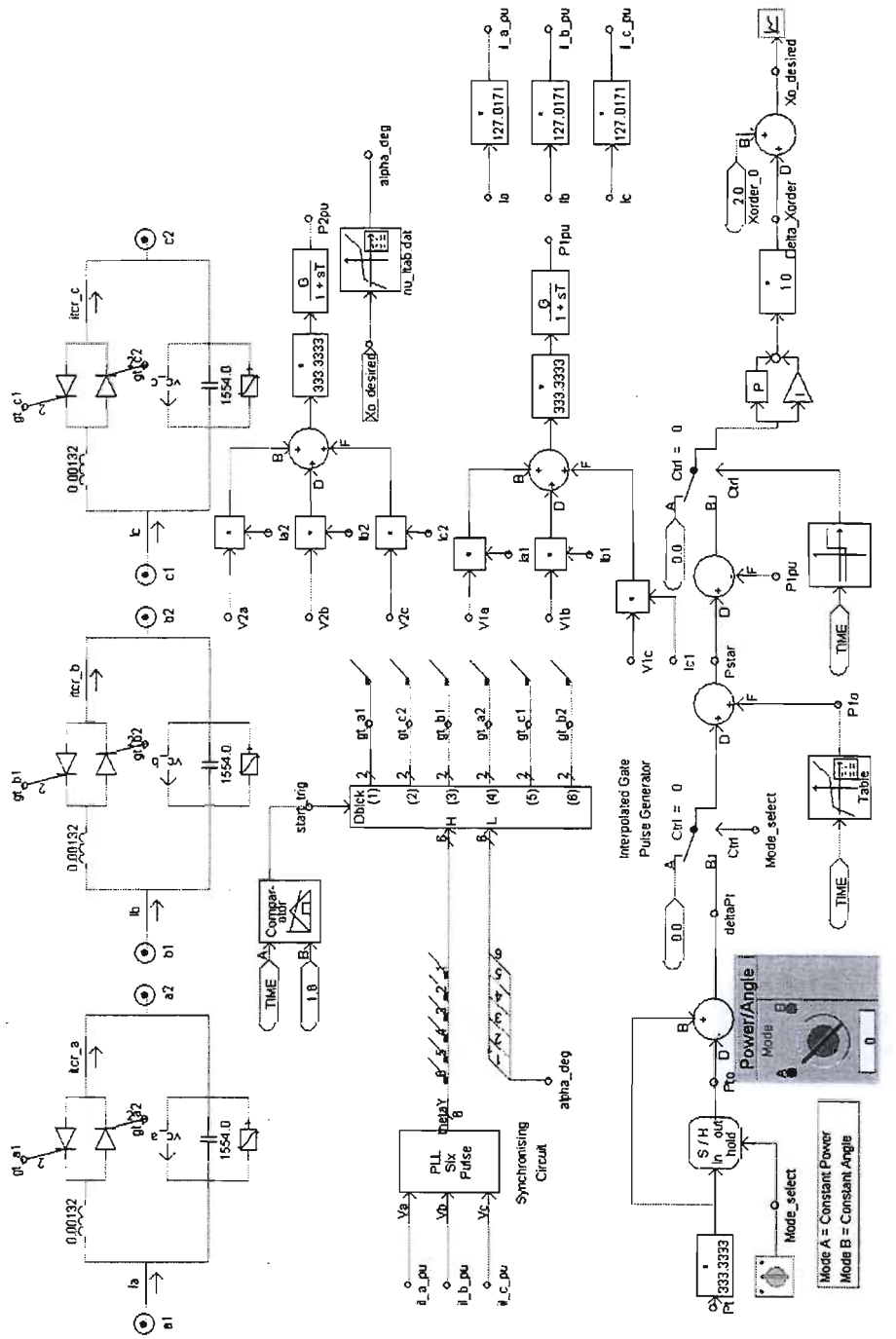

Fig A.2: Detailed PSCAD representation of the TCSC and power flow controller model.

APPENDIX B

PARAMETERS OF THE FOUR-GENERATOR SYSTEM AND THE DESIGN OF THE CONTROLLER GAINS

This Appendix lists the parameters used in the four-generator study system in Chapter Six and outlines the method used to design the power flow controller gains in the four-generator system. In addition this appendix includes the RCSAD representation of the four-generator system complete with the TCSC internal controls and power flow controller model.

B.1. Parameters of the Study System

B.1.1 Generators

R_a = 0.0025 p.u

X_l = 0.2 p.u

X_d = 1.8 p.u

X_d' = 0.3 p.u

X_d'' = 0.25 p.u

X_q = 1.7 p.u

X_q' = 0.55 p.u

X_q'' = 0.25 p.u

T_{d0}' = 8.0 s

T_{d0}'' = 0.03 s

T_{q0}' = 0.4 s

T_{q0}'' = 0.05 s

H = 6.5s [for G1 and G2]

H = 6.175s [for G3 and G4]

Base Voltage = 20 kV

Base Power = 900 MVA

B.1.2 Transmission Line System

r	= 0.0001 p.u./km
x_L	= 0.001 p.u./km
b_C	= 0.00175 p.u./km
Base power	= 900MVA
Base voltage	= 230kV

B.1.3 Transformer

R_{TRFR}	= 0.0 p.u
X_{TRFR}	= 0.15 p.u
Base power	= 900MVA
Base voltage	= 20 / 230 kV

B.1.4 Initial Conditions

G1:	P = 700MW,	Q = 185MVar,	$E_t = 1.03\angle 20.2°$
G2:	P = 700MW,	Q = 235MVar,	$E_t = 1.01\angle 10.5°$
G3:	P = 719MW,	Q = 176MVar,	$E_t = 1.03\angle -6.8°$
G4:	P = 700MW,	Q = 202MVar,	$E_t = 1.01\angle -17.0°$

B.1.5 Loads

Bus 7:	P_L = 967MW,	Q_L = 100MVar,	Q_C = 200MVar
Bus 9:	P_L = 1767MW,	Q_L = 100MVar,	Q_C = 350MVar

B.1.6 Thyristor-Controlled Series Capacitor

C	= 0.255 p.u
L	= 0.044 p.u
Base power	= 900MVA
Base voltage	= 230kV

B.2. Design Method for Power Flow Controller Gains

This particular subsection illustrates the design method followed for obtaining the proportional and integral gains for the power flow controller in the studies of Chapter Six. However before getting into the computational steps, a brief overview of the parameters of the system will be highlighted. Firstly in order to decide on a desired operating point, the TCSC's reactance order (X_{order}) was set to a value of 2. For this steady state reactance order a detailed simulation model in Fig B.2 was executed with the power flow controller loop disabled. During this condition the relevant parameters were measured:

Power Flow in the Transmission Line

P_{TCSC} = 0.178 p.u
P_{L2} = 0.1408 p.u.
P_{L3} = 0.1408 p.u.

Output Power of Generator's

P_{G1} = 0.83 p.u.
P_{G2} = 0.82 p.u
P_{G3} = 0.85 p.u
P_{G4} = 0.82 p.u

Bus Voltages

Similarly as in section 3.3.3, the bus voltages are measured at the coupling point of the transmission lines. The bus voltages measured were:

V_S = 0.991 p.u

V_R = 0.999 p.u

TCSC Data

The set-point value for the TCSC's reactance order ($X_{order\ 0}$) was chosen to be a fixed value of 2. This resulted in the net compensating reactance ($X_{TCSC\ 0}$) having a magnitude of 0.509 p.u.

Transmission Line Data

In order to apply the design approach adopted in Chapter 3, the four-generator study system has to be simplified into a parallel transmission network with two equivalent transmission lines. Thus the transmission lines L2 and L3 are simplified to form one equivalent line $L_{2//3}$. The parameters of line $L_{2//3}$ are:

$R_{2//3}$ = 0.099 p.u

$X_{2//3}$ = 0.99 p.u

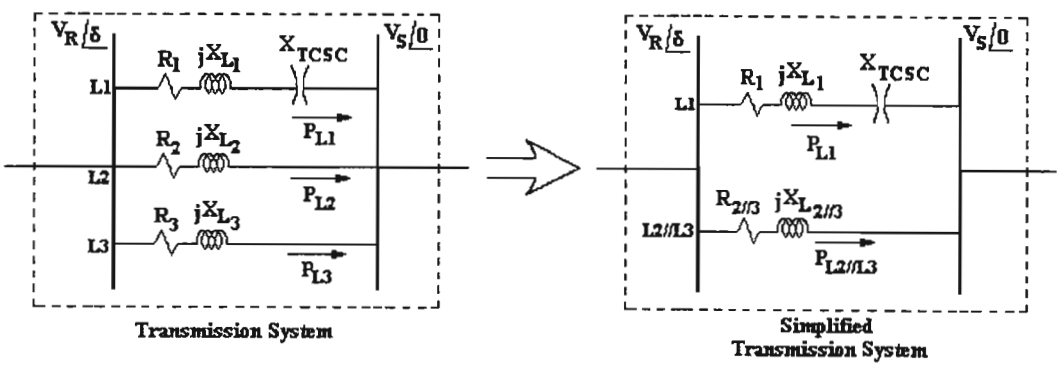

Fig. B.1 Diagram of the actual transmission system and simplified system for power flow controller design purposes

Using the parameters obtained from the RSCAD simulation, the transmission angle δ can be computed from equation 5.

Rearranging equation 5, and solving for δ, yields,

$$\delta = \frac{P_{TCSC}\,|X_L - X_{TCSC}|}{|\overline{V_S}||\overline{V_R}|}$$

$$= \frac{0.178\,|1.980 - 0.509|}{|0.991||0.999|}$$

$$= 15.32^0$$

Now using the transmission angle δ, the plant gain can be calculated using equation (12),

$$K_{PLANT} = X_C \frac{|\overline{V_S}||\overline{V_R}|}{(X_L - X_{TCSC0})^2}\sin\delta$$

$$= (0.255)\frac{|0.991||0.999|}{(1.980 - 0.509)^2}\sin(15.32)$$

$$= 0.0308$$

In this example a settling time (T_S) of 5s will be considered. For this settling time, a desired time constant τ_P = 1s and the τ_Z = 0.1s is specified. With the values for K_{PLANT}, τ_P, τ_Z established, the controller gains K_P and K_I can be determined using equations (15) and (16) as follows:

$$K_I = \frac{1}{0.0308(1-0.1)} = 36.07$$

$$K_P = \frac{0.1}{0.0308(1-0.1)} = 3.607$$

The numerical example shown above illustrates how the feedback controller can be designed to achieve a specific settling time for power flow control in the four-generator study system of Fig B.2 at a particular operating point. The same design procedure can thus be used to obtain a range of different power flow controller response times for comparative analysis.

B.3. Four-Generator Study system

An eleven-bus four-generator study system considered for analysis in Chapter Four and Six is depicted in Fig B.2 below.

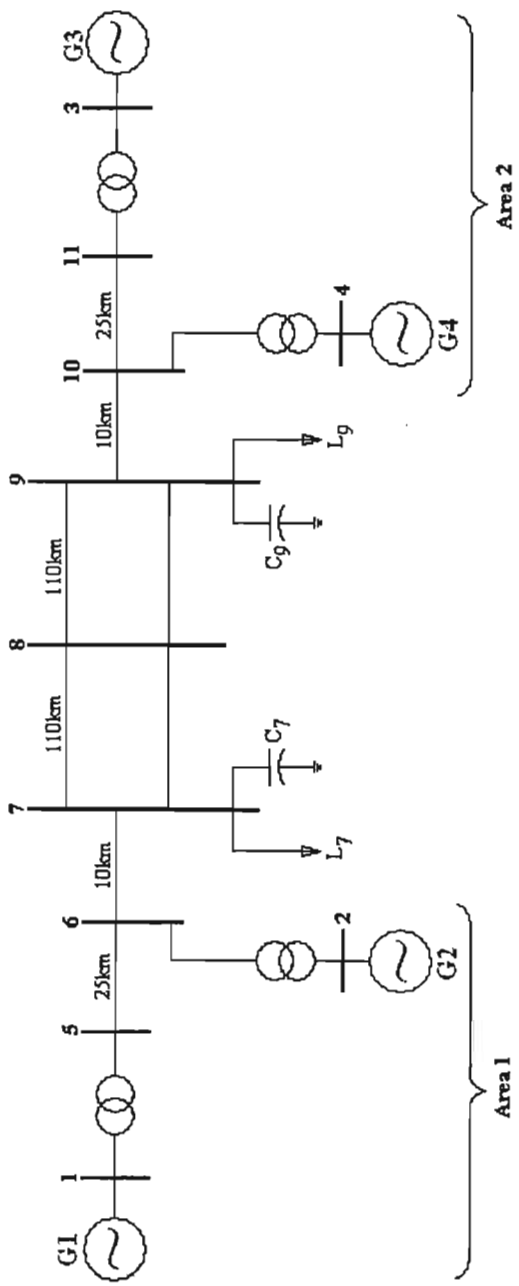

Figure B.2: An eleven bus four-generator study system

B.4. RSCAD Representation of the Four-Generator Model

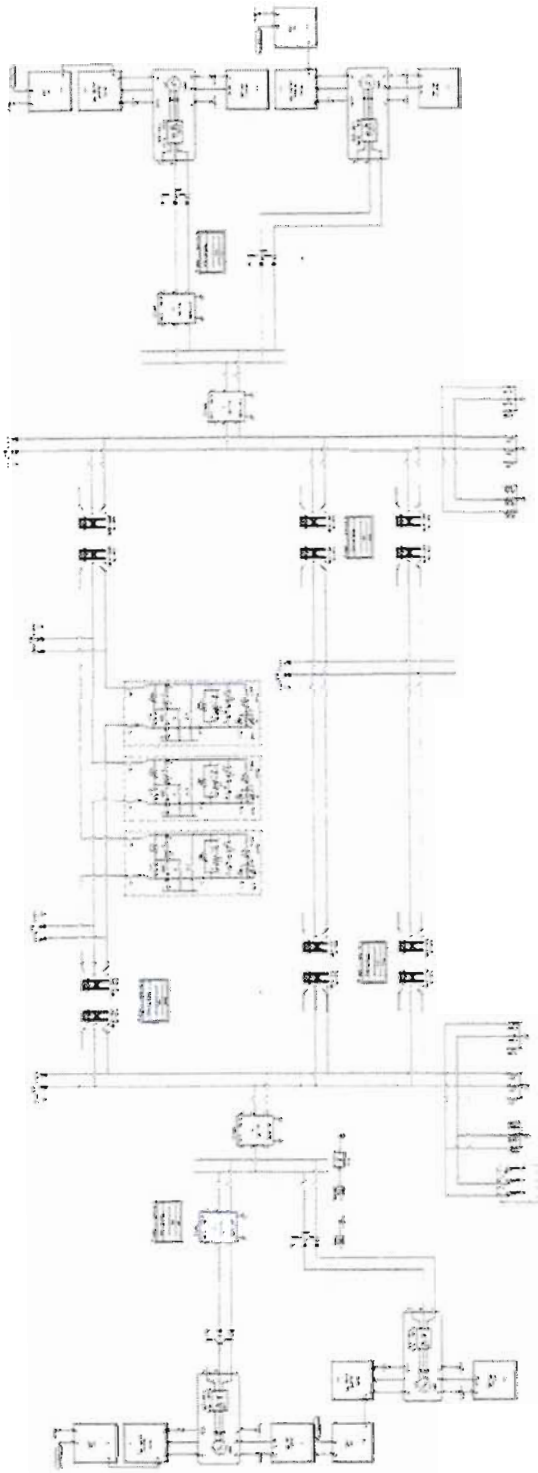

Fig B.3: Detailed RSCAD representation of the modified four-generator study system

B.5. TCSC Internal Control Model and Power Flow Controller Model

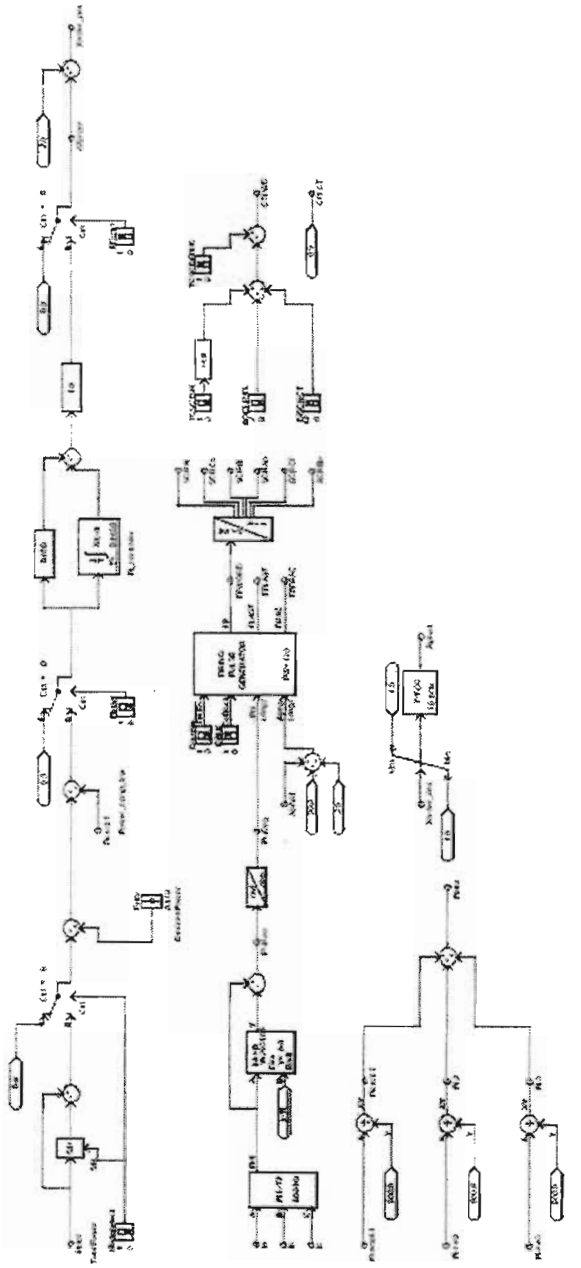

Fig B.4: Detailed RSCAD representation of the TCSC internal controls and power flow controller model

REFERENCES

[1] Hingorani N.G, Gyugyi L, Understanding FACTS: Concepts and Technology of Flexible AC Transmission System, *IEEE Press*, Piscataway New Jersey, 1999, ISBN 0-7803-3455-8.

[2] Edris A-A, Adapa R, Baker M.H, Habashi K, L.K. Bohmann Clark, Gyugyi L, Lemay J, Mehraban A.S, Myers A.K, Reeve J, Sener F, Torgerson D.R, Wood R.R: "Proposed Terms and Definitions for Flexible AC Transmission System (FACTS)", *IEEE Transactions on Power Delivery*, Vol.12, No.4, 1997.

[3] Larsen EV, Bowler CEJ, Damsky B, Nilsson S: "Benefits of Thyristor Controlled Series Compensation", *CIGRE Paper* 14/37/38-04, Paris, 1992.

[4] Gyugyi L, Rietman T.R, Edris A, "The Unified Power Flow Controller: A New Approach to Power Transmission Control", *IEEE Transactions on Power Delivery*, Vol. 10, No.2, April 1995.

[5] Noroozian M, Andersson G, "Power Flow Control by use of controllable Series Components", *IEEE Transactions on Power Delivery*, Vol. 8, No.3, July 1993.

[6] Martins N, Pinto JCP, Paserba JJ: "Using a TCSC for Line Power Scheduling and System Oscillation Damping – Small Signal and Transient Stability Studies", *Proceedings IEEE PES Winter Meeting*, Singapore, January 2000.

[7] Mihalič R, Papič I, "Power Flow Control using Static Synchronous Series Compensator", *Proceedings UPEC '97*, pp 174-177.

[8] Kundur P, Power System Stability and Control, McGraw Hill Inc, New York, 1994.

[9] Manitoba HVDC Research Centre Inc: "Introduction to PSCAD/EMTDC Version 3.0".

[10] Real-Time Digital Simulator Hardware Manual, Rev. 01, RTDS Technologies, Winnipeg, Manitoba, Canada, June 2001.

[11] Ally A, Rigby BS, "The Application of a Thyristor Controlled Series Capacitor for Closed-Loop Control of Transmission Line Power Flow, *Proceedings SAUPEC '04*, Stellenbosch, South Africa, Jan 2004.

[12] Ally A, Rigby BS, "An Investigation into the Impact of a Thyristor Controlled Series Capacitor-Based Closed-Loop Power Flow Controller Under Fault Conditions", *Proceedings IEEE Africon 2004*, Gaborone, Botswana, September 2004, pp. 675-681.

[13] Kimbark E.W, "Improvement of System Stability by switched Series Capacitors", *IEEE Transactions on Power Apparatus and Systems*, Vol. PAS-85, No.2, 1966.

[14] Song Y.H, Johns A.T.: "Flexible AC Transmission Systems" *IEEE Power & Energy Series 30*, ISBN 085 2 9677 13.

[15] Gyugyi L, "A Unified power Flow Controller Concept for Flexible AC Transmission Systems", *IEE Proceedings-C*, Vol.139, No.4, July 1992.

[16] Gama C, "Brazilian North-South Interconnection Control Application and Operating Experience with a TCSC", Proceedings of 1999 *IEEE PES Summer Meeting*, Edmonton, Canada, July 1999, pp. 1103-1108.

[17] Christl N, Hedin R, Johnson R, Krause P, Montoya A, "Power System Studies and Modelling for the Kayenta 230kV substation Advanced Series Compensation", *IEE Fifth International Conference on AC and DC Power Transmission*, London, September 1991.

[18] Piwko R.J, Damsky W.B.L, Furumasu B.C, Eden J.D, "The Slatt Thyristor Controlled Series Capacitor Project-Design, Installation, Commissioning and System Testing", *CIGRE paper* 14-104, Paris, 1994.

[19] Renz B.A, Keri A, Mehraban A.S, Schauder C, Stacey E, Kovalsky L, Gyugyi L, Edris A: "AEP Unified Power Flow Controller Performance", *IEEE Transactions on Power Delivery*, Vol 14, No 4, October 1999, pp 1374-1381.

[20] Gotham D.J, Heydt G.T, "Power Flow Control and Power Flow Studies for Systems with Facts Devices", *IEEE Transactions on Power Systems*, Vol.13, No.1, February 1998.

[21] Rigby B.S: "An AC Transmission Line Power Flow Controller Using a Thyristor Controlled Series Capacitor", *Proceedings IEEE Africon 2002*, George, South Africa, October 2002, pp.773-778.

[22] Mazibuko, R.H-B, "Design and Implementation of a Thyristor Controlled Series Capacitor for Research Laboratory Application", MScEng Thesis, University of Natal, Durban, South Africa, 2003.

[23] Pillay A, Rigby B.S: "Investigations into the effect of inductor size on the performance of thyristor controlled series capacitor", *Proceedings IEEE Africon 2004*, Gaborone, Botswana, September 2004, pp.1149-1154.

[24] Carpanen R.P, Rigby B.S: "Transient Stability Enhancement Using a Thyristor Controlled Series Capacitor", *Proceedings IEEE Africon 2004*, Gaborone, Botswana, September 2004.

[25] Klein M, Rogers G.J, Moorty S, Kundur P, "Analytical Investigation of Factors Influencing Power System Stabilizers Performance", *IEEE Transactions on Energy Conversion*, Vol. 7, No. 3, September 1992.

[26] Klein M, Rogers G.J, Kundur P, "A Fundamental Study of Inter-Area Oscillations in Power Systems, *IEEE Transactions on Power Systems*, Vol. 6, No.3, August 1991.

[27] Rigby B.S: "Validation of Models Used in Real Time Simulation", Eskom Research Report No. RES/RR/03/22445, December 2003.

[28] Chonco N.S, "The Application of Controllable Inverter-Based Series Compensation to Power Oscillation Damping", MScEng Thesis, University of Natal, Durban, South Africa, 2000.

[29] Fujita G, Goswami P.K, Yokoyama R, "Local Power Flow based Decentralised TCSC Controller", *IEEE 0-7803-4754-4/98*, 1998.

[30] Da X, Hui N, Chen C, Jishun W, "An Algorithm to Control the Power Flow in Large Systems Based on TCSC", *Proceedings of IEEE International Conference on Power Technology*, POWERCON98, pp 344-348.

[31] Guojie L, Lie T.T, Shrestha G.B, Lo K.L, "Real-time coordinated optimal FACTS controllers", *Electric Power Systems Research 52*, 1999, pp 273-286.

[32] MathWorks: "MATLAB for windows User's Guide", The MathWorks, Inc., 1991.